# Electron Solvation Dynamics in Photoexcited Iodide-Polar Solvent Clusters: A Theoretical Investigation

Chun C. Mak

A Thesis in the Department of Chemistry and Biochemistry

Presented in Partial Fulfilment of the Requirements for the

Degree of Doctor of Philosophy (Chemistry) at

Concordia University,

Montréal, Québec, Canada

August 2014

**CONCORDIA UNIVERSITY**
**SCHOOL OF GRADUATE STUDIES**

This is to certify that the thesis prepared

By: Chun Chi Mak

Entitled: Electron Solvation Dynamics in Photoexcited Iodide-Polar Solvent Clusters: A Theoretical Investigation

and submitted in partial fulfillment of the requirements for the degree of

Doctor of Philosophy (Chemistry)

complies with the regulations of the University and meets the accepted standards with respect to originality and quality.

Signed by the final examining committee:

Dr. V. Zazubovits — Chair

Dr. B. Schwartz — External Examiner

Dr. M. Frank — External to Program

Dr. A. English — Examiner

Dr. G. Lamoureux — Examiner

Dr. G. Peslherbe — Thesis Supervisor

Approved by: Dr. H. Muchall , Graduate Program Director

September 25, 2014 Dr. A. Roy, Dean
Faculty of Arts and Science

## Abstract

**Electron Solvation Dynamics in Photoexcited Iodide-Polar Solvent Clusters: A Theoretical Investigation**

Chun C. Mak, Ph.D.

Concordia University, 2014

Photoexcitation of halides dissolved in polar liquids results in charge-transfer-to-solvent (CTTS) states in which a halide valence electron has been transferred to a delocalised, solvent-supported orbital. Subsequent relaxation of CTTS excited solvated halides results in the formation of solvated electrons, ubiquitous species implicated in numerous chemical and biochemical transformations. Analogues of the CTTS excited states of solvated halides have also been observed in small iodide-polar solvent clusters, and the relaxation of CTTS excited iodide-polar solvent clusters, $[I^-(Solv)_n]^*$, has attracted significant interest as a paradigm for investigating the role of individual solvent molecules in trapping and solvating an excess electron.

In this work, a combination of high-level quantum chemical calculations and first-principles molecular dynamics simulations is employed to elucidate the relaxation mechanism of $[I^-(Solv)_n]^*$ (Solv = $H_2O$, $CH_3CN$ and $CH_3OH$) and to develop an in-depth understanding of the nature of the molecular motions and interactions involved in the associated electron solvation processes. A 'two-level' approach is employed, in which $[I^-(Solv)_n]^*$ trajectories are propagated on a potential energy surface computed with a relatively modest treatment of electron correlation and a medium-sized basis set while electronic properties of cluster configurations sampled from the trajectories are computed with a much more rigorous quantum-chemical method and significantly larger basis sets.

Results indicate that $[I^-(Solv)_n]^*$ relaxation involves rapid initial motion of the solvent molecules, leading to the separation of the excited electron from the iodine atom and a concomitant decrease in stability of the excited electron, followed by more gradual

reorganisation of the cluster, which can have variable effects on the stability of the excited electron, depending on the type of solvent molecule in the cluster. In clusters with a strong network of solvent-solvent interactions, such as $[I^-(H_2O)_n]^*$, stabilisation of the excited electron occurs, while in clusters with a weaker network of solvent-solvent interactions, such as $[I^-(CH_3OH)_n]^*$, solvent cluster fragmentation ultimately results in destabilisation of the excited electron. Subtle differences in the structural properties of the molecules within the cluster can thus heavily influence the electron solvation process in $[I^-(Solv)_n]^*$, a reflection of the important role of individual molecules in supporting a solvated electron.

## Acknowledgements and Dedication

I would like to first and foremost express my gratitude towards my research supervisor, Professor Gilles Peslherbe for his friendly encouragement, inspiration and advice, without which this work would not have been possible. I would also like to thank my committee members, Professor Ann English and Professor Guillaume Lamoureux, for offering constructive feedback on my research. Finally, I will fondly remember the many stimulating and fruitful conversations with my present and former colleagues, who brightened up my stay at Concordia University.

I am grateful for the generous financial support I have received from the Fonds de Recherche du Québec — Nature et Technologies (FQRNT), the Natural Sciences and Engineering Research Council of Canada (NSERC), and Concordia University throughout the course of my doctoral studies, and for the generous allocation of computational resources from the Centre for Research in Molecular Modeling (CERMM) and Compute Canada, without which many of the calculations reported in this thesis would not have been possible.

I dedicate this thesis to my family, for their unconditional love and encouragement.

## Contribution of the Authors

The research reported in this dissertation was largely carried out by me, Chun Mak, with guidance and feedback from co-authors Professor Qadir Timerghazin, of Marquette University, Milwaukee, Wisconsin, and Professor Gilles Peslherbe, my research supervisor. Specifically, my contributions to the manuscripts included in this dissertation are outlined below:

**Chapter 2:** I identified research questions, designed the computational approach needed to address these questions, performed the calculations, analysed the calculation results to answer the previously identified research questions and wrote the first draft of the entire manuscript.

**Chapter 3:** The research reported in this chapter began as unpublished work originally reported in Qadir Timerghazin's doctoral dissertation (2006). By revisiting the research results in light of subsequent findings from other research groups, and greatly expanding and improving the work with the help of more sophisticated computational approaches made possible by the more powerful computing facilities that became available after Qadir Timerghazin's dissertation was completed, I arrived at a very different picture of the system under study; the new conclusions derived from the expanded work then played a critical role in the interpretation of the results of the research presented in the other sections of this dissertation. I wrote most of the first draft of the manuscript myself, but in order to make the manuscript coherent, this chapter also retains text and figures originally included in Qadir Timerghazin's dissertation; paragraphs and figures incorporating a significant amount of material from Qadir Timerghazin's dissertation begin with **.

**Chapter 4:** I identified research questions, designed the computational approach needed to address these questions, performed the calculations, analysed the calculation results to answer the previously identified research questions and wrote the first draft of the entire manuscript.

**Chapter 5:** I compiled previous research findings and integrated them to develop a general picture of the class of systems investigated in this dissertation. I also wrote the first draft of the entire manuscript.

# Table of Contents

# List of Figures

# List of Tables

# List of Abbreviations

| | |
|---|---|
| **B3LYP** | **Becke's Three Parameter Hybrid Exchange/Lee-Yang-Parr** |
| **CASPT2** | **Complete-Active-Space Second-Order Perturbation Theory** |
| **CCSD(T)** | **Coupled-Cluster Theory with Single, Double and Non-Iterative Triples Correction** |
| **CIS** | **Configuration Interaction with Single Excitations** |
| **CTTS** | **Charge Transfer to Solvent** |
| **DFT** | **Density Functional Theory** |
| **DNA** | **Deoxyribonucleic acid** |
| **HF** | **Hartree Fock** |
| **HOMO** | **Highest Occupied Molecular Orbital** |
| **IP** | **Ionisation Potential** |
| **MP2** | **Møller-Plesset Second-Order Perturbation theory** |
| **MRCI** | **Multireference Configuration Interaction** |
| **ROHF** | **Restricted Open-Shell Hartree Fock** |
| **SA-CASSCF** | **State-Averaged Complete-Active-Space Self-Consistent-Field Theory** |
| **SO** | **Spin Orbit** |
| **SOC** | **Spin Orbit Coupling** |
| **SOMO** | **Singly Occupied Molecular Orbital** |
| **VDE** | **Vertical Detachment Energy** |

# 1. Introduction

### 1.1. Background

The solvated electron is best known as the species responsible for the deep blue colour of solutions formed upon addition of sodium metal to liquid ammonia, and in fact, this intriguing species, which is essentially a free electron, a subatomic particle, trapped in solvent, was first prepared more than 200 years ago. It was around 1807 when Sir Humphrey Davy noticed the formation of a golden brown to bluish substance when grains of potassium metal were exposed to gaseous ammonia.[*1*] Decades later, in 1864, the same blue colour was observed when alkali metals were dissolved in liquid ammonia.[*2*] The spectacular blue colour of these solutions was first attributed to the presence of solvated electrons in the early 20$^{th}$ century,[*3*] and since then, solvated electrons have been observed in a variety of other polar solvents, including water[*4*] and alcohols.[*5*] While being the most elementary anion of chemistry, consisting of one electron and no nuclei, the solvated electron is also an important species in numerous noteworthy chemical and biochemical transformations. The solvated electron serves as a reducing agent in several synthetically important chemical reactions, including the Birch reduction of benzene derivatives to substituted 1,4-cyclohexadienes,[*6-8*] the Bouveault-Blanc reduction[*9, 10*], in which esters are converted to primary alcohols, and the conversion of nitriles to aldehydes under aqueous conditions.[*11*] As a ubiquitous species in aqueous environments irradiated with high-energy ionising radiation, the solvated electron has also been implicated in the process of radiation induced damage to cellular genetic material. Despite the long history of the solvated electron and its importance in many chemical processes, including those relevant to living systems, the molecular properties of the solvated electron continues to be a subject of intense interest and controversy.[*12, 13*]

In order to obtain a clearer picture of the mechanism of solvated electron formation, substantial research has been carried out on the photochemistry of simple anions, such as halides, in solution.[*14*] Halides have long been known to exhibit broad absorption bands in the ultraviolet region of the electromagnetic spectrum that are associated with excited states in which a halide-localised valence electron has been transferred to an orbital supported by the collective electric field of the surrounding solvent molecules.[*15, 16*] CTTS excited halides relax to produce solvated electrons,[*14*] and in fact, the very same intermediates believed to be involved in the relaxation pathway of CTTS excited halides may be related to species involved in the process of

DNA damage induced by exposure to high-energy radiation, which can ultimately result in diseases, including cancer.[*17*] The development of a detailed understanding of the relaxation dynamics of CTTS excited species may therefore shed light on the chemical properties of solvated electron precursors that may be involved in chemically and biologically relevant reduction reactions taking place in solution.[*14*]

While there are no gas-phase analogues of halide CTTS states, excited states analogous to the CTTS states of halides in solution have been identified in small clusters consisting of an iodide anion and one or more complexed solvent molecules. In 1995, Johnson and co-workers observed using photofragmentation action spectroscopy bound excited states in small iodide-acetone, $I^-(CH_3COCH_3)$, and iodide-acetonitrile, $I^-(CH_3CN)_n$ (n = 1, 2), complexes that decay to produce acetone anions, $(CH_3COCH_3)^-$ and a combination of acetonitrile, $(CH_3CN)^-$, and acetonitrile dimer, $(CH_3CN)_2^-$, anions, respectively.[*18, 19*] Similar excited states were also observed for small iodide-water clusters, $I^-(H_2O)_n$ (n = 2-4), shortly after.[*20*] The observed excited states were believed to be dipole-bound, with the excited electron interacting weakly with the collective dipole moment of the solvent molecules attached to the iodine atom formed upon photoexcitation; later quantum-chemical calculations performed by Chen and Sheu[*21*] and Timerghazin and Peslherbe [*22*] confirmed the dipole-bound nature of these cluster excited states. These calculations indicate that the excited electron in small iodide-polar solvent molecule clusters occupy an extremely diffuse molecular orbital spanning a region of space greatly exceeding that of the neutral cluster framework itself, generally on one side of the neutral cluster. As such, the excited-state electronic structure of small iodide-polar solvent molecule clusters differs substantially from that of iodide in bulk solutions, which tend to be more confined, with the excited electron occupying mostly the region of space in the vicinity of the neutral iodine atom, typically surrounded by solvent molecules.[*23*] Nevertheless, small excited iodide-polar solvent molecule clusters can be loosely viewed as the gas-phase analogues of CTTS excited iodide in bulk solutions, and it can be surmised that the electronic structure of excited iodide-polar solvent molecule clusters would become increasingly similar to that of bulk CTTS excited iodide as the number of solvent molecules increases. Due to the intimate relationship between small excited iodide-polar solvent molecule clusters, $[I^-(Solv)_n]^*$, and CTTS excited solvated iodide, the former will henceforth be referred to as CTTS excited iodide-polar solvent molecule complexes in this thesis.

The relaxation processes of $[I^-(Solv)_n]^*$ have attracted substantial interest since they provide a unique opportunity to investigate the processes involved in trapping and possibly solvating an excess electron at the molecular level, and starting with their initial investigation of electron solvation dynamics in $[I^-(H_2O)_n]^*$ (n = 4-6) using femtosecond photoelectron spectroscopy,[*24*] Neumark and co-workers have performed a series of experiments using variants of the original technique for clusters with a variety of polar-solvent molecules, including ammonia,[*25*] alcohols,[*26-28*] and acetonitrile,[*29*] revealing rich and varied relaxation dynamics that exhibit remarkable solvent specificity. While all $[I^-(Solv)_n]^*$ examined to date undergo relaxation processes resulting in an increased stability of the excited electron at early times, it is the subsequent time evolution of the stability of the excited electron and the rate of decay of the clusters by vibrational autodetachment of the excited electron that exhibit the most intriguing variation with the nature of the solvent. $[I^-(H_2O)_n]^*$ and $[I^-(CH_3CN)_n]^*$ decay on a timescale of up to several nanoseconds, while $[I^-(CH_3OH)_n]^*$ and $[I^-(NH_3)_n]^*$ decay over a much shorter timescale not exceeding tens of picoseconds. Furthermore, the excited electron of $[I^-(CH_3OH)_n]^*$ undergoes a much more pronounced destabilisation at later times, before the clusters decay by autodetachment, a feature not observed in any of the other $[I^-(Solv)_n]^*$ investigated. The observed modulation in the stability of the excited electron in $[I^-(Solv)_n]^*$ resulted in much speculation as to the nature of the relaxation pathways involved and the manner in which small clusters can trap and solvate an excited electron, and almost all of the subsequent work to understand in greater detail the relaxation mechanisms of $[I^-(Solv)_n]^*$ focused on $[I^-(H_2O)_n]^*$ due to the significance of water as nature's most common solvent.

The observed increase in stability of the excited electron in $[I^-(H_2O)_n]^*$ was first rationalised by Neumark and co-workers in terms of the rearrangement of the solvent cluster moiety following excitation to trap and stabilise the excited electron,[*24*] in what came to be referred to as the "solvent-driven model" of $[I^-(H_2O)_n]^*$ relaxation dynamics. Much of the evidence in support of the solvent-driven model of $[I^-(H_2O)_n]^*$ relaxation dynamics came from earlier work on bare water cluster anions, which identified multiple conformers with different electron binding energies.[*30, 31*] It was proposed that, upon excitation, the water-cluster moiety of $[I^-(H_2O)_n]^*$ would rearrange from a conformer with a lower electron binding energy to one with a higher electron binding energy, accounting for the increase in stability of the excited electron of $[I^-(H_2O)_n]^*$ observed in the femtosecond photoelectron spectroscopy experiments.

The solvent-driven model of $[I^-(H_2O)_n]^*$ was subsequently challenged by Chen and Sheu, who proposed, based on quantum-chemical calculations of $[I^-(H_2O)_n]^*$ (n = 4, 5), that the observed increase in the stability of the excited electron in $[I^-(H_2O)_n]^*$ could be rationalised in terms of the relative motion of the iodine atom and the water-cluster moiety.[*32, 33*] This "iodine-driven model" of $[I^-(H_2O)_n]^*$ relaxation dynamics highlighted the importance of the effect of the iodine atom formed upon excitation on the stability of the excited electron in $[I^-(H_2O)_n]^*$, but in contrast to the solvent-driven model of Neumark and co-workers, did not consider the effect solvent cluster reorganisation could have on the stability of the excited electron.

In the first attempt to unravel the relaxation mechanism of $[I^-(H_2O)_n]^*$, Timerghazin and Peslherbe performed first-principles molecular dynamics simulations of $[I^-(H_2O)_n]^*$ (n = 3).[*34*] Results of these preliminary simulations indicate that the $[I^-(H_2O)_n]^*$ relaxation process is characterised by a combination of solvent and iodine motions, with the dynamics of both the solvent molecules and the iodine atom likely to contribute to the time evolution of the stability of the excited electron. While other researchers have subsequently carried out variants of the original first-principles molecular dynamics simulations of $[I^-(H_2O)_n]^*$ for different cluster sizes and initial cluster configurations,[*35-38*] none of the simulations performed to date have attempted to untangle the precise roles of the solvent molecules and the iodine atom in $[I^-(H_2O)_n]^*$ relaxation dynamics. Furthermore, there has to date not been any attempt to characterise in detail the molecular interactions that are critical in the electron solvation dynamics of $[I^-(Solv)_n]^*$. Finally, there remains no satisfactory explanation of the solvent specificity of $[I^-(Solv)_n]^*$ stability and electron solvation dynamics. Thoroughly addressing these issues is not only critical for the development of a complete understanding of the relaxation and electron solvation dynamics of $[I^-(Solv)_n]^*$, but also may shed light on to the fundamental molecular properties of the solvated electron.

### 1.2. Research Objectives

The purpose of this work is to obtain a comprehensive picture of the relaxation and electron solvation dynamics of $[I^-(Solv)_n]^*$ and to develop a molecular-level understanding of the most important factors that determine the nature of the electron solvation pathways in $[I^-(Solv)_n]^*$. This research project involves three primary aspects. Firstly, the relaxation mechanism of $[I^-$

$(Solv)_n]^*$ is elucidated. Secondly, the role of individual molecules and the associated molecular interactions in trapping and stabilising an excess electron in clusters are unequivocally determined. Finally, a detailed comparison of the relaxation and electron solvation dynamics of $[I^-(Solv)_n]^*$ for different solvent molecules is performed in order to develop an understanding of the general features of $[I^-(Solv)_n]^*$ relaxation and obtain a rational explanation of the solvent specificity of these processes. This work is organised into four sections, as outlined below.

In **chapter 2**, a detailed comparison of the relaxation dynamics of $[I^-(H_2O)_n]^*$ (n = 5) and the rearrangement dynamics of the closely related water pentamer anion, $(H_2O)_n^-$ (n = 5), which unequivocally establishes the roles of iodine and water in the electron solvation process of CTTS excited iodide-water clusters, is reported.

In **chapter 3**, a detailed study of $[I^-(CH_3CN)]^*$ relaxation dynamics, which sheds light on the types of solvent motions involved in $[I^-(Solv)_n]^*$ relaxation and the nature of the iodine-electron interactions that may be important in electron solvation processes, is described. A fundamental understanding of these aspects of $[I^-(Solv)_n]^*$ relaxation dynamics and their dependence on the molecular structure of the solvent molecules in the cluster provides the basis for investigating the solvent specificity of electron solvation dynamics in small clusters, the subject of the remaining sections of this thesis.

**Chapter 4** reports results of an investigation of $[I^-(CH_3OH)_n]^*$ relaxation dynamics using quantum chemistry and first-principles molecular dynamics simulations that aim to address the similarities and differences between $[I^-(CH_3OH)_n]^*$ and $[I^-(H_2O)_n]^*$ relaxation dynamics. While providing a glimpse of the molecular basis of the solvent specificity of $[I^-(Solv)_n]^*$ relaxation dynamics, this work also demonstrates the manner in which subtle differences in the molecular interactions present within the cluster can result in stark differences in the relaxation and electron solvation dynamics.

**Chapter 5** provides a comprehensive overview of the main features of $[I^-(Solv)_n]^*$ relaxation dynamics and highlights the manner in which differences in the molecular structure of the solvent molecules found within the cluster contribute to the rich and varied relaxation dynamics of different $[I^-(Solv)_n]^*$. By comparing and contrasting the relaxation dynamics of $[I^-(Solv)_n]^*$ (Solv = $H_2O$, $CH_3CN$ and $CH_3OH$) and rationalising the similarities and differences in terms of

the findings of the previous chapters of this thesis, a framework for understanding the cluster analogues of electron solvation processes is proposed.

## 2. Photoinduced Electron Transfer and Solvation Dynamics in Aqueous Clusters: Comparison of the Photoexcited Iodide-Water Pentamer and the Water Pentamer Anion

**Published As:**

Chun C. Mak, Qadir K. Timerghazin and Gilles H. Peslherbe, *Physical Chemistry Chemical Physics,* 2012, 14: 6257-6265

## Abstract

Upon photoexcitation of iodide-water clusters, $I^-(H_2O)_n$, an electron is transferred from iodide to a diffuse cluster-supported, dipole-bound orbital. Recent femtosecond photoelectron spectroscopy experiments have shown that, for photoexcited $I^-(H_2O)_n$ ($n \geq 5$), complex excited-state dynamics ultimately result in the stabilisation of the transferred electron. In this work, *ab initio* molecular dynamics simulations of excited-state $I^-(H_2O)_5$ and $(H_2O)_5^-$ are performed, and the simulated time evolution of their structural and electronic properties are compared to determine unambiguously the respective roles of the water molecules and the iodine atom in the electron stabilisation dynamics. Results indicate that, driven by the iodine – hydrogen repulsive interactions, excited $I^-(H_2O)_5$ rearranges significantly from the initial ground-state minimum energy configuration to bind the excited electron more tightly. By contrast, $(H_2O)_5^-$ rearranges less dramatically from the corresponding configuration due to the lack of the same iodine – hydrogen interactions. Despite the critical role of iodine for driving reorganisation in excited $I^-(H_2O)_5$, excited-electron vertical detachment energies appear to be determined mostly by the water cluster configuration, suggesting that femtosecond photoelectron spectroscopy primarily probes solvent reorganisation in photoexcited $I^-(H_2O)_5$.

## 2.1. Introduction

Despite having no bound excited states in the gas phase, halides dissolved in polar solvents such as water exhibit broad absorption bands in the ultraviolet region of the electromagnetic spectrum resulting from the transfer of an electron originally localised on the halide ion to a delocalised solvent-supported molecular orbital.[*15, 16*] The halide excited states formed in solution are called charge-transfer-to-solvent (CTTS) states.[*16*] Relaxation of these CTTS states following photoexcitation results in the separation of the ejected electron from the neutral halogen atom and the formation of a solvated electron,[*39, 40*] a synthetically important chemical species[*11*] that is also implicated in radiation-induced cell damage.[*41, 42*] Analogous CTTS states have also been experimentally observed in various iodide-polar solvent clusters,[*18-20*] and electronic structure calculations indicate that, in each case, photoexcitation results in the transfer of an electron from iodide to a diffuse orbital stabilised by the dipole field of the solvent molecule(s).[*21-23, 43*] The CTTS process resulting from photoexcitation of solvated halides is one of the simplest examples of electron transfer reactions, which are ubiquitous in chemistry and biology.[*44, 45*]

Excited iodide-water clusters, $[I^-(H_2O)_n]^*$, provide an especially interesting paradigm for investigating the molecular details of electron transfer processes in aqueous systems. Neumark and co-workers applied femtosecond photoelectron spectroscopy to probe the relaxation dynamics of $I^-(H_2O)_n$ following photoexcitation to the CTTS excited state, uncovering interesting excited-state dynamics that ultimately result in the increased stability of the excited electron, especially for larger clusters with at least five water molecules.[*24-26, 46, 47*] For such clusters, the excited-electron binding energy, and thus its vertical detachment energy (VDE), decreases sharply immediately after photoexcitation by 0.03 to 0.38 eV, then it increases by 0.23 to 0.40 eV over a period of several ps, depending on the size of the cluster. Two somewhat conflicting models of $I^-(H_2O)_n$ excited-state dynamics have been proposed to explain the ultimate increase in the stability of the excited electron, one emphasising the role of solvent cluster reorganisation, hereafter referred to as the solvent-driven model,[*34*] and the other emphasising the role of iodine ejection, hereafter referred to as the iodine-driven model,[*34*] and both are to some extent consistent with available experimental[*24-26, 46-48*] and theoretical data.[*21, 32, 33*]

The solvent-driven model of $I^-(H_2O)_n$ excited-state dynamics, first proposed by Neumark and co-workers, attributes the increase in the excited-electron VDE following photoexcitation to the rearrangement of the $(H_2O)_n$ moiety to a conformation that binds the excited electron more tightly.[*24-26, 46-48*] Multiple isomers of water cluster anions, $(H_2O)_n^-$, have been identified,[*49-52*] and the similarity between the minimum and maximum excited-electron VDEs attained by $[I^-(H_2O)_n]^*$ and the excess-electron VDEs of the more weakly and strongly bound $(H_2O)_n^-$ isomers provide convincing evidence for water cluster isomerisation as the primary stabilisation mechanism of the excited electron.[*46, 47*] The solvent-driven model essentially assumes $[I^-(H_2O)_n]^*$ to resemble a water cluster anion with an iodine atom acting as a spectator, with little effect on the stability of the excited electron.

Based on "static" *ab initio* electronic structure calculations, which showed that the neutral iodine atom exerts a destabilising effect on the excited electron in $[I^-(H_2O)_n]^*$,[*21*] Chen and Sheu proposed that the experimentally-observed increase in the $[I^-(H_2O)_n]^*$ excited-electron VDE could be explained by the ejection of the iodine atom from the excited cluster.[*32, 33*] The calculated increase in the excited-electron VDE upon removal of the iodine atom without changing the geometry of the water cluster was found to be in excellent agreement with the experimentally-measured increase in the excited-electron VDE following photoexcitation of $I^-(H_2O)_n$. [*32, 33*] Results of more recent photofragment coincidence imaging[*53*] and *ab initio* electronic structure calculations[*54, 55*] of CTTS excited-state $I^-(H_2O)_n$ provide further evidence in support of this iodine-driven model of $I^-(H_2O)_n$ excited-state relaxation dynamics. In contrast to the solvent-driven model of $I^-(H_2O)_n$ excited-state dynamics, the iodine-driven model emphasises the role of iodine ejection while neglecting the solvent dynamics in CTTS excited-state $I^-(H_2O)_n$.

Timerghazin and Peslherbe performed *ab initio* molecular dynamics simulations of $[I^-(H_2O)_n]^*$ (n = 3) in order to gain further insight into the main features of $I^-(H_2O)_n$ excited-state dynamics.[*34*] Despite the small size of the cluster and the absence of the significant shift in excited-electron VDE observed experimentally in larger $I^-(H_2O)_n$, results of the preliminary simulations of this small system suggested that the dynamics of $[I^-(H_2O)_n]^*$ is characterised by rapid oscillatory motion of the water molecules and gradual increase in the distance between the iodine atom and the water cluster centre of mass. While it was proposed that the time evolution

of the excited-electron VDE is determined primarily by the changes in the dipole moment of the water cluster moiety, effects arising from the very presence of the iodine atom could not be ruled out. Despite the several theoretical studies of $I^-(H_2O)_n$ that followed,[*35-38, 54, 55*] there continues to be much speculation about this process and, as yet, no consensus picture of the respective roles played by the iodine atom and the water molecules has been achieved for the electron stabilisation dynamics of $I^-(H_2O)_n$ ($n \geq 5$).

In order to develop a conclusive understanding of the roles of the iodine atom and the water molecules in the electron transfer and stabilisation process in CTTS excited-state $I^-(H_2O)_n$, *ab initio* molecular dynamics simulations of $[I^-(H_2O)_5]^*$ and the water pentamer anion, $(H_2O)_5^-$, are performed using a model that provides a consistent description of the two related systems. The simulated electron stabilisation dynamics and excess-electron VDE profiles of the two systems are then compared to untangle the roles of iodine and solvent in the electron stabilisation process. A detailed understanding of the iodine and solvent roles in $I^-(H_2O)_5$ excited-state dynamics may prove crucial for the design and interpretation of further femtosecond photoelectron spectroscopy experiments that could lead to new insights into the general features of electron transfer and solvation in diverse solvent clusters.

### 2.2. Computational Methods

Several *ab initio* molecular dynamics simulations of $[I^-(H_2O)_5]^*$ and $(H_2O)_5^-$ are performed to uncover the similarities and differences in the electron stabilisation dynamics of the two systems. The trajectories are propagated in quaternion coordinates,[*56*] with the geometry of the water molecule taken as the experimental gas-phase one,[*57*] using a fifth-order Gear predictor-corrector algorithm[*58*] with a time step of 0.7 fs to solve the classical equations of motion, and forces and energies at each time step are obtained from an electronic structure calculation. The free flow of vibrational energy between all modes has been a long-standing issue in classical simulations (see Ref. [*59*] and references therein), and it is therefore crucial to keep the water molecules rigid in order to avoid the artificial transfer of zero-point vibrational energy from the high-frequency intramolecular vibrational modes of the water molecules to the low-frequency intermolecular modes of the cluster. Another approach, which involves constraining the energy in each of the vibrational modes above the zero-point level, has recently been described by

Bowman and co-workers.[*60*] While this approach has the added advantage of allowing possible fluctuations in the water geometry during the relaxation/rearrangement of $[I^-(H_2O)_5]^*$ and $(H_2O)_5^-$, the use of rigid water molecules remains a more feasible option in the present simulations due to the system size and the computational cost of the selected model chemistry; freezing the intramolecular (high-frequency) modes of the water molecules allows the use of a larger time step in the integration of the equations of motion.

The model chemistries employed in the present work are similar to those originally used by Timerghazin and Peslherbe for the preliminary simulations of $[I^-(H_2O)_3]^*$,[*34*] but they are slightly modified to afford a consistent description of both $I^-(H_2O)_5$ and $(H_2O)_5^-$, a crucial requirement to allow an unbiased comparison of the rearrangement dynamics and the separation of the effects of iodine and water in the process of electron transfer and stabilisation. For $[I^-(H_2O)_5]^*$, the State-Averaged Complete-Active-Space Self-Consistent-Field (SA-CASSCF) level of theory[*61, 62*] is used to compute the energies and energy gradients used in the molecular dynamics simulations. The same (4,3) active space that was used in the $[I^-(H_2O)_3]^*$ simulations[*34*] is used here; it consists of the two nearly-degenerate 5*p* orbitals of iodide and the lowest unoccupied molecular orbital of the ground state, which accommodates the excited electron in the excited state. Excited-electron VDEs, which are crucial in the interpretation of the simulation results and connection with experiment, are computed using Second-Order Complete-Active-Space Perturbation Theory (CASPT2)[*63*] with the CASSCF wave function as the reference wave function. As for $(H_2O)_5^-$, in order to keep a description of the system equivalent to that of $[I^-(H_2O)_5]^*$, Restricted Open-Shell Hartree-Fock (ROHF) theory is employed for the computation of the energies and energy gradients, while Møller-Plesset Second-Order Perturbation theory (MP2)[*64, 65*] is used to compute the excess-electron VDEs. The 6-31++G(d,p) basis set[*66-68*] is used for hydrogen and oxygen atoms, while the ECP46MWB effective core potential and valence basis set[*69*] is used for iodine. In order to properly describe the highly diffuse dipole-bound electron in $[I^-(H_2O)_5]^*$ and $(H_2O)_5^-$, a set of diffuse basis functions consisting of 3 *s* functions with exponents 0.004, 0.000444 and 0.0000494, and one set of *p* functions with exponent 0.004 are added to the hydrogen atoms that form hydrogen bonds with iodide in the ground-state cluster geometry.[*70*] All electronic structure calculations are performed with the MOLPRO 2006.1 suite of programs.[*71*]

Of the several *ab initio* molecular dynamics simulations performed, the first one revisits the excited-state dynamics of $I^-(H_2O)_5$ initiated at the optimized Y41 structure, which was reported to be the lowest energy structure of ground-state $I^-(H_2O)_5$ by Kim and co-workers.[*72*] The Y41 structure of $I^-(H_2O)_5$, shown in the left panel of Figure 2.1a, consists of the iodide anion hydrogen-bonded to a crown-shaped water tetramer, with a fifth water molecule hydrogen-bonded to both iodide and a water molecule of the tetramer. The initial linear and angular velocities are selected from a Maxwell-Boltzmann distribution at 200 K,[*73*] which is believed to be the approximate temperature of water clusters,[*74*] using an approach reminiscent of the one used by Herbert and Head-Gordon for their simulations of $(H_2O)_4^-$.[*75*] Two different simulations of $(H_2O)_5^-$ are then performed in order to understand the solvent dynamics that results in the stabilisation of the excess electron. In the first one, the initial water cluster geometry is that of the initial geometry of the $[I^-(H_2O)_5]^*$ simulation, with the iodine removed; this allows investigation of the water cluster isomerisation alone to stabilise the excess electron in the absence of the iodine atom, by including the polarisation effects on the initial water cluster geometry due to the presence of iodide in the ground state, but removing any iodine effect on the water cluster rearrangement process in $[I^-(H_2O)_5]^*$ relaxation. In the second simulation of $(H_2O)_5^-$, the initial water cluster geometry is obtained by removing the iodine atom from the $[I^-(H_2O)_5]^*$ geometry after 50 fs of relaxation; this allows to probe the dynamics of the excess electron in the water cluster after the cluster has been heated up significantly during the initial rapid relaxation, again in the absence of the iodine atom. For both simulations of $(H_2O)_5^-$, the initial linear and angular velocities of the water molecules were taken to be identical to the corresponding velocities of $[I^-(H_2O)_5]^*$ at the time the iodine atom was removed (0 and 50 fs, respectively).

The excited/excess-electron VDEs of $[I^-(H_2O)_5]^*$ and $(H_2O)_5^-$ configurations sampled along the trajectories are computed in order to probe the effect of cluster reorganisation on the stability of the excess electron and make a connection with previous experimental work.[*24-26, 47*] In addition, the excess-electron VDEs of $(H_2O)_5^-$ in the geometry of the water cluster moiety of $[I^-(H_2O)_5]^*$ sampled along the trajectory are also computed to evaluate the effect of the presence of the iodine atom on the stability of the excited electron. All simulations are performed for 1 ps, a length of time sufficient to reproduce the major features of the time evolution of the excited-

electron VDE of $[I^-(H_2O)_5]^*$, including the initial sharp decrease and the subsequent gradual rise of the excited-electron VDE. [*24-26, 47*]

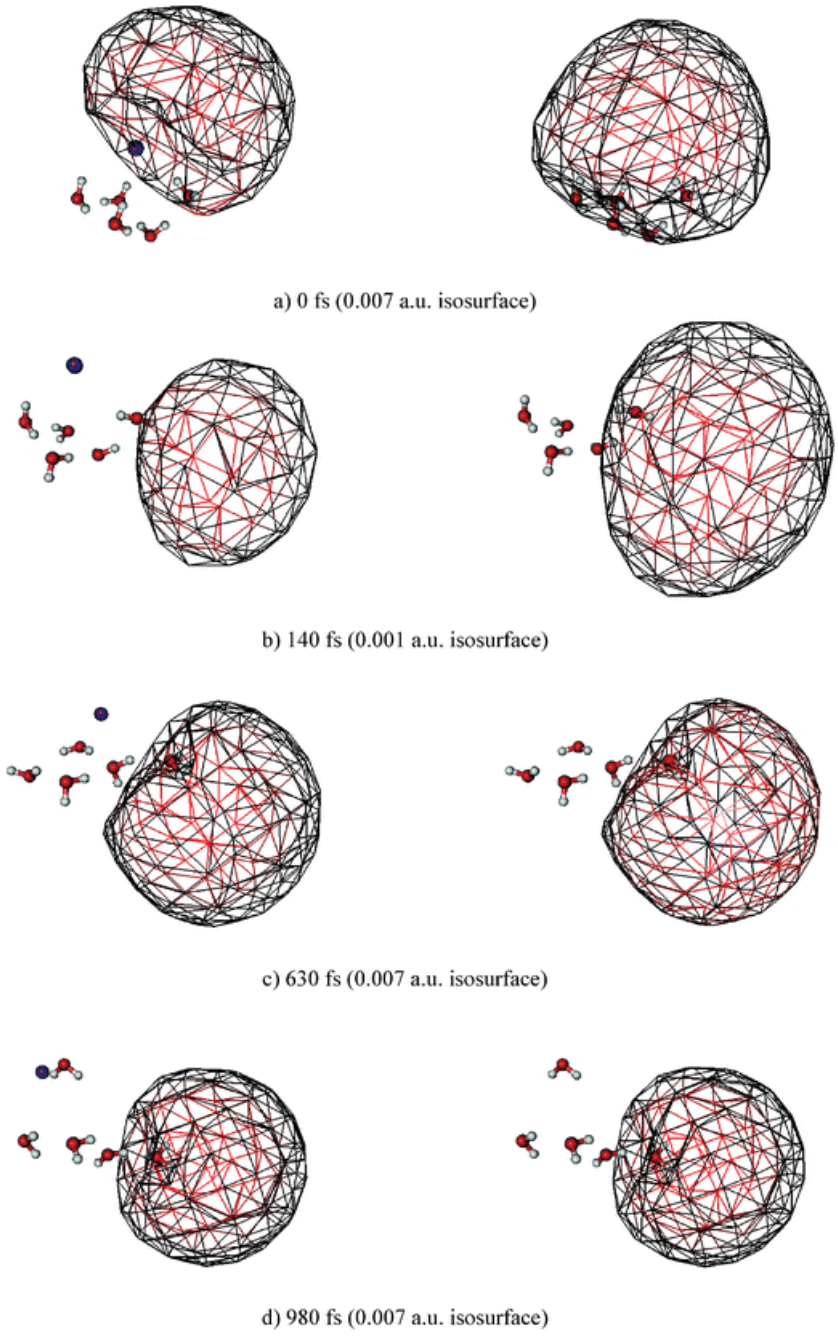


Figure 2.1. Snapshots of $[I^-(H_2O)_5]^*$ geometries and HOMO surface plots at various times along the trajectory initiated at the Y41 optimised geometry (left) along with SOMO surface plots of $(H_2O)_5^-$ at the $[I^-(H_2O)_5]^*$ water cluster geometries (right).

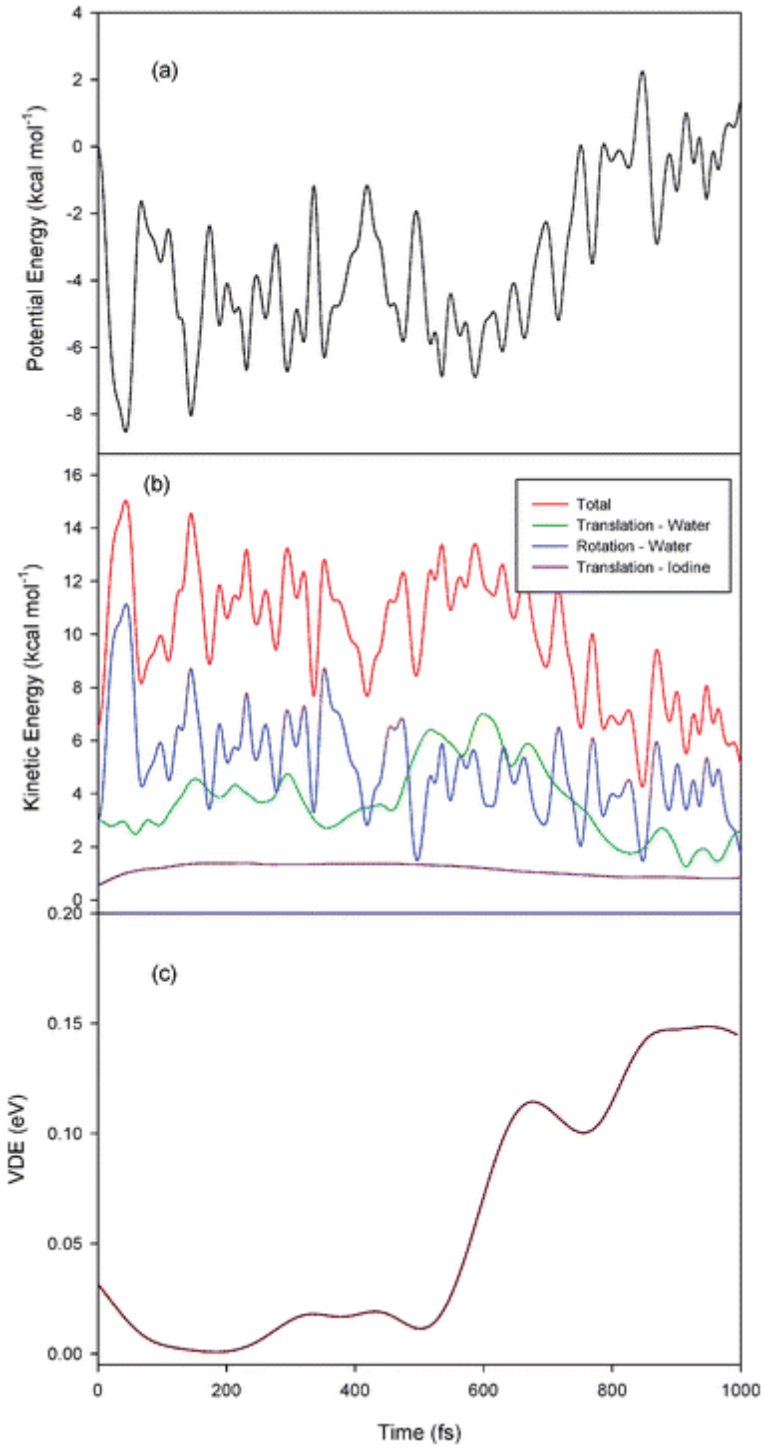


Figure 2.2. Time evolution of various properties for $[I^-(H_2O)_5]^*$ along the trajectory initiated at the Y41 optimised ground-state geometry: a) potential energy; b) kinetic energy; c) excess-electron VDE.

## 2.3. Results and Discussion

### *2.3.1. Rearrangement dynamics of excited $I^-(H_2O)_5$*

Snapshots of the simulated geometries and surface plots of the highest occupied molecular orbitals (HOMO) of $[I^-(H_2O)_5]^*$ at different times along the trajectory are shown in the left panel of Figure 2.1, while the time evolution of the cluster potential energy, kinetic energy (and its various rotational and translational components) and excited-electron VDE of the cluster are shown in Figure 2.2. Upon excitation, $I^-(H_2O)_5$ undergoes extensive rearrangement, eventually leading to the formation of a structure with a higher excited-electron VDE, a process that is accompanied by significant changes in the excited-electron distribution (*cf*. Figure 2.1).

During the first 50-100 fs of the trajectory, the water molecules originally hydrogen-bonded to iodide in the ground state of $I^-(H_2O)_5$ rotate synchronously so that the "dangling hydrogen atoms" (i.e. those not involved in water – water interactions) move away from the neutral iodine atom. This rapid initial relaxation, which is accompanied by a sharp decrease in cluster potential energy (Figure 2.2a) and increase in the rotational energy of the water molecules (Figure 2.2b), appears to be a manifestation of the repulsive nature of the excited-state potential energy surface in the vicinity of the ground-state minimum-energy geometry of $I^-(H_2O)_n$, as first reported by Vila and Jordan, who computed the potential energy profiles of ground and excited-state $I^-(H_2O)_4$ along the dihedral angle formed by the dangling hydrogen atoms and the plane of the water cluster oxygen atoms.[*76*]

Within 140 fs, the dipoles of the water molecules are oriented in different directions (Figure 2.1b), resulting in a very low total dipole moment for the water cluster moiety. At this point, the excited-electron VDE of the cluster (Figure 2.2c) has already reached a minimum value. Both the magnitude of the decrease in the excited-electron VDE (0.03 eV) and the time at which the minimum value is attained (150 fs) are in close agreement with previously reported experimental values.[*47*]

After the initial sharp increase, the rotational kinetic energy of the water molecules eventually decreases as energy is transferred to the intermolecular translational degrees of freedom of the water molecules in the cluster (Figure 2.2b). This ultimately results in major reorganisation of

the water cluster network, which changes from the Y41 structure of the ground state to a branched structure with a single water molecule connected to a linear chain of four water molecules (Figures 2.1c and 2.1d), and a concomitant increase in the cluster potential energy. In the final, relaxed structure of $[I^-(H_2O)_5]^*$, the water molecules are oriented such that the positive ends of their dipoles point in the direction of the excited-electron distribution, away from the iodine atom, resulting in a large net cluster dipole moment. Accordingly, the excited-electron VDE increases, eventually attaining a value of 0.15 eV after 1 ps. The magnitude of the increase in VDE is slightly underestimated, although still in good agreement with the experimental value of 0.226 ± 0.03 eV.[*47*]

The present simulation results agree with the consensus picture in which gradual solvent reorganisation is a key aspect of the electron stabilisation process in $[I^-(H_2O)_5]^*$.[*34-38*] The role of the iodine atom in the excited-state dynamics of $I^-(H_2O)_5$ however continues to be a matter of controversy. Various *ab initio* molecular dynamics simulations of $[I^-(H_2O)_n]^*$ have addressed the issue of iodine departure in the relaxation of $[I^-(H_2O)_n]^*$. [*34-38*] Timerghazin and Peslherbe reported an increase in the iodine – water cluster center of mass separation from 3.4 Å to 6.3 Å over 900 fs and pointed out the possible effect of iodine on the excited-electron VDE of $[I^-(H_2O)_n]^*$ as the clusters relax following photoexcitation.[*34*] Similarly, Kim and co-workers have observed the gradual increase in the distance between the iodine atom and the water molecules in their simulations of $[I^-(H_2O)_n]^*$.[*35, 38*] On the other hand, Takayanagi and Takahashi failed to observe the departure of iodine from the excited clusters in their simulations, although they acknowledged that this could be due to overestimation of the strength of the iodine–water interactions by the B3LYP/6-31(1+,3+)G* model chemistry that they employed.[*36, 37*]

The apparent discrepancies in the iodine motion observed in the different simulations reported are presumably due to the differences in simulation methodology and model chemistry employed. Previous reports tended to emphasise changes in the iodine – water cluster centre-of-mass separation in the excited state of $I^-(H_2O)_n$, but a more important issue that has not been rigorously addressed is the importance of the iodine atom in driving the rearrangement of $[I^-(H_2O)_n]^*$ and its effect on the stability of the excited electron as the clusters relax, regardless of the position of iodine. In the following sections, results of $(H_2O)_5^-$ simulations are reported that

provide a conclusive picture of the iodine effect on the $[I^-(H_2O)_n]^*$ excited electron stabilisation process.

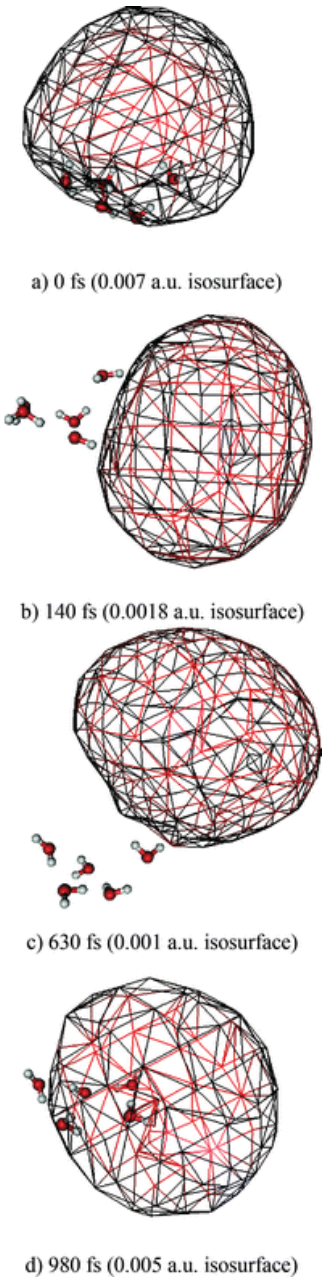


Figure 2.3. Snapshots of $(H_2O)_5^-$ geometries and SOMO surface plots at various times along the trajectory initiated at the Y41 geometry.

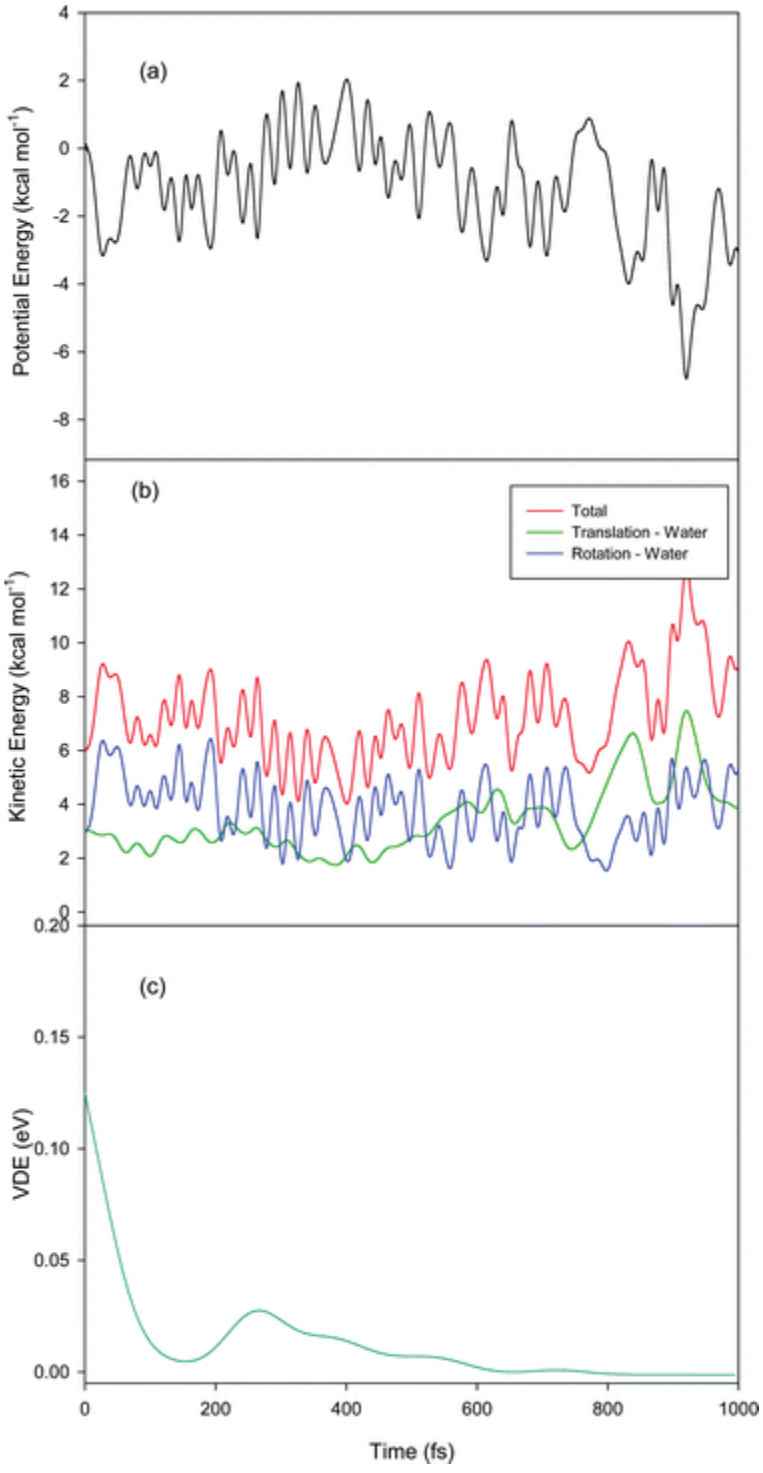


Figure 2.4. Time evolution of various properties for $(H_2O)_5^-$ along the trajectory initiated at the Y41 geometry: a) potential energy; b) kinetic energy; c) excess-electron VDE.

### *2.3.2. Rearrangement dynamics of $(H_2O)_5^-$*

Snapshots of the geometries and Singly-Occupied Molecular Orbital (SOMO) surface plots of $(H_2O)_5^-$ from the trajectory initiated at the Y41 optimised structure are displayed in Figure 2.3, while plots of the time evolution of the cluster potential energy, kinetic energy (and its various rotational and translational components) and excess-electron VDE are shown in Figure 2.4. These results suggest that $(H_2O)_5^-$, unlike $[I^-(H_2O)_5]^*$, does not undergo isomerisation from the Y41 structure to a structure with a more tightly bound excess electron. As for $[I^-(H_2O)_5]^*$, the initial dynamics is characterised by rapid synchronous rotation of the water molecules that results in a near flattening of the crown-shaped water tetramer structure within the water pentamer (Figures 2.3a and 2.3b) and a corresponding decrease in the cluster potential energy and excess-electron VDE (Figures 2.4a and 2.4c). However, the decrease in cluster potential energy is smaller in magnitude by 5 kcal $mol^{-1}$ for $(H_2O)_5^-$, compared to that for $[I^-(H_2O)_5]^*$. The water molecules continue to rotate, but in a less synchronous fashion than in the initial relaxation. In contrast with $[I^-(H_2O)_5]^*$, a cyclic water cluster structure with 5 water – water hydrogen bonds and a small excess-electron VDE is eventually formed.

The most important reason for the profound difference between the dynamics of $[I^-(H_2O)_5]^*$ and $(H_2O)_5^-$ appears to be the lack of iodine – hydrogen repulsive interactions in the latter. The iodine – hydrogen repulsion energy is roughly 5 kcal $mol^{-1}$ for $[I^-(H_2O)_5]^*$ near its initial geometry,[*77*] which is a sizeable contribution to the 15 kcal $mol^{-1}$ kinetic energy gained by $[I^-(H_2O)_5]^*$ after the initial relaxation. The additional kinetic energy gained in the initial relaxation of $[I^-(H_2O)_5]^*$ because of the more repulsive dynamics appears to overcome the water – water hydrogen bond dissociation energy, and thus allows the formation of the branched cluster structure with high excited-electron VDE. In contrast, the smaller amount of energy acquired for $(H_2O)_5^-$ results in a less dramatic rearrangement. As noted previously by Herbert and Head-Gordon, the water cluster configurations that bind an excess electron most tightly generally have higher potential energies.[*75*] While the warmer $[I^-(H_2O)_5]^*$ would possess sufficient kinetic energy to sample these high potential energy configurations, the cooler $(H_2O)_5^-$ would not, resulting in smaller excess-electron VDEs for the latter.

In order to further understand the role of the neutral iodine atom on the long-term dynamics

leading to the stabilisation of the excited electron in $[I^-(H_2O)_5]^*$, we turn our attention to the trajectory of $(H_2O)_5^-$ initiated with the structure obtained by removing the iodine atom from the configuration of $[I^-(H_2O)_5]^*$ after the initial fast (50 fs) relaxation. By that time, the hydrogen atoms initially forming hydrogen bonds with iodide have moved away from the neutral iodine atom, and the kinetic energy of the cluster has reached its maximum value. Snapshots of the cluster geometries and SOMO surface plots at different times along the $(H_2O)_5^-$ trajectory (Figure 2.5) show that the water cluster eventually rearranges to a linear structure, similar to the final water cluster geometry in $[I^-(H_2O)_5]^*$ at 1 ps. Plots of the time evolution of the cluster potential energy, kinetic energy (and its various rotational and translational components) and excess-electron VDE are shown in Figure 2.6. The potential and kinetic energy profiles (Figures 2.6a and 2.6b) resemble closely those of $[I^-(H_2O)_5]^*$ (Figures 2.2a and 2.2b), at least until 600 fs. The potential energy gradually rises, accompanied by a decrease in the rotational kinetic energy of the water molecules, which is increasingly transferred to the translational modes of the water molecules. Eventually, this leads to the formation of a linear water cluster structure with high excess-electron VDE, in a process analogous to that occurring in $[I^-(H_2O)_5]^*$. The iodine atom therefore appears to be important primarily for initiating the rearrangement process through the rapid initial relaxation that results from the iodine – hydrogen repulsive interactions in the Franck-Condon geometry. Once the amount of kinetic energy acquired is sufficiently high, the cluster can rearrange to a higher energy, high excess-electron VDE structure, regardless of the presence of the iodine atom.

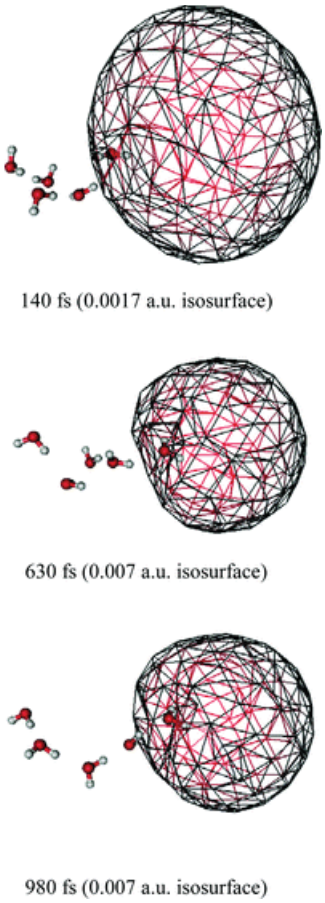


Figure 2.5. Snapshots of $(H_2O)_5^-$ geometries and SOMO surface plots at various times along the trajectory initiated at the $[I^-(H_2O)_5]^*$ water cluster geometry after 50 fs of relaxation.

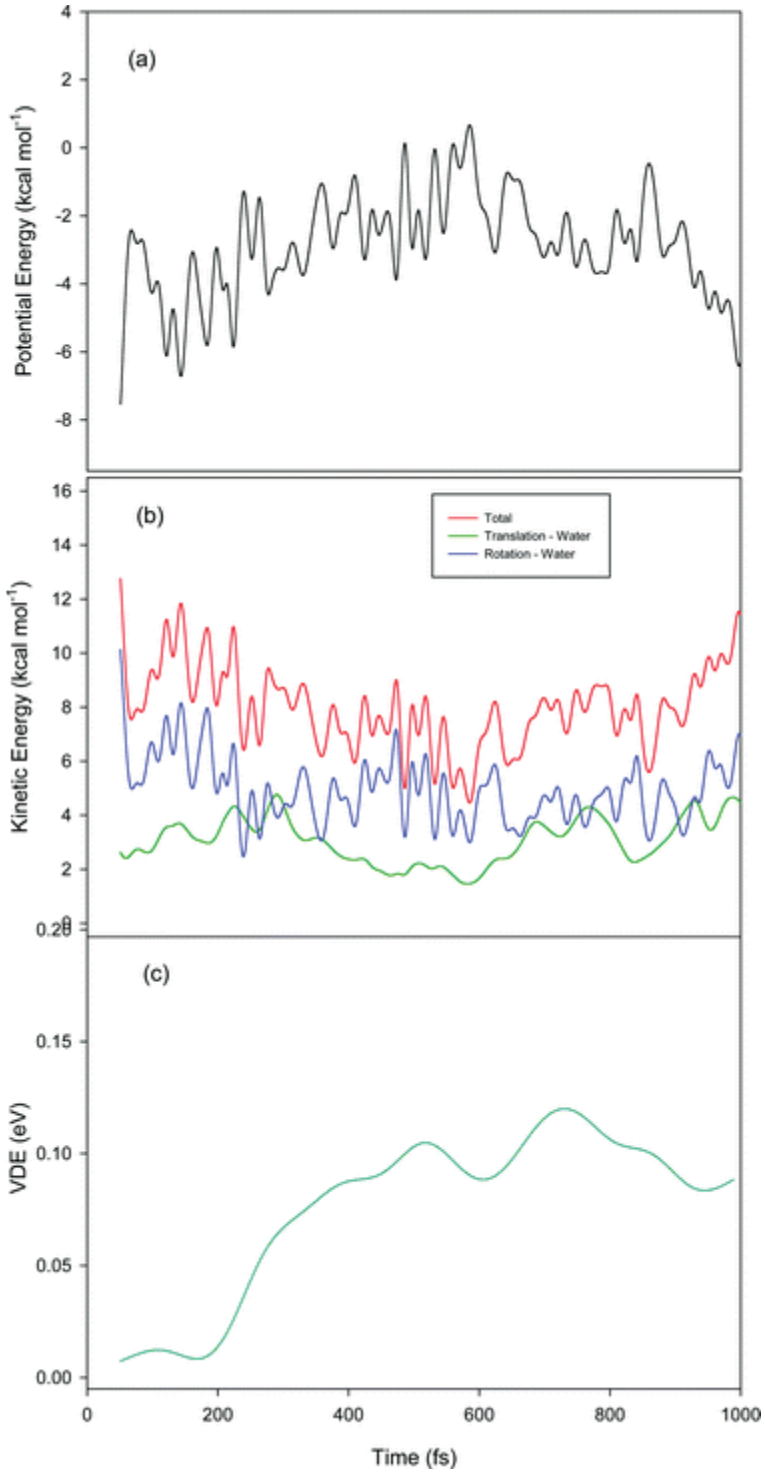


Figure 2.6. Time evolution of various properties for $(H_2O)_5^-$ along the trajectory initiated at the $[I^-(H_2O)_5]$* water cluster geometry after 50 fs of relaxation: a) potential energy; b) kinetic energy; c) excess-electron VDE.

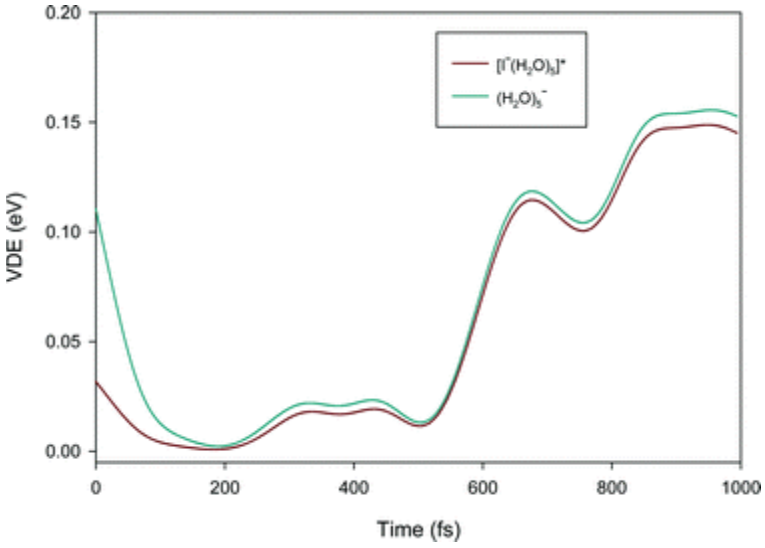


Figure 2.7. Comparison of excess-electron VDEs of $[I^-(H_2O)_5]^*$ and $(H_2O)_5^-$ at the $[I^-(H_2O)_5]^*$ water cluster geometries.

### *2.3.3. Iodine effect on the excited electron of $[I^-(H_2O)_5]^*$*

Figure 2.7 displays the excited-electron and excess-electron VDE of $[I^-(H_2O)_5]^*$ and $(H_2O)_5^-$, respectively, computed at the water cluster configurations of $[I^-(H_2O)_5]^*$, while the corresponding HOMO and SOMO plots for selected $[I^-(H_2O)_5]^*$ and $(H_2O)_5^-$ structures, respectively, are shown in Figure 2.1. At early times (0-200 fs), when the water cluster geometry is close to that of ground-state $I^-(H_2O)_5$, the excess-electron VDE of $(H_2O)_5^-$ is higher than that of $[I^-(H_2O)_5]^*$ by 0.08 eV. Chen and Sheu rationalised this observation by noting that, due to the fact that the excited electron is essentially excluded from the region occupied by the electrons of the neutral iodine atom, the diffuse excited electron of $[I^-(H_2O)_5]^*$ is generally located further away from the water cluster moiety than in $(H_2O)_5^-$, resulting in a lower excited-electron VDE.[*21, 32, 43*] Comparison of the HOMO plots for $[I^-(H_2O)_5]^*$ and SOMO plots for $(H_2O)_5^-$ (Figure 2.1a) confirms that there is indeed a shift of electron density further away from the water

cluster moiety in $[I^-(H_2O)_5]^*$ compared to $(H_2O)_5^-$ at the initial Y41 geometry of $I^-(H_2O)_5$. As mentioned earlier, Chen and Sheu further hypothesised that the excited-electron VDE increase observed in the femtosecond photoelectron spectroscopy experiments of Neumark and co-workers[*24*] is due to the ejection of iodine from $I^-(H_2O)_5$ in the excited state.[*32, 33*]

The results of the present simulations of $[I^-(H_2O)_5]^*$ suggest that the iodine atom remains within the vicinity of the water cluster, at least for the first 1 ps following photoexcitation. While the excess-electron VDE of $(H_2O)_5^-$ is initially much higher than the excited-electron VDE of $[I^-(H_2O)_5]^*$, as described in Section IIIA, rapid rotation of the water molecules drive the distribution of the excited electron away from the neutral iodine atom in the $I^-(H_2O)_5$ excited state (Figure 2.1b). Within 200 fs, the excited/excess-electron distributions and VDEs of $[I^-(H_2O)_5]^*$ and $(H_2O)_5^-$ become essentially identical, indicating that the destabilising effect of the iodine atom on the excited electron is no longer present, and the cluster could be viewed as a water cluster anion with an additional, spectator, iodine atom.

Nevertheless, the excited electron is not yet fully stabilised, contrary to the hypothesis of Chen and Sheu,[*32, 33*] since the rapid initial water rotations result in a water cluster moiety with a very small net dipole moment. The present simulations suggest that the subsequent experimentally-observed increase in the excited-electron VDE of $[I^-(H_2O)_5]^*$ can be attributed almost entirely to the rearrangement of the water cluster moiety to a branched structure that binds the excited electron more tightly. Therefore, the *geometry of the water cluster essentially determines the VDE of the excited electron in* $[I^-(H_2O)_5]^*$, as long as the iodine atom is not located between the water cluster and the excited-electron distribution, as is the case in the Franck-Condon region. As shown earlier, however, the *rearrangement process of the water cluster moiety itself is driven by the kinetic energy acquired by the cluster because of the repulsive interactions between the neutral iodine atom and the hydrogen atoms of the water cluster in the Franck-Condon geometry*. Nevertheless, the modulation of the experimental VDEs determined by femtosecond photoelectron spectroscopy is determined almost exclusively by the structural rearrangement of the water cluster moiety in $[I^-(H_2O)_n]^*$, which is driven by the initial presence of iodine.

## 2.4. Concluding Remarks

In this work, *ab initio* molecular dynamics simulations were performed to characterise the cluster relaxation/rearrangement dynamics of $[I^-(H_2O)_5]^*$ and $(H_2O)_5^-$, unravelling profound differences between the two systems. On one hand, $[I^-(H_2O)_5]^*$ undergoes significant rearrangement from the initial ground-state geometry, which ultimately leads to the formation of a branched water cluster that binds the excited electron much more tightly. On the other hand, $(H_2O)_5^-$ undergoes much less drastic rearrangement from the same geometry, ultimately resulting in a cyclic water cluster with a very weakly bound excess electron. The sharp contrast in the dynamics of $[I^-(H_2O)_5]^*$ and $(H_2O)_5^-$ demonstrates unambiguously that the iodine atom plays a critical role in the relaxation process in $[I^-(H_2O)_5]^*$. Despite the great importance of iodine in driving the relaxation process leading to the excited electron stabilisation in $[I^-(H_2O)_5]^*$, its effect on the excited-electron VDE appears negligible except in the short period of time (< 200 fs) following photoexcitation. Therefore, femtosecond photoelectron spectroscopy experiments may probe mainly the resulting solvent cluster reorganisation aspects of the electron stabilisation process. It remains to be explored whether this statement regarding femtosecond photoelectron spectroscopy experiments would still hold for other iodide-polar solvent clusters.

# 3. Photoexcitation and Charge-Transfer-to-Solvent Relaxation Dynamics of the $I^-(CH_3CN)$ Complex

**Published As:**

Chun C. Mak, Qadir K. Timerghazin and Gilles H. Peslherbe, *The Journal of Physical Chemistry A*, 2013, 117:7595-7605

## Abstract

Photoexcitation of iodide-acetonitrile clusters, $I^-(CH_3CN)_n$, to the charge-transfer-to-solvent (CTTS) state and subsequent cluster relaxation could result in the possible formation of cluster analogues of the bulk solvated electron. In this work, the relaxation process of the CTTS excited iodide-acetonitrile binary complex, $[I^-(CH_3CN)]^*$, is investigated using rigorous *ab initio* quantum chemistry calculations and direct-dynamics simulations to gain insight into the role and motion of iodine and acetonitrile in the relaxation of CTTS excited $I^-(CH_3CN)_n$. Computed potential energy curves and profiles of the excited electron vertical detachment energy for $[I^-(CH_3CN)]^*$ along the iodine-acetonitrile distance coordinate reveal for the first time significant dispersion effects between iodine and the excited electron, which can have a significant stabilising effect on the latter. Results of direct-dynamics simulations demonstrate that $[I^-(CH_3CN)]^*$ undergoes dissociation to iodine and acetonitrile fragments, resulting in decreased stability of the excited electron. The present work provides strong evidence of solvent translational motion and iodine ejection as key aspects of the early-time relaxation of CTTS excited $I^-(CH_3CN)_n$ that can also have a substantial impact on the subsequent electron solvation processes, and further demonstrates that intricate details of the relaxation process of CTTS excited iodide-polar solvent molecule clusters make it heavily solvent-dependent.

### 3.1. Introduction

** Charge-transfer-to-solvent (CTTS) excited states constitute one of the most important features of the photochemistry of inorganic anions in polar solvent media.[*16*] Excitation to CTTS states involves the transfer of an excess electron from the anion to an orbital bound by the collective electric field of several solvent molecules. The bulk CTTS excited state is believed to be very similar in nature to the solvated electron and, in fact, the latter can be easily produced from the former.[*39, 78, 79*] The nature of the CTTS states has been a topic of long-standing interest from both experimentalists and theoreticians,[*16*] and the ultra-fast excited electron and solvent dynamics following CTTS excitation has attracted considerable attention.[*79-83*] Whereas the gas-phase analogues of the solvated electron, *i.e.* small solvent cluster anions, have been known for a few decades,[*84*] the CTTS precursor states in finite anion-solvent clusters were first observed much more recently.[*85*] Interestingly, just before the first experimental observations of CTTS states in clusters were reported,[*18-20*] Combariza *et al.* speculated, based on quantum chemistry calculations,[*86*] that CTTS states might potentially be observed only for very large halide-solvent clusters. However, Johnson and co-workers reported experimental observations of bound excited states just below the photodetachment threshold for a number of clusters formed by iodide and a few polar solvent molecules, including acetone, acetonitrile and water: $I^-(CH_3CN)_{1\text{-}2}$, $I^-(CH_3COCH_3)$ and $I^-(H_2O)_{1\text{-}4}$.[*18-20*] By analogy to the bulk situation, where the relaxation of CTTS states leads to solvated electrons, the relaxation of the CTTS-precursor states in clusters was found to produce solvent cluster anions with high yields.[*18, 19*]

The relaxation of iodide-polar solvent clusters excited to the CTTS state, $[I^-(Solv)_n]^*$, has attracted considerable interest since the detailed molecular mechanism directly reflects the role of individual solvent molecules in the electron solvation process. In a series of femtosecond photoelectron spectroscopy experiments, Neumark and co-workers have investigated the relaxation of $[I^-(Solv)_n]^*$ (Solv = $H_2O$, $NH_3$, $CH_3OH$, $CH_3CH_2OH$ and $CH_3CN$), revealing the intriguing influence of the type of solvent on the electron solvation processes occurring during $[I^-(Solv)_n]^*$ relaxation.[*24-29, 46-48*] Complementary theoretical work[*21, 32-38, 54, 55, 76, 87*] has primarily focused on the electronic properties and dynamics of $[I^-(H_2O)_n]^*$ due to the importance of water as nature's most abundant and ubiquitous solvent, but recently, preliminary *ab initio* molecular dynamics simulations of $[I^-(CH_3OH)_n]^*$ have offered some important

insights into the pronounced solvent dependence of the relaxation mechanism of $[I^-(Solv)_n]^*$.[*88*] While it has been shown unequivocally that $[I^-(H_2O)_n]^*$ undergoes dramatic reorganisation of the water cluster moiety initiated by repulsive iodine-hydrogen interactions that leads ultimately to the stabilisation of the excited electron,[*87*] $[I^-(CH_3OH)_n]^*$ relaxation on the other hand, which involves a much more complicated modulation of the excited electron stability, appears to involve multiple pathways characterised by dissociation to $I^\bullet$ and $(CH_3OH)_n^-$, and fragmentation of the solvent cluster moiety. These results highlight the central role of solvent-solvent and electron-solvent interactions in the electron solvation processes occurring in $[I^-(Solv)_n]^*$ and provide a rational explanation for the pronounced effect of solvent type on the nature of $[I^-(Solv)_n]^*$ relaxation pathways; more limited hydrogen-bonding in methanol clusters relative to water clusters facilitates fragmentation in $[I^-(CH_3OH)_n]^*$, thereby reducing the propensity for the excited electron to be trapped and stabilised in the solvent cluster relative to $[I^-(H_2O)_n]^*$.

While extensive experimental and theoretical work on the relaxation of $[I^-(H_2O)_n]^*$ and $[I^-(CH_3OH)_n]^*$ have led to important insights into the molecular basis of solvent-dependent electron solvation pathways in $[I^-(Solv)_n]^*$, $[I^-(CH_3CN)_n]^*$ have also attracted interest as they offer the opportunity to investigate the dynamics of a more "internalised" electron at the molecular level.[*29*] $I^-(CH_3CN)_n$ are believed to adopt "interior" solvation states,[*89, 90*] in contrast to $I^-(H_2O)_n$ and $I^-(CH_3OH)_n$, in which iodide is primarily located at the cluster surface,[*91-96*] and as such, the excited electron in $[I^-(CH_3CN)_n]^*$ is also expected to be internalised, at least initially. Femtosecond photoelectron spectroscopy experiments performed on $[I^-(CH_3CN)_n]^*$ by Neumark and co-workers indicate that the excited electron vertical detachment energy (VDE) for $[I^-(CH_3CN)_n]^*$, which reflects the stability of the excited electron, decreases over several hundred femtoseconds by 0.10 to 0.35 eV before subsequently increasing by 0.30 to 0.45 eV over several picoseconds.[*29*] Based on limited earlier molecular dynamics simulations employing density-functional theory,[*97*] the initial drop in the excited electron VDE was attributed to an expansion of the cavity occupied by the excited electron and the I atom formed in the excitation process, combined with possible localisation of the excited electron on one or two acetonitrile molecules. The subsequent increase in the excited electron VDE could be attributed to contraction of the solvent cavity, along with possible iodine ejection, perhaps leading to the formation of an internally trapped electron. The proposed pathway remains

speculative, however, and no conclusive insights into the detailed molecular motions involved in the relaxation and electron solvation process of $[I^-(CH_3CN)_n]^*$ have been obtained to date.

In this respect, $I^-(CH_3CN)_n$ (n=1) lends itself as the simplest case for detailed computational studies of the photoexcitation process and CTTS excited state dynamics of $I^-(CH_3CN)_n$, and in fact, recent photoelectron spectroscopy experiments performed on $I^-(CH_3CN)$ have highlighted the need for an in depth understanding of the dynamics and electron molecule interactions involved in the process of electron detachment through CTTS states.[*98*] The small size and high symmetry of this binary complex also allow quantum chemistry calculations at relatively high levels of theory, which are very important for benchmarking various theoretical procedures that can be used for large-scale molecular dynamics simulations of larger $[I^-CH_3CN)_n]^*$ clusters. In addition, with only one acetonitrile molecule, which alone possesses a sufficient dipole moment to trap an excess electron in a dipole-bound state, $[I^-(CH_3CN)]^*$ presents a unique opportunity to examine by itself the solvent molecular motion that is of paramount importance in the electron transfer and solvation dynamics of iodide-polar solvent molecule clusters. In fact, $(CH_3CN)^-$, the final product produced upon CTTS excitation of $I^-(CH_3CN)$,[*19*] is among the smallest systems with an excess electron trapped in a dipole-bound state, *i.e.* one of the smallest cluster precursors of the solvated electron.

** In the present article, we report high-level quantum chemistry calculations and *ab initio* molecular dynamics simulations of the CTTS state of the $I^-(CH_3CN)$ binary complex. The nature of the electronic transitions involved and various components of the excitation energy are revisited in detail, and the role of spin-orbit coupling in the CTTS state of iodide-solvent clusters is examined for the first time. The potential energy profiles for the excited and ionised states are characterised using rigorous quantum chemistry calculations and are used to validate an inexpensive yet reliable computational procedure, which is subsequently used in realistic first-principles excited-state molecular dynamics simulations of $[I^-(CH_3CN)]^*$ relaxation. The outline of this article is as follows: the computational methods are outlined in section 2, the static picture of the photoionisation and photoexcitation of $I^-(CH_3CN)$ is presented in section 3, the potential energy profiles of the excited and ionised states are discussed in section 4, the dynamics of the excited state in section 5, and concluding remarks follow in section 6.

### 3.2. Computational Methods

** The structure of the $I^-(CH_3CN)$ complex was optimised and its harmonic vibrational frequencies were calculated using second-order Møller-Plesset (MP2) perturbation theory.[*99*] The Dunning's correlation-consistent polarised double-zeta basis set augmented with diffuse functions (aug-cc-pVDZ) was used for the hydrogen, carbon and nitrogen atoms,[*100*] and the relativistic large-core ECP46MDF pseudopotential and corresponding basis set by Stoll *et al*.[*101*] were used for the iodine atom. This basis set combination will be further referred to simply as the DZ basis set for brevity.

** The excited and ionised states of the $I^-(CH_3CN)$ complex were calculated with multi-reference second-order perturbation theory (CASPT2)[*63*] with the state-averaged complete active space self-consistent field (CASSCF)[*61, 62*] reference wavefunction. CASSCF calculations used a (6,4) active space consisting of the three occupied 5*p*-orbitals of iodine and the lowest unoccupied orbital, resulting in 10 singlet configuration state functions (CSF) and 6 triplet CSFs. A total of 10 states (4 singlet states, 3 triplet states and 3 ionised states) were included in the state-averaging. For excited-state calculations the DZ basis set was further augmented by 8 diffuse *sp*-functions generated in an even-tempered manner from the average of the outmost *s*- and *p*-functions of the aug-cc-pVDZ basis set using the geometric progression ratio of 3.2,[*102*] resulting in an exponent of $1.9414 \times 10^{-6}$ au for the most diffuse *sp*-basis function. The augmented DZ basis set will be simply referred to as DZ+. In most calculations, the additional diffuse *sp*-functions were centred on the methyl group carbon atom. In a number of calculations, the "floating centre" technique[*103*] was used, with the position of the diffuse centre optimised with CASPT2 using numerical gradients.

** Spin-orbit coupling calculations were performed with the interacting states method, using the effective one-electron spin-orbit (SO) operator included in the relativistic effective core potential of the iodine atom.[*101*] The CASPT2 energies of the lowest singlet and triplet electronic states were corrected on the basis of spin-orbit coupling (SOC) elements calculated using the CASSCF wavefunction. This approach is referred to as CASPT2-SOC.

In order to properly describe the excess-electron VDEs of dipole-bound systems such as $[I^-(CH_3CN)]^*$ a higher order treatment of electron correlation effects is required,[*102, 104-107*] and

as such, the excited electron VDEs of $[I^-(CH_3CN)]^*$ were computed with the coupled cluster method with single, double and non-iterative triple excitations (CCSD(T)) for open-shell systems.[*108, 109*] In these calculations, the aug-cc-pVTZ basis set[*100*] was used for carbon, hydrogen and nitrogen, while the ECP46MWB pseudopotential[*69*] and the corresponding triple-zeta basis set were used for iodine.[*110*] In addition, 9 sets of diffuse functions were added to the carbon atom of the methyl group to describe the excited electron.[*102*] The exponents were generated in an even-tempered manner with a progression ratio of 3.2, beginning with the average of the outermost *sp* exponents of the aug-cc-pVTZ basis set. The four tightest sets of functions contained functions of *s*, *p* and *d* symmetry, while the remaining sets of functions were of *s* and *p* symmetry, and the smallest exponent was $1.5 \times 10^{-6}$. This basis set will hereafter be denoted TZ+.

Beginning with our early work on $I^-(H_2O)_n$ (n=3),[*34*] first-principles excited-state molecular dynamics simulations have been used extensively to elucidate the CTTS excited-state relaxation of iodide-solvent clusters,[*35-38, 87, 88, 97*] as they paint a real-time dynamic picture that can be connected with state-of-the-art ultra-fast photoelectron spectroscopy experiments. In this approach, the energy and atomic forces are calculated "on the fly" during the propagation of the atomic equations of motion by *ab initio* methods.[*111*] Unfortunately, molecular dynamics simulations employing high-level *ab initio* methods such as CASPT2 with large basis sets, which is used to compute the potential energy curves, are not yet feasible within the limits of current computational resources. Large-scale first-principles excited-state molecular dynamics simulations require a fast and robust model chemistry for which analytic energy gradients are readily available for efficient calculation of the forces.

In order to develop a suitable model chemistry for use in *ab initio* molecular dynamics simulations of $[I^-(CH_3CN)]^*$, two approaches were employed. The first approach was based on the triplet approximation for the calculation of CTTS states first employed by Bradforth and Jungwirth.[*23*] The triplet CTTS states are the lowest states of that multiplicity, and as such, single reference methods such as restricted open-shell Hartree Fock (ROHF) theory and MP2 theory are appropriate for calculating the energies and forces of $I^-(CH_3CN)$. As will be shown below, the triplet states approximate the actual spin-orbit excited states of $[I^-(CH_3CN)]^*$ as well as the singlet states. In these calculations, the 6-31++G(d,p) basis set[*66-68*] was used for

carbon, hydrogen and nitrogen, while the effective core potential and corresponding valence basis set of Kurtz and co-workers were used for iodine.[*112, 113*] This basis set was augmented with four *s* diffuse functions (exponents 0.012, 0.004, 0.00133 and 0.000444) on hydrogen and two sets of *sp* diffuse functions (exponents 0.008667 and 0.0009630) on iodine. This basis set will be referred to as Mid+. The second approach for modelling the excited state of [$I^-$ ($CH_3CN$)]* involved the use of the configuration interaction with single excitations (CIS) [*114*] method. ** An economic double-zeta basis set referred to as Min+ was developed for use in these calculations. The Min+ basis set is constructed from the small double-zeta quality basis set of Mitin *et al*.[*115*] augmented by a diffuse *s*-function for hydrogen and diffuse *sp*-functions for carbon and nitrogen.[*67*] For iodine, the large-core effective core potential and corresponding basis set by Stevens *et al.*,[*116*] augmented by one diffuse *sp* shell,[*117*] was employed. To accommodate the dipole-bound electron, the basis set was further augmented by three additional diffuse *sp*-shells centred on the carbon atom of the methyl group and two *sp*-shells on the iodine atom. The diffuse exponents were generated from the outmost diffuse functions of the main basis set in an even-tempered manner using a geometric progression factor of 5.0.

** Initial conditions for the excited-state molecular dynamics simulations were generated using the thermal Monte-Carlo sampling technique[*118*] implemented in the VENUS reaction dynamics program[*119*] on the ground-state $I^-(CH_3CN)$ HF/Min+ potential energy surface for T = 150 K. While there is a wide uncertainty about the actual temperature of $I^-(CH_3CN)_n$ clusters generated in experiments, this temperature estimate was obtained using Klots theory of the evaporative ensemble.[*74*] 128 constant-energy trajectories were then propagated using the dynamic reaction coordinate technique[*120*] employing the velocity Verlet algorithm,[*111*] as implemented in the GAMESS package,[*121*] with a time-step of 0.3 fs for up to 2 ps.

In order to probe the effect of the relaxation process on the stability of the excited electron in [$I^-$ ($CH_3CN$)]*, the excited electron VDEs of the complex at the Franck-Condon geometry and at the end of the 2 ps relaxation process were computed with the CCSD(T)/TZ+ model chemistry as described above.

All CASSCF, CASPT2 and CCSD(T) calculations were performed with the MOLPRO package,[*71*] HF and MP2 calculations were performed with the MOLPRO and GAMESS[*121*] packages, and all CIS calculations were performed with GAMESS.

### 3.3. Photoexcitation and Photoionisation of $I^-(CH_3CN)$

** Figure 3.1 shows a general energetic scheme of photoionisation and photoexcitation for iodide in the gas phase and in clusters. Free $I^-$ does not possess bound excited states, and absorption of a photon with sufficient energy to overcome the ionisation potential (IP) simply leads to photodetachment of the excess electron. Due to strong electrostatic and polarisation interactions, complexation with one or more polar solvent molecules significantly stabilises the ion (typically with anion binding energies $D_{anion}$ larger than 10 kcal/mol or ~0.5 eV), whereas the stabilisation by solvent molecules of the neutral iodine atom which forms upon photodetachment is rather small. This differential solvation leads to the well-known increase of the ionisation potential of the solvated anion with an increasing number of solvent molecules in the cluster. If the solvent cluster possesses a dipole moment high enough ($\mu \geq 2.5$ D)[*84*] to bind the excess electron ejected from $I^-$ upon photoexcitation, then a dipole-bound CTTS-precursor excited state can be formed, slightly lower in energy than the photodetachment limit (Figure 3.1). Thus, the CTTS excitation energy is lower than the IP of iodide in the cluster ($IP_{cluster}$) by the excited electron VDE. In small clusters this value is rather small (tens of meV), but the stabilisation of the excited electron increases dramatically with cluster size and the CTTS excitation energy can be significantly lower than the IP in larger clusters. Thus, in order to quantitatively reproduce experimentally observed CTTS excitation energies, one must be able to reproduce various energy components, including the ionisation potential of free iodide, the binding energies of iodide and neutral iodine to the solvent cluster and, finally, the stabilisation energy of the dipole-bound excited/excess electron to the solvent molecule(s).

As immediately obvious from Figure 3.2**,** the excited electron distribution in the photoexcited iodide-acetonitrile complex is very similar to the excess electron distribution in the dipole-bound acetonitrile anion, in agreement with previous studies.[*21, 22*]

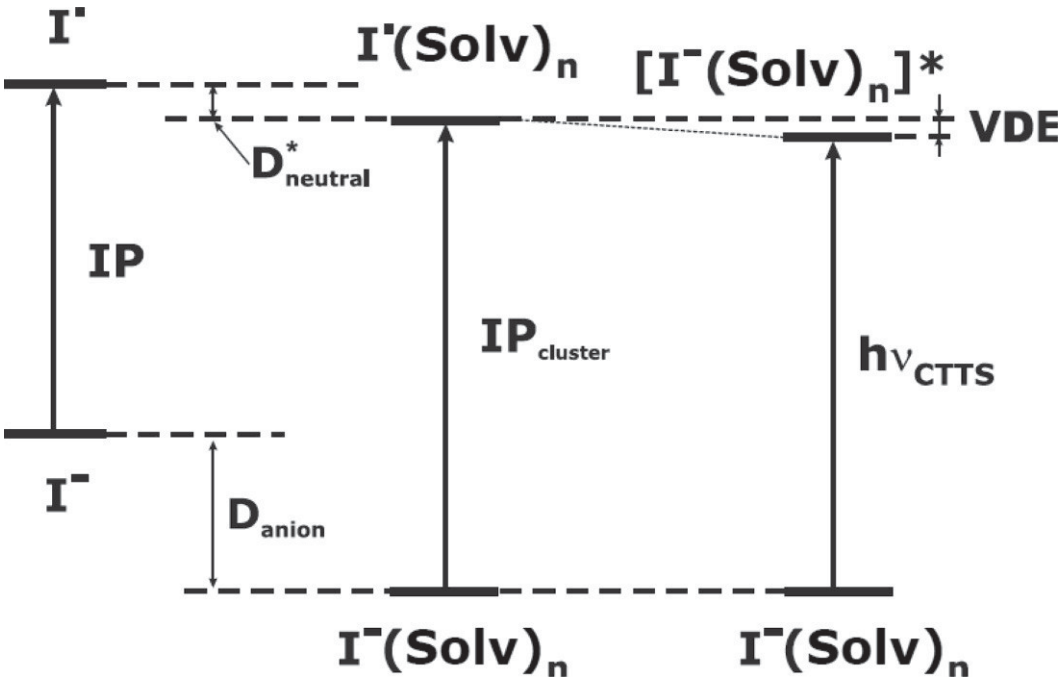


** Figure 3.1. Photoionisation and photoexcitation of free iodide and iodide-solvent clusters. $D^*_{neutral}$ is the vertical detachment energy of the $I^{\bullet}(Solv)_n$ cluster in the equilibrium geometry of the $I^-(Solv)_n$ cluster

** Similarly to other intermolecular complexes formed by $^2P$ halogen atoms,[*122, 123*] the interaction of the iodine atom formed upon photoionisation/excitation of $I^-(CH_3CN)$ with the acetonitrile molecule gives rise to two possible electronic states that differ by the orientation of the half-filled 5*p*-orbital relative to the $C_3$ axis of the $CH_3CN$ molecule. In the lower, doubly-degenerate $1^2E$ state, the half-filled *p*-orbital of iodine is perpendicular to the $C_3$ axis and, in the$1^2A$ state, the half-filled *p*-orbital is aligned along the symmetry axis (the singlet CTTS excited states are $1^1E$ and $2^1A_1$, respectively). However, since the interaction of the iodine atom with the acetonitrile molecule is relatively weak and significantly smaller than the spin-orbit coupling constant of the free iodine atom (0.94 eV),[*124*] a typical Hund case (c) situation arises, and the value of the total spin is not a good quantum number to describe the ionised and excited states of iodide-solvent clusters. The spin-orbit mixing of the $1^1E$ and $2^1A_1$ states of the ionised complex gives rise to three spin-orbit states, labeled *I*, *II* and *III* (*X* is used for the ground state of

the $I^-(CH_3CN)$ complex, which is essentially the $1^1A_1$ state); the first two states correlate with the $^2P_{3/2}$ limit of the free iodine atom, whereas the third one correlates with the $^2P_{1/2}$ limit.[*122, 123*] For a complex with cylindrical symmetry, such as $Na^{+\cdots}I^{\bullet}$ or $I^{\bullet}(CH_3CN)$, one of the doubly degenerate states retains its character, whereas the other two spin-orbit states have mixed $A_1$ and $E$ character. The spin quantum number is not a good quantum number for weak intermolecular complexes formed by iodine, so the singlet and triplet CTTS excited states of iodide-solvent clusters are strongly mixed. Therefore, the lowest triplet excited state(s) can be as good an approximation to the actual (spin-orbit) excited CTTS states as the first singlet state(s), further validating the "triplet approximation" approach employed by Bradforth and Jungwirth to model the CTTS states in water clusters and in the bulk.[*23*]

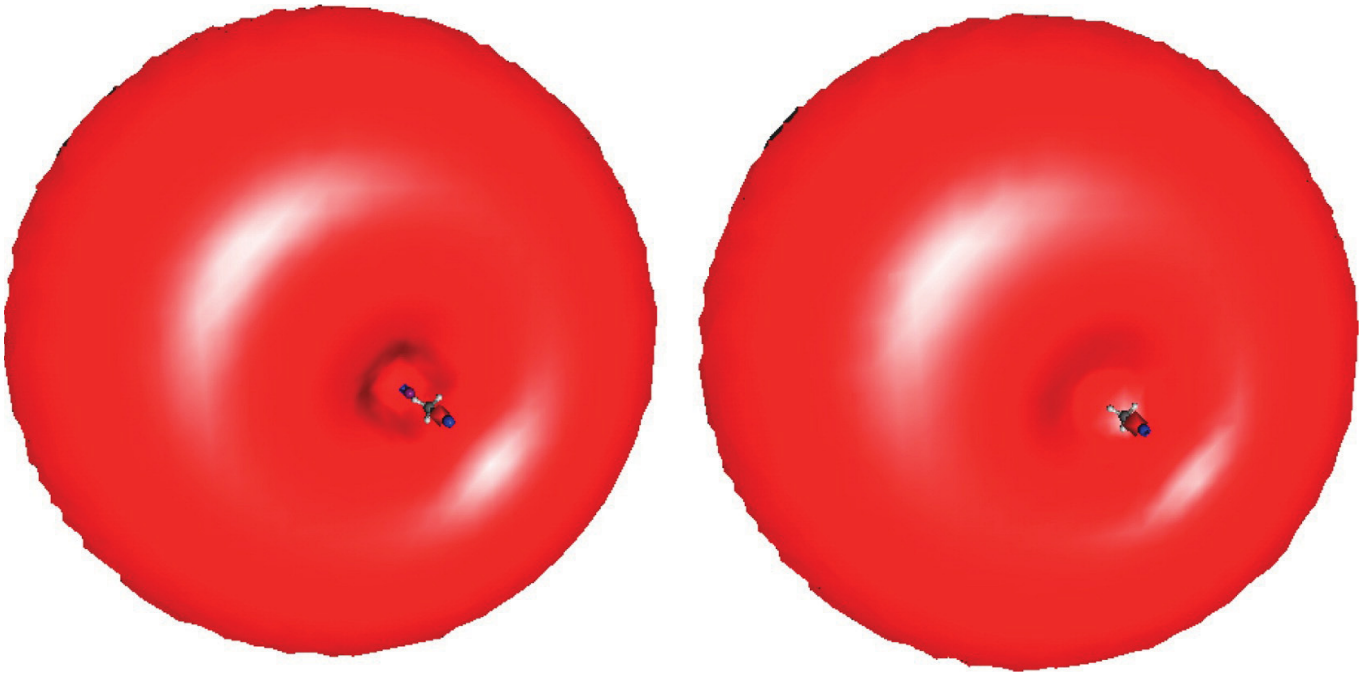

Figure 3.2. Distribution of the excited/excess electron in the excited iodide-acetonitrile complex and the dipole-bound acetonitrile anion (CASPT2/DZ+ natural orbitals, isosurfaces both enclose 45% of electron density)

Table 3.1. Calculated and experimental binding energies and other properties relevant to the photoexcitation and photoionisation of the $I^-(CH_3CN)$ complex[a]

| | ** CASPT2/DZ+ | ** CASPT2-SOC/DZ+ | CCSD(T)/TZ+ | ** Expt. |
|---|---|---|---|---|
| **$D_e[I^-(CH_3CN)]$** | 0.511 | 0.511 | 0.495 | |
| **$D_0[I^-(CH_3CN)]$** | 0.509 [b] | 0.509 [b] | 0.493[b] | 0.494 ± 0.040 [c] |
| **$D_e^*[I^\bullet(CH_3CN)]$** | 0.032 ($1^2E$)<br>0.021 ($2^2A$) | 0.032 (I)<br>0.025 (II)<br>0.026 (III) | 0.051 ($1^2E$) | |
| **VDE $[CH_3CN^-]$** | $11.0 \times 10^{-3}$ | | $14.0 \times 10^{-3}$ | $(11 - 18) \times 10^{-3}$ [d] |
| **IP($I^-$)** | 2.979 | 2.674 | 3.17 | 3.059 [e] |
| **IP$[I^-(CH_3CN)]$** | 3.470 ($1^1A_1 \rightarrow 1^2E$)<br>3.480 ($1^1A_1 \rightarrow 1^2A_1$) | 3.165 (X→I)<br>3.171 (X→II)<br>4.084 (X→III) | 3.67 ($1^1A_1 \rightarrow 1^2E$) | 3.54, 4.48 |
| **$E_{CTTS}$** | 3.463 ($1^1A_1 \rightarrow 1^1E$)<br>3.474 ($1^1A_1 \rightarrow 2^1A_1$) | 3.158 (X→I)<br>3.164 (X→II)<br>4.078 (X→III) | 3.64 ($1^1A_1 \rightarrow 1^3E$) | 3.53, 4.47 |
| **VDE $[I^-(CH_3CN)]$*** | $6.7 \times 10^{-3}$ ($1^1E$)<br>$5.9 \times 10^{-3}$ ($2^1A_1$)<br>$7.0 \times 10^{-3}$ ($1^3E$)<br>$6.3 \times 10^{-3}$ ($1^3A_1$) | $7.0 \times 10^{-3}$ (I)<br>$6.4 \times 10^{-3}$ (II)<br>$6.7 \times 10^{-3}$ (III) | $2.5 \times 10^{-2}$ ($1^3E$) | $\cong 10.0 \times 10^{-3}$ |

[a] All values in eV
[b] Zero-point energy-corrected value with vibrational frequencies calculated with MP2/DZ
[c] From ref.[*125*]
[d] From refs.[*126*] and [*19*]
[e] From ref.[*124*]

** We now turn our attention to more quantitative aspects of the photoionisation and photoexcitation of $I^-(CH_3CN)$. As we have demonstrated previously,[*127*] *ab initio* (MP2) calculations predict binding energies for the binary halide-acetonitrile clusters in excellent agreement with experimental data. Indeed, the binding energy of the $I^-(CH_3CN)$ complex calculated with CASPT2/DZ+ of 0.51 eV (11.74 kcal/mol) is well within the experimental range of 0.484 ± 0.040 eV (Table 3.1), and furthermore, is in close agreement with the values obtained with the more rigorous CCSD(T)/TZ+ model chemistry. Interestingly, the iodide-acetonitrile complex is the only complex in the $X^-(CH_3CN)$ series (X = F, Cl, Br, I) to adopt a linear structure, resulting from the fact that iodide interacts with acetonitrile through ion-dipole interactions only, while complexes formed with the other halides exhibit less symmetric, hydrogen-bonded minimum-energy structures.[*127*] The calculated binding energy of the iodine atom to an acetonitrile molecule in the equilibrium geometry of the parent $I^-(CH_3CN)$ cluster,

$D_e^*$, is relatively small (0.02-0.03 eV or 0.5-0.7 kcal/mol with CASPT2/TZ+, and 0.051 eV or 1.2 kcal/mol with CCSD(T)/TZ+, Table 3.1). Thus, the shift of the ionization potential of iodide upon complexation with acetonitrile is practically equal to the $I^-(CH_3CN)$ binding energy $D_{anion}$ (Figure 3.1) and arises mainly from ground-state stabilisation of iodide by the acetonitrile polar solvent molecule.

The quantum-chemical treatment of systems with an extremely diffuse dipole-bound electron, such as the excited $I^-(CH_3CN)$ complex or the acetonitrile anion $CH_3CN^-$, is a challenging but well-understood problem.[*84*] The diffuse nature of the excited/excess electron dictates the use of extremely diffuse basis sets, which may cause severe convergence problems.[*102*] Dispersion interactions are also very important in the stabilisation of the dipole-bound electron,[*104-107*] so inclusion of dynamic electron correlation is necessary to produce reliable VDEs of the dipole-bound electron. Inspection of Table 3.1 suggests that both the CASPT2/DZ+ and CCSD(T)/TZ+ approaches provides an adequate description of the dipole-bound electron binding energy for the acetonitrile anion, as they predict values in agreement with experiment and previously reported high-level *ab initio* quantum chemistry calculations.[*107*]

** The ionisation potential of the free iodide anion is reproduced relatively well with both CASPT2/DZ+ and CCSD(T)/TZ+, although introduction of spin-orbit coupling leads to an underestimated value for the IP in the case of the CASPT2 calculations (by *ca*. 0.4 eV, Table 3.1). In fact, the ionisation potential of iodide (*i.e.* the electron affinity of iodine) is known to converge very slowly with basis set size, and even calculations employing the quintuple-zeta basis set aug-cc-pV5Z-PP still yield a slightly underestimated value.[*128*] Not surprisingly, the IP of the $I^-(CH_3CN)$ complex is also underestimated with CASPT2-SOC/DZ+ by almost 0.4 eV. The IP values uncorrected for spin-orbit coupling are closer to experimental data, most likely, due to a cancellation of errors. Although the absolute value of the IP for the iodide-acetonitrile complex is reproduced poorly, the calculated shift of the IP between the free and complexed iodide (0.44-0.49 eV) is very close to the one observed in experimental studies (0.48 eV).[*19*] CASPT2-SOC/DZ+ calculations thus paint a correct quantitative picture of the photoexcitation and photoionisation of the binary iodide-acetonitrile complex once the systematic error in the calculated ionisation potential of iodide is taken into account. The splitting between the $1^2E$ and $1^2A_1$ ionized states of $I^-(CH_3CN)$ is small (~0.01 eV), and even smaller for the two lowest spin-

orbit states *I* and *II*, which may explain why it is not possible to distinguish them experimentally.[*19*]

** Experimental data concerning the electron binding energy of the excited electron in the CTTS excited state of $I^-(CH_3CN)$ in the Franck-Condon region is rather uncertain, but photoneutral and photofragment action spectra suggest that the CTTS state lies *ca.* 10 meV below the ionised states.[*19*] Our calculated results fall within the range of these values, with CASPT2/DZ+, predicting ionisation energies of around 6-7 meV, and CCSD(T)/TZ+ predicting a slightly larger value of 25 meV (Table 3.1). Not surprisingly, the triplet excited states are 0.3-0.4 meV more stable than the singlet states, and the spin-orbit mixing of the singlet and triplet *E* and $A_1$ states leads to slightly higher VDEs.

** To summarise, CASPT2 and CASPT2-SOC *ab initio* quantum chemistry calculations with the highly diffuse DZ+ basis set provide a description of the photoionisation and photoexcitation of $I^-(CH_3CN)$ in the Franck-Condon region in close agreement with experiment and higher-level electronic structure calculations. However, a complete understanding of the subsequent CTTS relaxation process requires information about extended regions of the excited-state potential energy surface, to which we now turn our attention.

### 3.4. Potential Energy Curves for the Ionised and Excited States of $I^-(CH_3CN)$

Potential energy curves of the ionised and excited states of $I^-(CH_3CN)$ are important for understanding the relaxation and electron solvation pathways of $[I^-(CH_3CN)_n]^*$ and, computed with rigorous *ab initio* quantum chemistry methods, they may serve to benchmark the reliability of more efficient computational models for describing $[I^-(CH_3CN)]^*$ relaxation dynamics. **Owing to the symmetry of $I^-(CH_3CN)$, it is relatively easy to map the potential energy surfaces of its ground, excited and ionised states. Although the ground-state potential energy surface is known to be rather flat with respect to tilting of the iodide off the acetonitrile $C_3$ symmetry axis and the iodine is relatively free to float in the "methyl pocket" at non-zero temperatures,[*127*] the most relevant coordinate for ionised and excited state relaxation dynamics is the C–I stretch coordinate along the $C_3$ axis (** Figure 3.3). The rigidity of the acetonitrile molecule further simplifies the evaluation of the potential energy curves, in which the acetonitrile geometry is kept fixed and only the iodine-acetonitrile distance is varied. ** Figure 3.3 shows potential

energy curves along the C–I stretch coordinate for the non-spin-orbit-coupled ionised and excited states of $I^-(CH_3CN)$, while ** Figure 3.4 shows potential energy curves for the spin-orbit states.

** The potential energy curves for the $1^2E$ and $1^2A_1$ states of $I^{\bullet}(CH_3CN)$ have substantially different well depths due to the non-spherical distribution of the electron density of the iodine atom, giving rise to a non-zero quadrupole moment and relatively large differences in the polarisability along different axes.[*123*] In the lower $1^2E$ state the interaction between acetonitrile and the iodine atom (located on the methyl group side) is relatively strong, with a potential well of *ca.* 50 meV (~1.2 kcal/mol) at a C–I distance of *ca.* 4 Å (** Figure 3.3*a*). The well depth for the $1^2A_1$ state is only 23 meV (~0.5 kcal/mol), and the potential energy minimum is located at a shorter acetonitrile-iodine distance, with r(C–I) = 3.8 Å. The weaker stabilisation of the $1^2A_1$ state can be explained by the destabilising interaction of the iodine atom quadrupole moment with the positive end of the acetonitrile molecular dipole, and the lower polarisability of the iodine atom in the direction of the half-filled *p*-orbital.

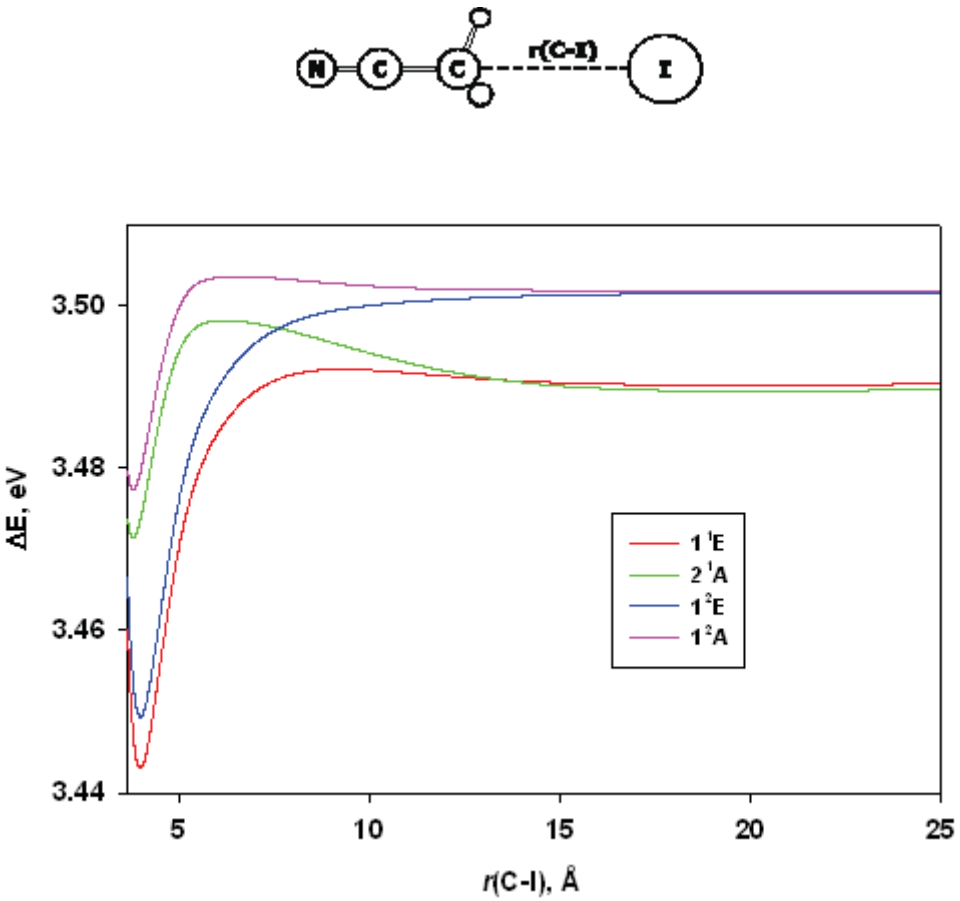


** Figure 3.3. Potential energy curves (CASPT2/DZ+) for the non-spin-orbit-coupled singlet CTTS excited and doublet ionised states of the $I^-(CH_3CN)$ complex along the C–I stretch coordinate. The equilibrium ground-state energy of $I^-(CH_3CN)$ defines the energy reference and the equilibrium C–I distance of $I^-(CH_3CN)$ corresponds to the onset of the curves.

** Generally, the potential energy curves for the CTTS excited states are similar to the corresponding ionised states, but 5-12 meV lower in energy (** Figure 3.3*a*). However, the differences in the $E$–$A_1$ curves due to anisotropy are somehow amplified: unlike the $1^1E$ state, the $2^1A_1$ state has a distinct maximum at a C–I distance of around 6 Å which is *ca.* 6 meV above the dissociation limit. The well depths for both singlet excited states, 45 and 16 meV (~1.1 and ~0.4 kcal/mol, respectively), are smaller than for their ionised counterparts. The triplet excited states $1^3E$ and $1^3A_1$ (not shown) are very similar to the singlet CTTS states, but they lie slightly lower by 1-1.5 meV.

** Since the excited dipole-bound electron distribution may change significantly depending on the position of the iodine atom, the diffuse basis set centred on the methyl group carbon atom may become inadequate for some regions of the potential energy surface. Hence, potential energy curves were also evaluated with the "floating centre" approach, where the position of the 8 *sp*-diffuse functions used to describe the excited/excess electron was optimised at each point. The resulting potential energy curves are essentially the same as those shown in ** Figure 3.3*b*.

** Taking into account spin-orbit coupling does not significantly change the character of the potential energy curves for the ionised and excited states of $I^-(CH_3CN)$. The lower ionised and excited states (*I*) are practically identical to the corresponding $1^2E$ and $1^1E/1^3E$ states, respectively, and they are simply shifted down in energy by *ca.* 0.3 eV, since the *I* state has pure *E* parentage, similarly to other complexes of halogen atoms with cylindrical symmetry.[*122, 123*] The *II* and *III* spin-orbit states (** Figure 3.4*a*, where only *II* is shown for clarity) have mixed *E* and $A_1$ character, and therefore exhibit deeper energy wells than the corresponding non-spin-orbit states, with well depths of 33 and 29 meV (0.8 and 0.7 kcal/mol) for the ionised and excited states, respectively.

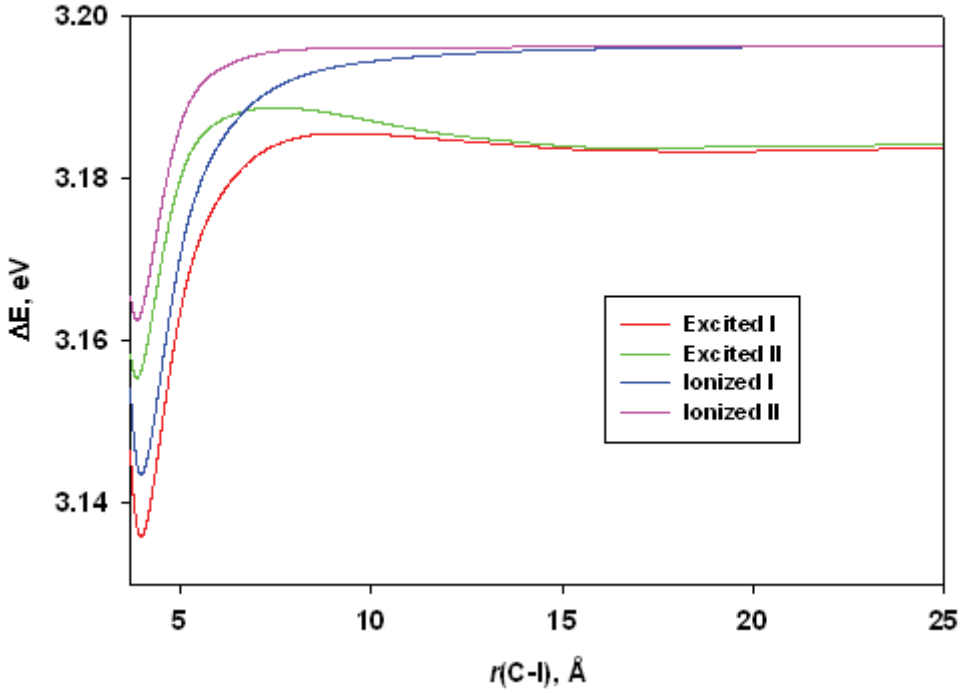


** Figure 3.4. Potential energy curves (CASPT2-SOC/DZ+) for the lowest spin-orbit CTTS excited and ionised states of the $I^-(CH_3CN)$ complex along the C–I stretch coordinate. The equilibrium ground-state energy of $I^-(CH_3CN)$ defines the energy reference and the equilibrium C–I distance of $I^-(CH_3CN)$ corresponds to the onset of the curves.

Figure 3.5 shows the distance profiles of the $[I^-(CH_3CN)]^*$ excited electron VDE computed with both CASPT2/DZ+ (for the non-spin orbit coupled singlet and triplet CTTS states, VDE profiles for the spin orbit CTTS excited states are very similar and not shown) and CCSD(T)/TZ+ (for the $1^3E$ triplet CTTS state only). The CASPT2/DZ+ curves for the various CTTS states are all very similar, and show that, for each state, the excited electron VDE increases by roughly 7 meV as the iodine-acetonitrile distance increases, reaching a maximum at $r$(C-I) ≈ 17 Å before decreasing by less than 1 meV to around 11 meV at larger $r$(C-I). These VDE profiles resemble those reported by Chen and Sheu for $[I^-(H_2O)_n]^*$,[*32*] but appear qualitatively different from the CCSD(T)/TZ+ VDE profile. In the latter case, the excited

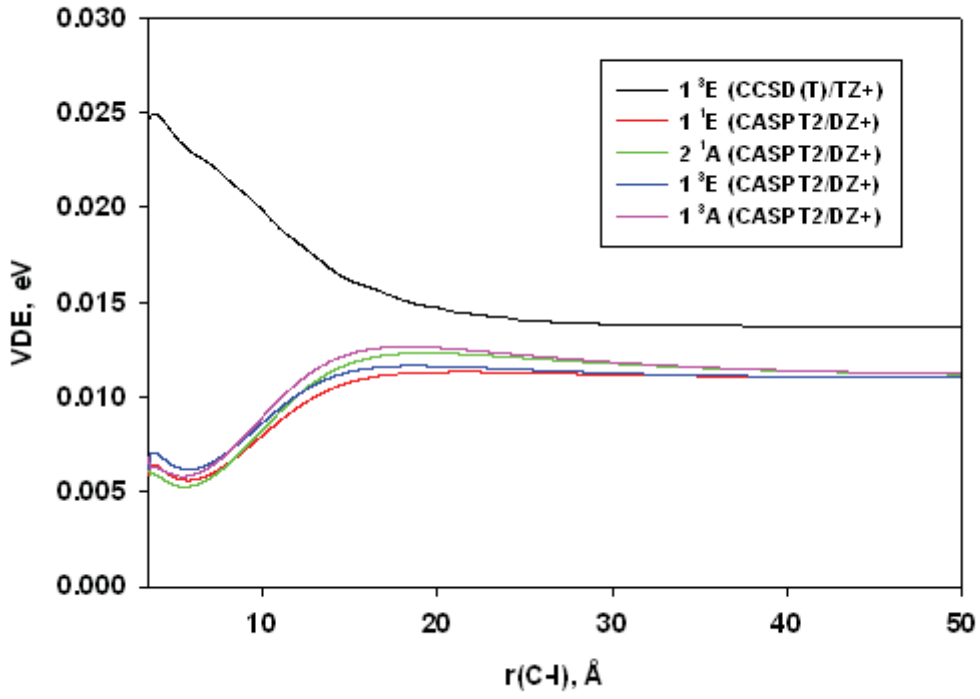


Figure 3.5. Excited electron vertical detachment energies for the singlet and triplet excited states of the $I^-(CH_3CN)$ complex along the C-I stretch coordinate.

electron VDE is highest at the ground-state equilibrium geometry of $I^-(CH_3CN)$ (25 meV) and decreases by around 10 meV as *r*(C-I) increases to 20 Å. Furthermore, CCSD(T)/TZ+ predicts a larger excited electron VDE for $[I^-(CH_3CN)]^*$ at all values of *r*(C-I). The discrepancies between the CASPT2/DZ+ and CCSD(T)/TZ+ VDE profiles appear to be due to the better treatment of dispersion effects between the diffuse excited electron and the electrons of the iodine atom by the second model chemistry. While exclusion effects have been invoked by Chen and Sheu to rationalise the destabilisation of the excited electron distribution by the iodine atom in the case of $[I^-(H_2O)_n]^*$,[*21, 32*] the present results suggest that more subtle dispersion interactions between the diffuse excited electron and the polarisable iodine atom, which can only be described with CCSD(T), appear to dominate. Indeed, higher order electron correlation effects have been shown to contribute significantly to the stability of excess electrons in dipole-bound anions,[*102,*

*104-107*] and the presence of the highly polarisable iodine atom in the region occupied by the excited electron distribution may make these effects even more important.

The stabilising effect of the iodine atom on the excited electron distribution may at least partially account for the observed decrease of the excited electron VDE in $[I^-(Solv)_n]^*$ at long times as the iodine and solvent cluster depart from one another.[*27, 29, 47*] As shown earlier in the case of $[I^-(H_2O)_5]^*$,[*87*] separation of the excited electron distribution from the iodine atom is indeed a critical aspect of the relaxation process, but the subsequent electron solvation process was highly dependent on the solvent reorganisation in that case. The shape of the potential energy curves for the excited states of $I^-(CH_3CN)$ and the associated profiles of the excited electron VDE indicate that separation of the iodine atom from the acetonitrile moiety is also expected to contribute to the observed modulation of the stability of the excited electron in $[I^-(CH_3CN)_n]^*$; a detailed picture of the intricate molecular dynamics involved in the trapping of the excited electron can, however, only be obtained from accurate molecular dynamics simulations, the topic of the following section.

### 3.5. Dynamics of Photoexcited $I^-(CH_3CN)$

#### *3.5.1. Method validation*

Potential energy curves of the ground and excited states of $I^-(CH_3CN)$ computed with different model chemistries are shown in Figures 3.6. For ground-state $I^-(CH_3CN)$, the HF/Min+ potential energy curve is in close agreement with those computed with the more rigorous CASPT2/DZ+ and CCSD(T)/TZ+ model chemistries once it is shifted by –0.16 Å. On the other hand, HF/Mid+ underestimates the depth of the potential energy well by 0.07 eV (1.6 kcal/mol), while MP2/Mid+ overestimates

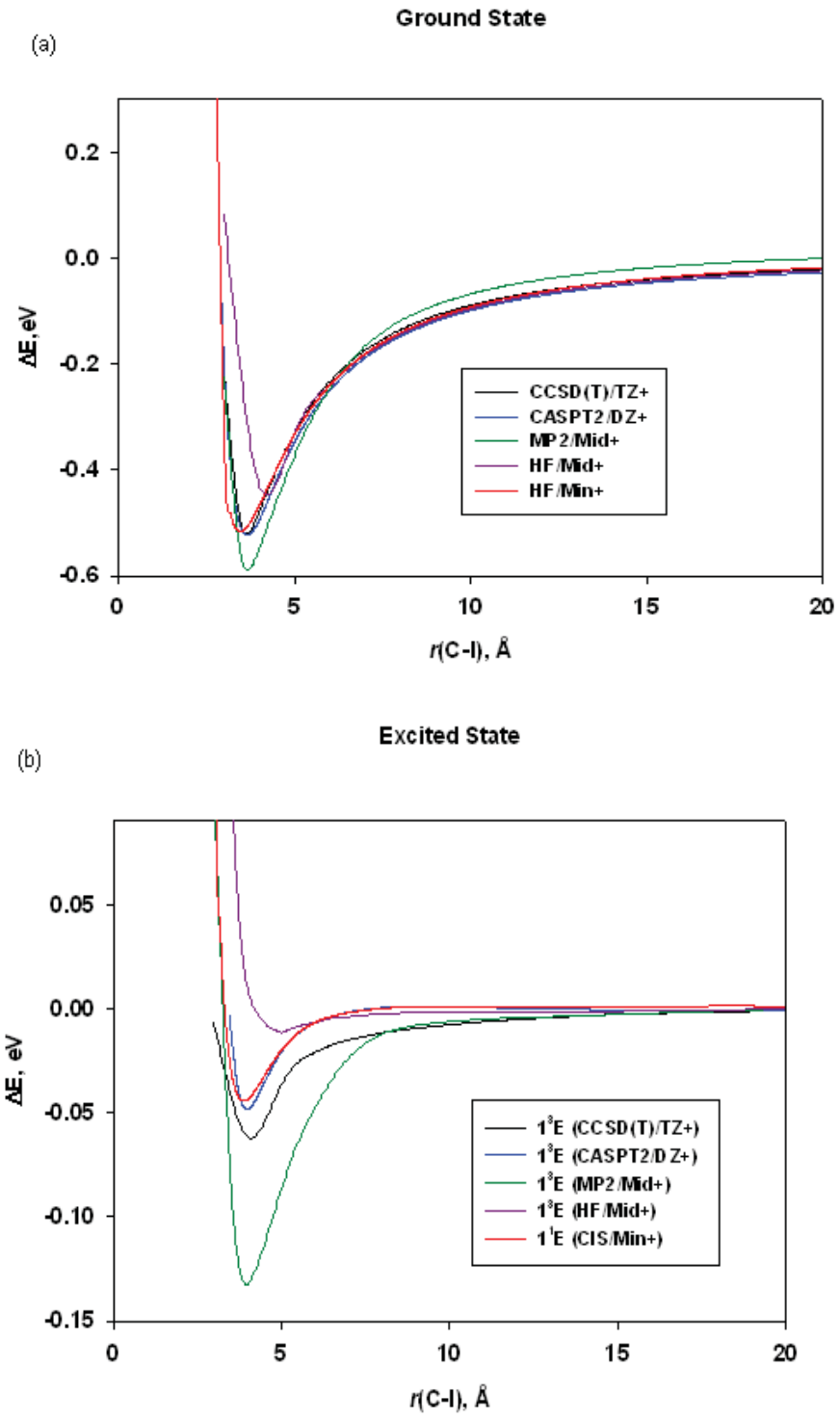


Figure 3.6. Ground and excited state potential energy curves of the $I^-(CH_3CN)$ complex computed with different model chemistries. Note that the vertical scale is different for the two plots. The asymptotic limit is set to zero for all curves.

the depth of the potential energy well by a similar amount relative to the CASPT2/DZ+ or CCSD(T)/TZ+ curves. CIS also appears to provide a reasonable description of the excited

state of $I^-(CH_3CN)$; the CIS and CASPT2 curves practically coincide once the CIS curves are shifted by *r*(C-I) = -0.16 Å. Relative to CCSD(T)/TZ+, however, the well-depth of the CIS/Min+ is slightly underestimated by 0.015 eV (0.35 kcal/mol), an amount that is not likely to have a significant impact on the nature of the excited-state dynamics given the amount of kinetic energy present in the system at 150 K (~0.3 eV). On the other hand, MP2/Mid+ overestimates the well-depth significantly by around 0.07 eV (1.6 kcal/mol), while HF/Mid+ underestimates it by a similar amount. Thus, the CIS/Min+ model chemistry was selected for use in the molecular dynamics simulations of the CTTS excited-state relaxation dynamics of $I^-(CH_3CN)$.

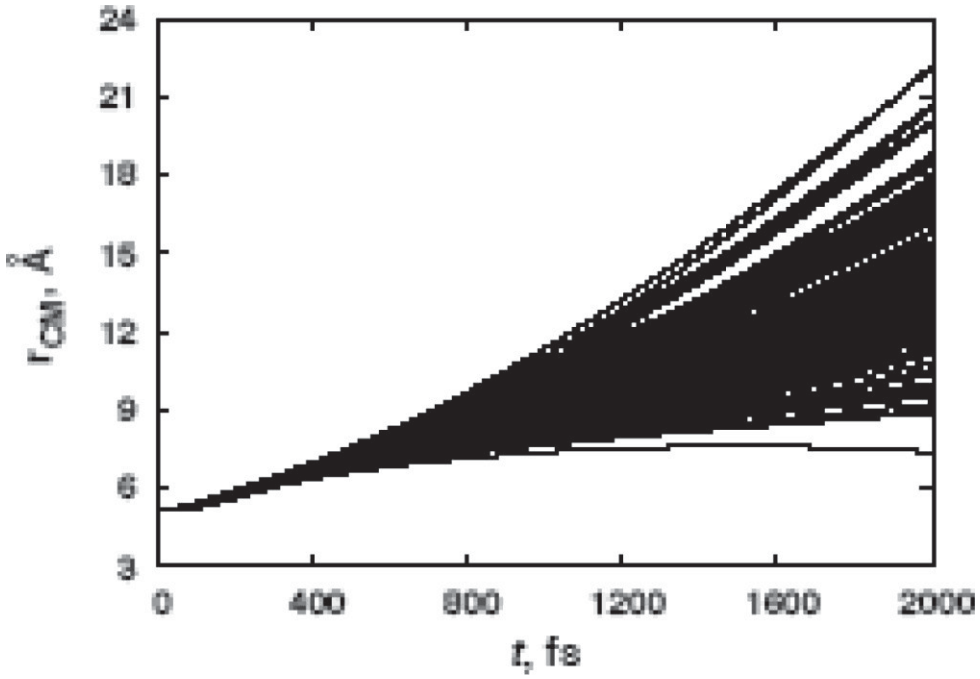


** Figure 3.7. CTTS relaxation dynamics of the $I^-(CH_3CN)$ complex: evolution of the inter-fragment distance (measured as the distance between the fragment centres of mass, $r_{CM}$).

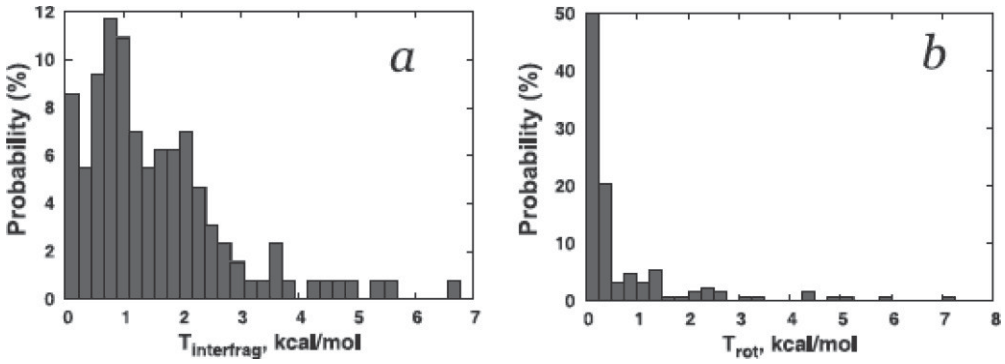


** Figure 3.8. CTTS relaxation dynamics of the $I^-(CH_3CN)$ complex: inter-fragment relative kinetic energy $T_{rel}$ (*a*) and rotational energy of the acetonitrile moiety $T_{rot}$ (*b*). All energies are averaged over the last 75 fs of the simulation.

### *3.5.2. CTTS relaxation dynamics*

** The time evolution of the excited $I^-(CH_3CN)]^*$ complex during CTTS relaxation and the fragment energy distributions at the end of the simulation time (2 ps) are shown in Figures 3.7 and 3.8, respectively. The relaxation of $[I^-(CH_3CN)]^*$ is generally characterised by reasonably fast dissociation of the complex into I• and $CH_3CN^-$ fragments. By the end of the simulation time, the distance between iodine and acetonitrile is larger than 10 Å for most of the trajectories, the inter-fragment distance exceeds 20 Å for a few trajectories, and only one trajectory results in a complex loosely trapped in the excited-state potential energy well. These results are in good agreement with the experimental observation of the acetonitrile dipole-bound anion as the only negatively charged product of $[I^-(CH_3CN)]^*$ relaxation.[19]

** Further insight into $[I^-(CH_3CN)_n]^*$ relaxation can be obtained by examining the final relative translational and rotational energies of the acetonitrile molecules (Figure 3.8a and 3.8b respectively). Most of the trajectories result in acetonitrile molecules with moderate translational kinetic energy (0.5-3 kcal/mol), with a comparatively smaller number of trajectories resulting in acetonitrile molecules with high translational kinetic energy (up to 7 kcal/mol) The acetonitrile rotational energy, on the other hand, is negligible for more than half of the trajectories (Figure 3.8b), with dissociation predominantly proceeding by elongation of the iodine-acetonitrile distance along the $C_3$ axis of the complex, *i.e.* along the coordinate of the potential energy curve in ** Figure 3.4, though a small number of trajectories lead to acetonitrile molecules with substantial rotational energy (*ca.* 7 kcal/mol).

These results tentatively suggest that translation of $CH_3CN$ away from the iodine may dominate the initial relaxation of $[I^-(CH_3CN)_n]^*$, consistent with the hypothesis by Neumark and co-workers that the solvent cage surrounding iodine undergoes expansion in the early stages of the relaxation process.[*29*]

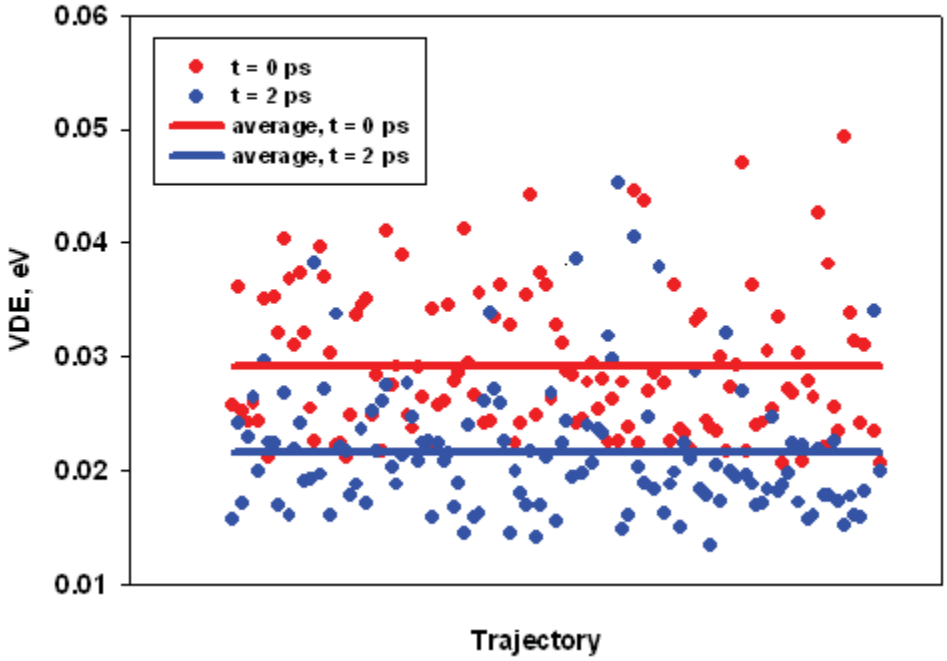


Figure 3.9. Scatter plot of the excited electron VDE of $[I^-(CH_3CN)]^*$ from the simulated trajectories, calculated with CCSD(T)/TZ+ // CIS/Min+. Solid lines indicate the average VDE over 128 trajectories at each time.

Comparison of the initial and final (after 2 ps) distributions of the $[I^-(CH_3CN)]^*$ excited electron VDEs obtained from the molecular dynamics simulations (Figure 3.9) provide important insights into the influence of the relaxation process on the stability of the excited electron. Furthermore, since $I^-(CH_3CN)$ lacks the solvent network characteristic of larger $I^-(Solv)_n$, $[I^-(CH_3CN)]^*$ offers a unique opportunity to investigate the importance of iodine-solvent relative motion in the electron solvation process. At t = 0 ps, the excited electron VDEs of $[I^-(CH_3CN)]^*$ are distributed around an average value of 0.030 eV, although VDEs for individual starting configurations can vary widely. These VDE values are significantly larger than those at 2 ps, which are distributed around an average value of only 0.021 eV. These findings are not surprising in light of the nature of the excited electron VDE profile of $[I^-(CH_3CN)]^*$ along the C-I stretch coordinate (Figure 3.5) and the overall tendency of the

complex to dissociate along this coordinate as the relaxation proceeds (Figure 3.7). Even if translational motion seems to prevail in the relaxation process, rotation of the acetonitrile molecule may also have a significant impact on the excited electron VDE, since the excited electron can move away from the region occupied by the iodine atom as it follows the rotating acetonitrile dipole, as in the early stages of $[I^-(H_2O)_n]^*$[*87*] relaxation. Molecular translational motion is, however, expected to play a far greater role in $[I^-(CH_3CN)_n]^*$ relaxation and the corresponding modulation of the stability of the excited electron; this unique aspect of $[I^-(CH_3CN)_n]^*$ might be due to the high moment of inertia of acetonitrile compared with that of water and methanol, and the resulting hindrance towards rotational excitation.

While substantial differences exist between $[I^-(CH_3CN)]^*$ and $[I^-(CH_3CN)_n]^*$ due to the absence of solvent-solvent interactions in the former complex, it is instructive to consider the simulated $[I^-(CH_3CN)]^*$ relaxation dynamics in the context of the recent femtosecond photoelectron spectroscopy experiments on $[I^-(CH_3CN)_n]^*$ performed by Neumark and co-workers.[*29*] These experiments indicate that, during the first ~300 fs following excitation, the excited electron VDE of $[I^-(CH_3CN)_n]^*$ decreases substantially by 0.1 to 0.3 eV depending on the number of solvent molecules present, before increasing again by up to 0.45 eV over the next few picoseconds. While the average decrease in the simulated excited electron VDE of $[I^-(CH_3CN)]^*$ is an order of magnitude smaller, the present results indicate that translational motion of the solvent molecules is likely to reduce the attractive excited electron-iodine interactions and the associated VDE in the early stages of $[I^-(CH_3CN)_n]^*$ relaxation. Indeed, expansion of the solvent cage was observed in the preliminary molecular dynamics simulations of Takayanagi, in which a very limited number of trajectories were propagated from mostly local minimum energy $I^-(CH_3CN)_n$ (n=2,3) configurations.[*97*] The present results also highlight the possible contribution of rotational motion in the $[I^-(CH_3CN)_n]^*$ relaxation process; solvent rotation can not only modulate the excited-electron iodine interaction, but it can also assist in opening up the solvent "ring" surrounding iodine[*96*] in the Franck-Condon geometry of larger $[I^-(CH_3CN)_n]^*$ ($n \geq 5$), which would then facilitate the departure of iodine and the subsequent formation of the actonitrile cluster anion with an internally solvated electron with higher VDE. Thus, while the present simulations of $[I^-(CH_3CN)]^*$ relaxation have provided some important insights into the types of solvent motion involved in the initial relaxation of $[I^-(CH_3CN)_n]^*$, extensive simulations of larger $[I^-(CH_3CN)_n]^*$ ($n \geq 2$) using the present approach may prove critical for

understanding the unique aspects of CTTS relaxation leading to the formation of a possibly internally trapped electron in $[I^-(CH_3CN)_n]^*$.

### 3.6. Concluding Remarks

In this article, we report a detailed investigation of the photoexcitation and photoionisation of the binary iodide-acetonitrile complex using high-level *ab initio* quantum chemistry methods. These calculations reproduce qualitative and quantitative aspects of the photoexcitation and photoionisation of the $I^-(CH_3CN)$ complex, in excellent agreement with available experimental data, thus providing solid ground for the computational investigation of the charge-transfer-to-solvent (CTTS) excited state relaxation processes. To this end, potential energy curves for the ionised and CTTS excited states were calculated in order to unveil the dependence of the excited electron binding energy on the complex geometry. A stabilising interaction between the iodine atom and the excited electron at short distance, which could influence the modulation of the excited electron VDE of $[I^-(CH_3CN)_n]^*$, was identified. An efficient two-level scheme for first-principles excited-state molecular dynamics simulations of the $I^-(CH_3CN)$ complex was developed, which makes use of a low-level economic model chemistry to propagate the equations of motion along the trajectories, and high-level calculations to obtain the time profile of the excited electron VDE. Extensive simulations with realistic initial conditions were then performed of the CTTS relaxation dynamics of the iodide-acetonitrile complex. The present results highlight the importance of iodine detachment from the complex in the relaxation and electron solvation process of $[I^-(CH_3CN)_n]^*$, a critical aspect of the relaxation dynamics that appears to be shared with all $[I^-(Solv)_n]^*$.

# 4. Relaxation Pathways of Photoexcited Iodide-Methanol Clusters: A Computational Investigation

**Published As:**

Chun C. Mak and Gilles H. Peslherbe, *The Journal of Physical Chemistry A*. 2014, 118:4494-4501

## Abstract

Upon photoexcitation of iodide-methanol clusters, $I^-(CH_3OH)_n$, to a charge-transfer-to-solvent (CTTS) excited state, extensive relaxation was found to occur, accompanied by a convoluted modulation of the stability of the excited electron, which ultimately decreases substantially. In order to develop a molecular-level understanding of the relaxation processes of CTTS excited $I^-(CH_3OH)_n$, high-level quantum-chemical calculations are first used to investigate the ground, excited and ionised states of $I^-(CH_3OH)_n$ (n = 2). Due to the relatively small size of $I^-(CH_3OH)_2$ it was possible to characterise the contributions of solvent-solvent interactions to the stability of the CTTS excited cluster relative to dissociation into methanol, iodine and a free electron, which exhibits a substantial dependence on the cluster geometric configuration. *Ab initio* molecular dynamics simulations of CTTS excited $I^-(CH_3OH)_3$ are then performed to shed some light onto the nature of the relaxation pathways involved in the modulation of the stability of the excited electron in larger clusters. Simulation results suggest that separation of I and $(CH_3OH)_3^-$ accompanied by solvent reorganisation in the latter can initially stabilise the excited electron, while gradual cluster fragmentation to I, $(CH_3OH)_2^-$ and $CH_3OH$ ultimately destabilises it. This work shows, for the first time, that the inability of small CTTS excited $I^-(CH_3OH)_n$ to retain a solvated electron may be attributed to the limited hydrogen-bonding capacity of $CH_3OH$, which increases the propensity for fragmentation to smaller clusters with lower excess-electron binding energies, and highlights the critical role of intricate molecular interactions in the electron solvation process.

## 4.1. Introduction

Photoexcitation of halide-polar solvent clusters, $X^-(Solv)_n$ (X = Cl, Br and I), results in the transfer of an electron from the halide to a diffuse, cluster-supported orbital, leading to cluster analogues of the charge-transfer-to-solvent (CTTS) excited states of halides in polar liquids.[*18-23, 43*] Furthermore, CTTS excited solvated halides relax to produce solvated electrons,[*14*] ubiquitous species involved in various synthetically important chemical reactions such as the Birch reduction[*6-8*] and the Bouveault-Blanc reduction.[*9, 10*] Since CTTS excited $X^-(Solv)_n$ are among the smallest gas-phase molecular aggregates that support a diffuse excess electron, their relaxation pathways are intricately connected to the role of the halogen atom and the solvent molecules in the process of solvated electron formation from CTTS excited halides.

Recently, Neumark and co-workers have investigated the relaxation of iodide-polar solvent clusters excited to the CTTS state, $[I^-(Solv)_n]^*$, using femtosecond photoelectron spectroscopy, revealing intriguing relaxation processes that exhibit a remarkable dependence on the type of solvent molecule.[*24-29, 46-48*] Due to the importance of water in biological and environmental systems, $[I^-(H_2O)_n]^*$ ($3 \leq n \leq 28$) have attracted the most interest both experimentally[*24, 26, 46-48*] and theoretically,[*32-38, 54, 55, 87, 129*] and there is now consensus that, upon excitation, the water cluster moiety undergoes substantial reorganisation to a configuration that binds the excited electron more tightly in a process that may be loosely viewed as the cluster analogue of electron solvation. Experimental work on other $[I^-(Solv)_n]^*$, however, suggests that similar electron solvation processes are absent in some types of clusters, though the molecular basis of the solvent effects remains elusive.[*25-28*]

While water is the most important solvent for chemical reactions in biological systems and in the environment, simple alcohols are commonly used as solvents in many synthetic reactions, particularly those involving solvated electrons,[*6-10*] and the relaxation of $[I^-(CH_3OH)_n]^*$ ($4 \leq n \leq 11$) has recently been probed with femtosecond photoelectron spectroscopy.[*27, 28*] In stark contrast with $[I^-(H_2O)_n]^*$ the excited electron is ultimately destabilised in these clusters. Depending on the cluster size, the vertical detachment energy (VDE) of the excited electron, which reflects its stability in the cluster, decreases by 0.040 to 0.12 eV before increasing by roughly the same amount during the first 1 to 4 ps. Subsequently, the VDE gradually decreases by 0.060 to 0.22 eV and the clusters decay by ejection of the excited electron over tens of picoseconds. These experimental observations were rationalised by the fact that

$CH_3OH$, unlike $H_2O$, is a single hydrogen-bond donor, and thus there would be a competition between the electron•••$CH_3OH$ interactions and the stronger $CH_3OH$•••$CH_3OH$ interactions; $[I^-(CH_3OH)_n]^*$ would thus reorganise to maximise the latter interactions, resulting in lower potential energy cluster configurations that have a smaller excited-electron VDE. The proposed relaxation pathway of $[I^-(CH_3OH)_n]^*$ provided a plausible explanation for the observed electron destabilisation, but alternative pathways could not be ruled out.[*26, 27*]

In this article, computational methods are used to investigate the relaxation dynamics of $[I^-(CH_3OH)_n]^*$. High-level quantum-chemical calculations are first performed to characterise the energetic properties of ground, excited and ionised $I^-(CH_3OH)_n$ (n = 2) and gain insights into the molecular interactions involved in the $[I^-(CH_3OH)_n]^*$ relaxation process. Due to the limited number of intermolecular interactions present in $I^-(CH_3OH)_2$, analysis of the ground, excited and ionised-state energies of different $I^-(CH_3OH)_2$ conformers can de-convolute the relative contributions of the $I^-$ ••• $CH_3OH$, $e^-$ ••• $CH_3OH$ and $CH_3OH$ ••• $CH_3OH$ interactions to the stabilities of $I^-(CH_3OH)_n$ and $[I^-(CH_3OH)_n]^*$, which may have a profound influence on the relaxation dynamics. *Ab initio* molecular dynamics simulations of $[I^-(CH_3OH)_n]^*$ (n = 3) are then performed to obtain a clear picture of the $[I^-(CH_3OH)_n]^*$ relaxation processes that result in the experimentally observed modulation of the stability of the excited electron in larger $I^-(CH_3OH)_n$ . Results of this work are used to understand how subtle molecular interactions can influence the electron solvation process of iodide-polar solvent molecule clusters excited to the CTTS state.

### 4.2. Computational Methods

The ground-state geometries of $I^-(CH_3OH)_n$ (n = 2) were optimised with second-order Moller-Plesset (MP2) perturbation theory[*64*] and the aug-cc-pVDZ basis set.[*100*] The cluster dissociation energies of the ground and CTTS excited states, the vertical CTTS excitation energies and the excess electron VDEs of the CTTS states were computed for the optimised $I^-(CH_3OH)_2$ geometries using coupled cluster theory for open shell systems with single, double and non-iterative triple excitations [CCSD(T)][*108, 109, 130*] combined with a large triple-zeta basis set augmented with a set of diffuse basis functions (referred to as TZ+) to provide an adequate description of the excited-electron distribution. In these calculations, the CTTS state energies of $I^-(CH_3OH)_2$ were estimated as CCSD(T) triplet ground-state energies, thus eliminating the need to use a multireference electronic structure method to obtain these energies. As shown in our earlier work, the singlet and triplet CTTS states of

iodide-polar molecule clusters are heavily coupled due to significant spin-orbit coupling effects, and as such, the triplet ground state and the singlet excited states provide equal-quality approximations of the actual spin-orbit CTTS states.[*131*] The TZ+ basis set consisted of the standard aug-cc-pVTZ basis set for carbon, hydrogen and oxygen atoms,[*100, 132*] the Stuttgart-Dresden effective core potential and corresponding triple-zeta basis set for iodine,[*69, 110*] and an additional set of 9s9p4d diffuse functions centred at the cluster centre of mass . The values of the exponents of the diffuse functions were obtained in an even-tempered manner from the smallest exponents in the aug-cc-pVTZ basis set, using a progression factor of 3.2, as in our previous work.[*131*]

First-principles molecular dynamics simulations of $I^-(CH_3OH)_n$ (n = 3) were performed in quaternion coordinates[*56*] using a fifth-order Gear predictor-corrector algorithm[*58*] with a time step of 0.7 fs, and the trajectories were propagated for 2.3 ps. As in our previous work on $I^-(H_2O)_n$,[*87*] this approach keeps the geometry of the solvent molecules rigid, thus preventing the transfer of energy from the high frequency intramolecular vibrational modes of the solvent molecules to the lower frequency intermolecular modes; this effect, known as "zero-point energy leakage" would artificially increase the available kinetic energy in the excited clusters and alter their dynamics.[*59, 60, 133*]

While high-level calculations at the second-order Moller-Plesset perturbation and coupled-cluster levels of theory using very large basis sets are used to obtain accurate values for the CTTS excitation energies and excited-electron VDEs of $I^-(CH_3OH)_2$, they cannot be used for first-principles molecular dynamics simulations of larger clusters, which require energy and gradient calculations for a large number of configurations. In the present work, we adopted an approach similar to the one we previously used for *ab initio* molecular dynamics simulations of $[I^-(H_2O)_n]^*$, where energies and gradients of the singlet excited state were computed at the state-averaged complete-active-space self-consistent-field (CASSCF) level of theory,[*61, 62*] with a [4,3] active space in which four electrons are distributed among the two highest energy *p* orbitals of iodine and the lowest unoccupied orbital of ground-state $I^-(CH_3OH)_n$, which accommodates the excess electron in the excited state. Excited-electron VDEs of configurations sampled from the molecular dynamics simulations were computed with second-order complete-active-space perturbation theory (CASPT2),[*63*] using the CASSCF(4,3) wavefunction as the reference wavefunction, in order to evaluate the effect of the cluster relaxation processes on the stability of the excited electron. For C, H and O

atoms, a 6-31++G(d,p) basis set,[*66-68*] was used while the effective core potential and corresponding valence basis set of Kurtz and co-workers[*112, 113*] were used for I. In order to describe the diffuse excited electron in $[I^-(CH_3OH)_n]^*$, four additional diffuse *s* functions with exponents 0.012, 0.004, 0.0013 and 0.00044 were placed on each hydrogen atom, and two sets of *sp* diffuse functions with exponents 0.008667 and 0.000963 were placed on the iodine atom. This moderate-size basis set will henceforth be referred to as the DZ+ basis set. This model chemistry is similar to the one used in our previous simulations of $[I^-(H_2O)_n]^*$,[*34, 87*] and as such, a direct comparison of the present simulations of $[I^-(CH_3OH)_n]^*$ with previous work on $[I^-(H_2O)_n]^*$ can offer valuable insights into the influence of the intricate features of the different solvent molecules on the relaxation dynamics of iodide-polar molecule clusters excited to the CTTS state. Furthermore, Hartree-Fock (HF) theory, which is essentially the ground-state reference for CASSCF(4,3), combined with the DZ+ basis set provides a reliable description of the $CH_3OH \bullet\bullet\bullet CH_3OH$ and $I \bullet\bullet\bullet CH_3OH$ dissociation energies when compared with the more rigorous CCSD(T)/TZ+, validating the more computationally efficient approach for describing the intermolecular interactions that are expected to play a critical role in $[I^-(CH_3OH)_n]^*$ relaxation dynamics (*cf*. Table 4.1). All electronic structure calculations were performed with the MOLPRO 2010.1 suite of programs.[*71*]

Table 4.1. Calculated energetic properties of $I^-(CH_3OH)_{1,2}$ and $(CH_3OH)_2$

| | HF/DZ+ | CCSD(T)/TZ+ |
|---|---|---|
| $E_{diss}(I(CH_3OH))$ | 0.5 | 1.6 |
| $E_{diss}((CH_3OH)_2)$ | 5.0 | 5.8 |
| $E_{diss}(\boldsymbol{ch2}\,(CH_3OH)_2)$[b] | 4.1 | 3.5 |
| $E_{diss}(\boldsymbol{mm}\,(CH_3OH)_2)$[b] | -0.5 | -0.6 |

[a] Energies in kcal/mol

[b] See Figure 4.1 for definition of configurations

## 4.3. Results and Discussion

### *4.3.1. $I^-(CH_3OH)_n$ (n=2) Ground and CTTS States*

In order to explore the geometric and energetic factors that can influence the relaxation pathways of $[I^-(CH_3OH)_n]^*$, it is instructive to examine the minimum energy geometries of $I^-(CH_3OH)_2$ and characterise the energetic properties of their ground, excited and ionised states. Unlike the larger $I^-(CH_3OH)_n$ that have been the subject of recent CTTS dynamics experimental work, $I^-(CH_3OH)_2$ is sufficiently small to be amenable to accurate quantum-chemical calculations using high levels of electron correlation and large basis sets, which have been shown to be critical for a quantitative description of the electron binding energies in CTTS excited iodide-polar solvent clusters.[*131*] As shown in earlier work,[*92*] ground-state $I^-(CH_3OH)_2$ possesses two nearly isoenergetic minimum energy configurations (Figure 4.1); in the ***ch2*** configuration, the iodide anion is bound to a hydrogen-bonded methanol dimer in which the two hydroxyl groups that form the "backbone" of the dimer are arranged in a short bent ***ch***ain, while two methanol molecules are hydrogen-bonded separately to the iodide anion in the ***mm*** (***m***onomer ***m***onomer) configuration.

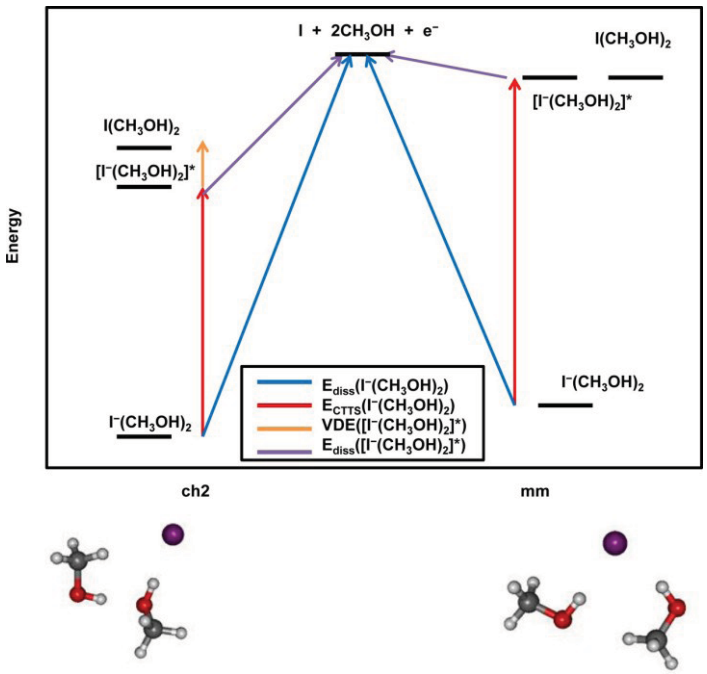


Figure 4.1. Energetics of ground, excited and ionised ***ch2*** and ***mm*** $I^-(CH_3OH)_2$.

Figure 4.1 provides a schematic representation of the relative energies of the ground, excited and ionised states of the two minimum energy configurations of $I^-(CH_3OH)_2$ and defines the various energetic quantities that are relevant in the photoexcitation and relaxation processes of $I^-(CH_3OH)_n$ (n = 2), including the vertical CTTS excitation energy, $E_{CTTS}$, the excited-electron VDE of $[I^-(CH_3OH)_n]^*$ and the dissociation energies for complete fragmentation of ground and excited $I^-(CH_3OH)_2$, $E_{diss}(I^-(CH_3OH)_2$ and $E_{diss}([I^-(CH_3OH)_2]^*)$, respectively, into an iodine atom, two methanol molecules and a free electron. The corresponding values are listed in Table 4.2. In agreement with earlier MP2/aug-cc-pVDZ

Table 4.2. CCSD(T)/TZ+ energetic properties of the ***ch2*** and ***mm*** $I^-(CH_3OH)_2$.[a]

| | ***ch2*** | ***mm*** |
|---|---|---|
| $E_{rel}$ | 0 | 0.5 |
| $E_{CTTS}$ ($I^-(CH_3OH)_2$) | 92 | 96 |
| VDE ($[I^-(CH_3OH)_2]^*$) | 0.3 | 0 |
| $E_{diss}(I^-(CH_3OH)_2)$ | 97 | 96.5 |
| $E_{diss}$ ($[I^-(CH_3OH)_2]^*$) | 5.3 | 0.5 |

[a] Energies are reported in kcal/mol

calculations performed on $I^-(CH_3OH)_2$,[*92*] ground-state ***ch2*** and ***mm*** are very close in energy, with the latter configuration only 0.5 kcal/mol higher in energy than the former. At an internal cluster temperature of 170 K, estimated to be that of experimental conditions from Klots theory,[*74*] both $I^-(CH_3OH)_2$ configurations are stable relative to dissociation to an iodine atom, two methanol molecules and a free electron [$E_{diss}(I^-(CH_3OH)_2)$ = 97 and 96.5 kcal/mol for ***ch2*** and ***mm***, respectively, *cf.* Table 4.2]; a combination of $I^-$ ••• $CH_3OH$ and $CH_3OH$ ••• $CH_3OH$ interactions stabilise the ***ch2*** configuration, while $I^-$ ••• $CH_3OH$ interactions alone stabilise the ***mm*** configuration. The CTTS states of ***ch2*** and ***mm*** $I^-(CH_3OH)_2$ lie 92 and 96 kcal/mol above the ground states, respectively, and the $I^-$ ••• $CH_3OH$ interactions that contributed to the stability of $I^-(CH_3OH)_2$ are no longer present in these states. While the $CH_3OH$ ••• $CH_3OH$ interaction, and to a lesser extent the excited electron ••• $I(CH_3OH)_2$ interaction [$VDE([I^-(CH_3OH)_2]^*)$ = 0.3 kcal/mol, *cf.* Table 4.2], stabilise ***ch2*** $[I^-(CH_3OH)_2]^*$ relative to dissociation ($E_{diss}$ = 5.3 kcal/mol, *cf.* Table 4.2), these

stabilising effects are much smaller in ***mm*** $[I^-(CH_3OH)_2]^*$ ($E_{diss}$ = 0.5 kcal/mol, *cf.* Table 4.2) due to the non-optimal arrangement of the two methanol molecules. As such, while ***ch2*** $[I^-(CH_3OH)_2]^*$ is stable relative to dissociation at 170 K, ***mm*** $[I^-(CH_3OH)_2]^*$ possesses sufficient thermal energy at this temperature to undergo dissociation into iodine and two methanol molecules and eject the excited electron. The present findings highlight the importance of solvent-solvent interactions for maintaining a bound excited electron during the $[I^-(CH_3OH)_n]^*$ relaxation process; in configurations where these interactions are absent, the excited electron would be destabilised and readily ejected as the cluster dissociates into smaller fragments.

### *4.3.2. Relaxation Pathways of $[I^-(CH_3OH)_n]^*$ (n=3)*

While high-level quantum-chemical calculations of $I^-(CH_3OH)_2$ have provided important insights into the various geometric and energetic factors and the underlying intermolecular interactions that influence the relaxation pathways of $[I^-(CH_3OH)_n]^*$, first-principles molecular dynamics simulations of larger clusters are needed to paint a clear picture of the molecular rearrangement taking place and its effect on the stability of the excited electron. Due to the small size of $I^-(CH_3OH)_2$, no substantial geometric rearrangement to stabilise the excess electron in the CTTS state is possible, and as such, simulations of the larger $[I^-(CH_3OH)_3]^*$ are performed to investigate the molecular rearrangement processes involved in the modulation of the stability of the excited electron. In order to examine the influence of the hydrogen-bonded network in the solvent cluster moiety of $I^-(CH_3OH)_n$ on the relaxation pathways, the simulations were initiated from two initial ground-state minimum energy $I^-(CH_3OH)_3$ geometries, ***ch3*** and ***dm*** (Figure 4.2); in the ***ch3*** configuration, a hydrogen-bonded ***ch***ain of ***3*** methanol molecules hydrogen-bonds to iodide, while in the ***dm*** configuration, a methanol ***d***imer and a methanol ***m***onomer are independently hydrogen-bonded to iodide. As the temperature of $I^-(CH_3OH)_n$ is estimated to be around 170 K under experimental conditions, the thermal energy is not significant compared to the kinetic energy gained by the system upon relaxation, and therefore simulations are initiated with no initial velocities (0 K conditions); this has the advantage of providing direct insight into the effects of the cluster configuration in the Franck-Condon region on the relaxation pathways, without possible thermal effects associated with the different initial velocities of the particles within the cluster.

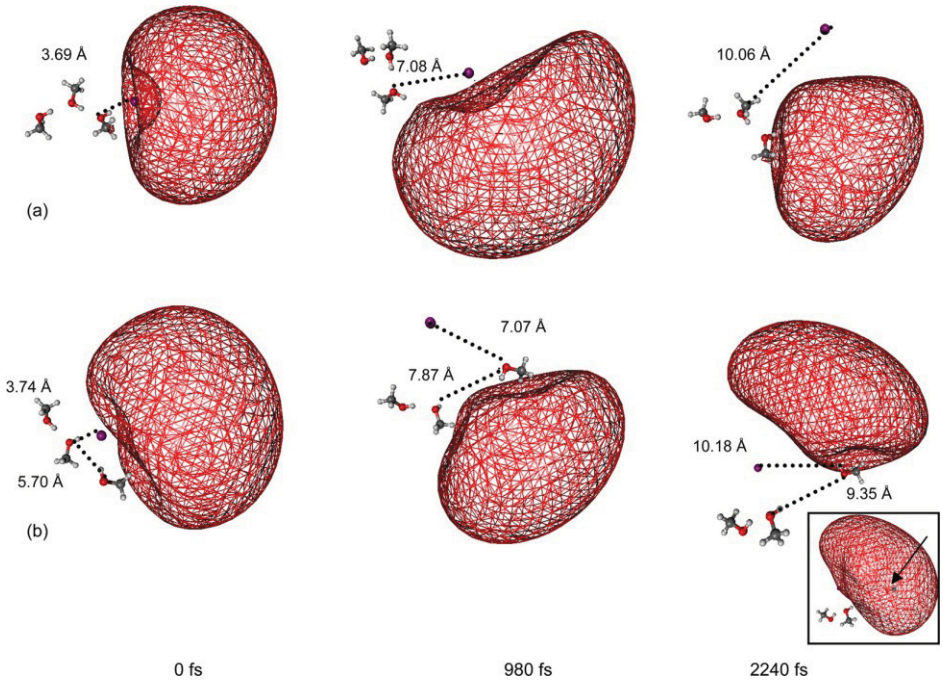


Figure 4.2. Snapshots of cluster configurations and HOMO surface plots from molecular dynamics simulations of (a) ***ch3*** $[I^-(CH_3OH)_3]^*$ and (b) ***dm*** $[I^-(CH_3OH)_3]^*$. The boxed inset at 2240 fs shows the HOMO surface plot of $(CH_3OH)_2^-$ at the geometry of ***dm*** $[I^-(CH_3OH)_3]^*$ (the arrow indicates the position of the $CH_3OH$ removed). Relevant distances are indicated on the figure. Isosurfaces encompass 25 % of the electron distribution.

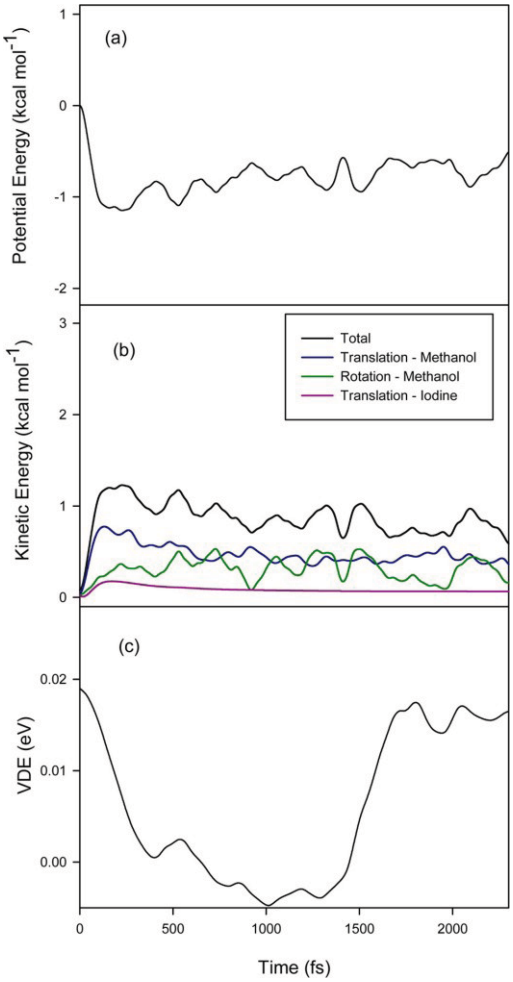


Figure 4.3. Time evolution of (a) the potential energy (b) the kinetic energy and its components and (c) the VDE for ***ch3*** $[I^-(CH_3OH)_3]^*$.

Snapshots of the simulated cluster geometries and surface plots of the highest-occupied molecular orbital (HOMO) for ***ch3*** and ***dm*** $[I^-(CH_3OH)_3]^*$ as the clusters relax following excitation are shown in Figure 4.2, while plots of the potential and kinetic energies and VDEs along the trajectory are shown in Figures 4.3 and 4.4 for ***ch3*** and ***dm*** $[I^-(CH_3OH)_3]^*$, respectively.

In the case of ***ch3*** $I^-(CH_3OH)_3$, simulation results suggest that, upon excitation, the clusters gradually separate into an iodine atom and a $(CH_3OH)_3^-$ moiety (Figure 4.2a). During the first 300 fs, the methanol molecule originally hydrogen-bonded to iodide in the ground state begins to rotate such that the hydroxyl hydrogen moves away from the neutral iodine in the CTTS state, resulting in a decrease of the cluster potential energy and an increase of the

kinetic energy (Figures 4.3a and 4.3b). As the rotation continues throughout the following 2 ps, the distance between $(CH_3OH)_3^-$ and I gradually increases, as more kinetic energy partitions into the translational motion of $CH_3OH$. This initial relaxation and energy lowering can be attributed to the difference in the optimal positions of an iodine atom and an iodide anion with respect to a methanol molecule. Quantum-chemical calculations with HF/6-31++G(d,p) and CCSD(T)/aug-cc-pVTZ both indicate that the energy of $I(CH_3OH)$ is around 1-2 kcal/mol higher at the minimum energy geometry of $I^-(CH_3OH)$ than at the minimum energy geometry of $I(CH_3OH)$, an effect similar to that observed for ***y41*** $[I^-(H_2O)_5]^*$.[*87*] The kinetic energy gained in the initial relaxation process is, however, significantly smaller for ***ch3*** $[I^-(CH_3OH)_3]^*$ (~ 1 kcal $mol^{-1}$) than for ***y41*** $[I^-(H_2O)_5]^*$ (~8 kcal $mol^{-1}$) since only one I ••• H close contact is present in the former cluster, resulting in a much less repulsive potential energy surface in the Franck-Condon region. As a consequence, the $(CH_3OH)_3$ hydrogen-bonded network is maintained, at least for 2.3 ps. Throughout the relaxation process, the excited-electron distribution remains roughly at the positive end of the $(CH_3OH)_3$ net dipole, and it gradually shifts away from the location of the neutral iodine atom (Figure 4.2a); this appears to be due to the combined rotation of the $CH_3OH$ molecules and gradual separation of $(CH_3OH)_3^-$ from I. As the relative orientations of the $CH_3OH$ dipoles fluctuate, the excited-electron VDE first decreases by around 0.02 eV over 1 ps, before increasing again by a similar amount over the following 1 ps (Figure 4.3c). While the simulated shifts in the excited-electron VDEs are small compared with those measured experimentally,[*27*] presumably due to the smaller size of the present cluster, the qualitative features of the simulated VDE profiles are in good agreement with the corresponding early-time experimental profiles. The present results suggest that dissociation to I and $(CH_3OH)_n^-$ combined with conformational changes in the $(CH_3OH)_3$ moiety may contribute to the experimentally observed modulation of the stability of the excited electron in $[I^-(CH_3OH)_n]^*$ early in the relaxation process.

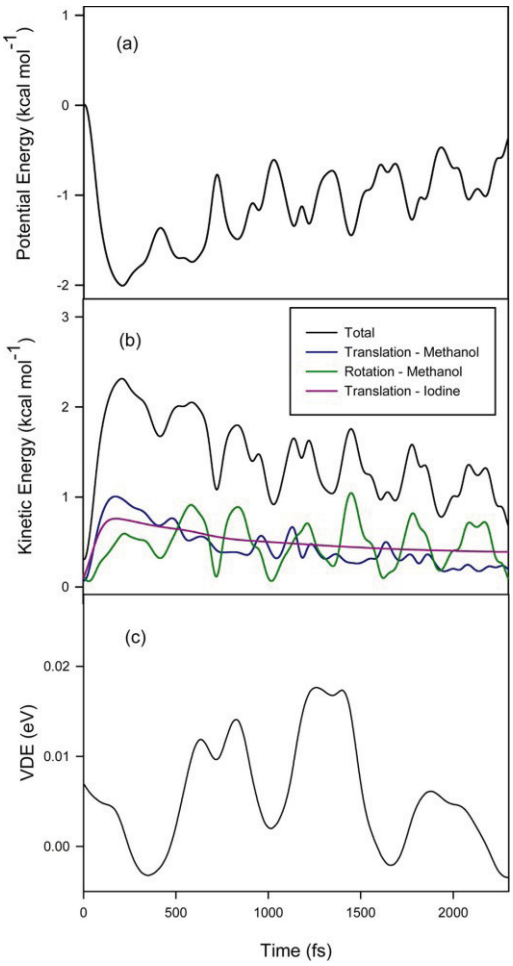


Figure 4.4. Time evolution of (a) the potential energy (b) the kinetic energy and its components and (c) the VDE for ***dm*** $[I^-(CH_3OH)_3]^*$.

In the case of ***dm*** $[I^-(CH_3OH)_3]^*$, snapshots of simulated cluster geometries and HOMO surface plots (Figure 4.2b) and profiles of the potential and kinetic energies and VDEs along the trajectory (Figure 4.4) paint a somewhat different picture of the relaxation mechanism. As in the case of ***ch3*** $[I^-(CH_3OH)_3]^*$, the inter-solvent hydrogen-bonding interactions originally present in the ground state are maintained as the clusters relax in the CTTS state. However, the cluster gradually separates into I, $(CH_3OH)_2^-$ and $CH_3OH$ fragments during the relaxation process due to the absence of a hydrogen-bonding interaction between the $(CH_3OH)_2$ and $CH_3OH$ moieties of the solvent cluster (Figure 4.2b). The potential energy initially decreases as the two $CH_3OH$ closest to I rotate to increase the I•••H separation, but then it gradually increases as the fragments slowly separate as a result of the kinetic energy gained in the initial relaxation (Figures 4.4a and 4.4b). Throughout the first 2.3 ps following

excitation, the rapid rotational motion of $CH_3OH$ (Figure 4.4b), particularly that of the $CH_3OH$ gradually departing from the cluster, results in oscillations of the cluster potential energy and the excited-electron VDE with a period of 200 - 500 fs (Figures 4.4a and 4.4c). The position of the excited-electron distribution changes dramatically as a result of fluctuations in the magnitude and direction of the net dipole moment of the cluster (Figure 4.2b). Furthermore, exclusion effects[*21, 32, 33, 43, 87*] arising from the departing $CH_3OH$ and I fragments appear to shift the excited-electron distribution further away from the remaining $(CH_3OH)_2$ fragment, such that the $(CH_3OH)_2$ fragment and the excess electron distribution are located roughly on opposite sides of a line connecting the departing I and $CH_3OH$ (Figure 4.2b, 2240 fs). While the fragmentation process is still ongoing at 2.3 ps, it may reasonably be expected that a $(CH_3OH)_2^-$ fragment will eventually be formed once I and the departing $CH_3OH$ have moved sufficiently far away that exclusion effects disappear (Figure 4.2b, inset at 2240 fs). The excess electron will then occupy the region where the departing fragments were located at 2.3 ps. It should be noted that the excited electron can also undergo autodetachment from the cluster during the fragmentation process if the dipole moments of the cluster fragments become too low to effectively bind the excited electron, and indeed $[I^-(CH_3OH)_4]^*$ was found to decay by autodetachment with a timescale of 0.8 ps in the femtosecond photoelectron spectroscopy experiments of Neumark and co-workers.[*27, 28*] The present simulation approach, in which the trajectories evolve on a single excited-state potential energy surface, is not capable of capturing autodetachment events occurring during the relaxation process. While the development of a more sophisticated simulation approach that takes into account non-adiabatic effects such as excited electron autodetachment may result in a more complete picture of the $[I^-(CH_3OH)_n]^*$ relaxation and decay process, the present simulations already highlight the important contribution of cluster fragmentation to the observed modulation of the stability of the excited electron in $[I^-(CH_3OH)_n]^*$. Since excess-electron VDEs of $(CH_3OH)_n^-$ generally decrease with decreasing cluster size,[*134*] slow fragmentation of the solvent cluster moiety in $[I^-(CH_3OH)_n]^*$ may contribute to the final gradual decrease of the experimentally observed excited-electron VDE and the decay of the cluster population over time.[*27, 28*]

The present simulation results highlight the influence of the solvent cluster configuration on the $[I^-(CH_3OH)_n]^*$ relaxation pathways and provide a molecular-level explanation of the convoluted modulation of the experimentally determined excited-electron VDE of these clusters. In cluster configurations in which all solvent molecules are bound *via* $CH_3OH$ •••

$CH_3OH$ hydrogen bonds, as exemplified by ***ch3***, the most important aspect of the relaxation process would involve the limited reorientation of the solvent molecules, which can lead to an increase in the cluster dipole moment and excited-electron VDE over a period of several ps. On the other hand, for configurations in which $I^-$ ••• $CH_3OH$ interactions disrupt the solvent network (by replacing some of the $CH_3OH$ ••• $CH_3OH$ interactions), such as ***dm***, relaxation pathways involving fragmentation of the solvent moiety would be facilitated due to the lower dissociation energies of the excited cluster, as shown earlier for ***mm*** $[I^-(CH_3OH)_2]^*$; this process, which is expected to occur even more readily at the estimated cluster temperatures of around 170 K, would lead to a decrease in stability of the excited electron, a lowering of the excited-electron VDE and the ultimate autodetachment of the excited electron. Both classes of relaxation pathways are expected to contribute to the time profile of the $[I^-(CH_3OH)_n]^*$ excited-electron VDE, which should be an average over an ensemble of initial conditions. The earlier increase of the excited-electron VDE can be attributed to solvent reorientation effects, which take place over a relatively short timescale and dominate the signal at early times, while the subsequent gradual decrease of the excited-electron VDE and decay of the cluster population can be attributed to the dominant contribution of fragmentation, a much slower process in which cluster fragments gradually move away from each other, after the maximum excited-electron VDE has been attained.

Results of the present work also provide a rational explanation for the stark contrast between $[I^-(CH_3OH)_n]^*$ and $[I^-(H_2O)_n]^*$ relaxation dynamics. While solvent reorientation leading to stabilisation of the excited electron is an important aspect of the relaxation pathways of both types of clusters, fragmentation leading to destabilisation and autodetachment of the excited electron is expected to be much more important for $[I^-(CH_3OH)_n]^*$ due to the disruption of the $CH_3OH$ ••• $CH_3OH$ interactions in the solvent moiety by the $I^-$ ••• $CH_3OH$ interactions in the initial ground-state $I^-(CH_3OH)_n$ configurations. On the other hand, in most low energy $I^-(H_2O)_n$ configurations, water molecules simultaneously participate in both $I^-$ ••• $H_2O$ and $H_2O$ ••• $H_2O$ interactions since water is a double hydrogen-bond donor, unlike the single hydrogen-bond donor methanol, leading to $I^-(H_2O)_n$ configurations with an extensively hydrogen-bonded water network that resists fragmentation in the excited state.[*72*] Structural features of the solvent molecules within $I^-(Solv)_n$ can thus have a profound influence on electron solvation pathways in $[I^-(Solv)_n]^*$.

## 4.4. Concluding Remarks

In this work, high-level quantum-chemical calculations and *ab initio* molecular dynamics simulations have been performed to develop an understanding of the relaxation dynamics of $[I^-(CH_3OH)_n]^*$ in terms of the cluster geometric and energetic properties and the underlying intermolecular interactions, and to gain insights into the solvent effects on electron solvation pathways in CTTS excited iodide-polar molecule clusters. Our results indicate that $[I^-(CH_3OH)_n]^*$ may undergo multiple relaxation pathways depending on the initial configuration of the cluster, a finding attributed to differences in the solvent-solvent interactions within the solvent moiety, which can influence the stability of the cluster in the CTTS state. While solvent cluster reorganisation can initially stabilise the excited electron, subsequent cluster fragmentation can destabilise the excited electron and ultimately lead to its detachment, explaining the experimentally observed fluctuations in the excited-electron VDE of $[I^-(CH_3OH)_n]^*$.[*27*] Our results also provide, for the first time, a rational explanation for the contrasting relaxation dynamics of $[I^-(CH_3OH)_n]^*$ and $[I^-(H_2O)_n]^*$; the more limited inter-solvent hydrogen bonding in methanol clusters relative to water clusters appears to increase the propensity for $[I^-(CH_3OH)_n]^*$ to undergo fragmentation, resulting in the ultimate destabilisation of the excited electron in $[I^-(CH_3OH)_n]^*$ and more rapid decay by autodetachment of $[I^-(CH_3OH)_n]^*$ than for $[I^-(H_2O)_n]^*$. The contrasting dynamics of $[I^-(CH_3OH)_n]^*$ and $[I^-(H_2O)_n]^*$ highlight the profound effects the intrinsic solvent molecular structure can have on the relaxation processes leading to electron solvation in $[I^-(Solv)_n]^*$, as observed by Neumark and co-workers.[*24-29, 46-48*]

# 5. New developments in first-principles excited-state dynamics simulations: unveiling the solvent specificity of excited anionic cluster relaxation and electron solvation

**Published As:**

Chun C. Mak and Gilles H. Peslherbe, *Molecular Simulation,* 2015, 41:156-167

## Abstract

Charge-transfer-to-solvent excited iodide-polar solvent molecule clusters, $[I^-(Solv)_n]^*$, have attracted substantial interest over the past 20 years as they can undergo intriguing relaxation processes leading ultimately to the formation of gas-phase molecular analogues of the solvated electron. In this review article, we present a comprehensive overview of the development and application of state-of-the-art first-principles molecular dynamics simulation approaches to understand and interpret results of femtosecond photoelectron spectroscopy experiments on $[I^-(Solv)_n]^*$ relaxation, which point to a high degree of solvent specificity in the electron solvation dynamics. The intricate molecular details of the $[I^-(Solv)_n]^*$ relaxation process are presented, and by contrasting the relaxation mechanisms of clusters with several different solvents (water, methanol, acetonitrile), the molecular basis of the solvent specificity of electron solvation in $[I^-(Solv)_n]^*$ is uncovered, leading to a more refined view of the manifestation of electron solvation in small gas-phase clusters.

## 5.1. Introduction

Photoexcitation of halides dissolved in polar liquids such as water, alcohols and acetonitrile results in the formation of charge-transfer-to-solvent (CTTS) excited states, in which an electron has been transferred from a halogen localised valence orbital to a more delocalised and solvent-supported orbital.[*15, 16*] Subsequent relaxation of CTTS excited halides in solutions results in the formation of solvated electrons,[*39*] ubiquitous species that play important roles in numerous chemical transformations. While CTTS excited states are intrinsically associated with bulk solutions, small complexes of iodide with polar solvent molecules such as acetone, acetonitrile and water do possess analogous excited states, and excitation to these states results in the formation of small electron-polar solvent complexes, which can be viewed as molecular analogues of the solvated electron.[*18-20*] CTTS iodide-polar solvent molecule complexes have thus served as important paradigms for understanding the transition from a free electron to the bulk solvated electron.

Substantial experimental work has been carried out to probe the nature of the relaxation processes of CTTS excited iodide-polar solvent molecule complexes, denoted hereafter $[I^-(Solv)_n]^*$, resulting in intriguing new insights into the manifestation of electron solvation processes in finite gas-phase systems.[*24-29, 46-48, 53*] Nevertheless, the development of a molecular-level understanding of the electron solvation dynamics of $[I^-(Solv)_n]^*$ and their relationship to the corresponding processes of solvated electron formation from CTTS excited halides in the solution phase has been a major challenge for modern theoretical and computational chemistry.

In this review article, we provide a comprehensive view of theoretical work on the properties and dynamics of $[I^-(Solv)_n]^*$, emphasising how an advanced molecular dynamics simulation approach combined with state-of-the-art electronic structure calculations have been used to unravel the relaxation mechanisms of $[I^-(Solv)_n]^*$ and to gain substantial new insights into the solvent specificity of electron solvation processes in clusters. By comparing the molecular details of the relaxation mechanism of different $[I^-(Solv)_n]^*$, we will also develop an understanding of the role of different molecular interactions for supporting and solvating an excess electron. The remainder of this article is organised as follows. In Section 2, an overview of the key experimental findings on $[I^-(Solv)_n]^*$ relaxation and a discussion of models of the relaxation process that have been proposed to explain these experimental findings is presented. In Section 3, the development of approaches based on first-principles

molecular dynamics simulations for elucidating the molecular details of the relaxation and electron solvation processes of $[I^-(Solv)_n]^*$ is described. This is followed in Section 4 with an overview of the relaxation mechanisms of the different $[I^-(Solv)_n]^*$ (Solv = $H_2O$, $CH_3OH$ and $CH_3CN$) that have been investigated with first-principles molecular dynamics simulations. The molecular basis of the solvent specificity of $[I^-(Solv)_n]^*$ relaxation dynamics is then discussed in Section 5. Finally, key conclusions regarding the factors that govern the electron solvation dynamics of $[I^-(Solv)_n]^*$ and some possible future directions in this area of research are presented in Section 6.

### 5.2. $[I^-(Solv)_n]^*$ relaxation dynamics: experimental results and early models

The relaxation dynamics of $[I^-(Solv)_n]^*$ (Solv = $H_2O$, $NH_3$, $CH_3OH$ and $CH_3CN$) have been probed extensively in a series of femtosecond photoelectron spectroscopy experiments by Neumark and co-workers to investigate the manner in which electron solvation processes behave in gas-phase solvent clusters.[*24-29, 46-48*] These experiments have revealed an intriguing dependence of the nature of the relaxation and electron solvation dynamics of $[I^-(Solv)_n]^*$ on the identity of the solvent. In the cases of $[I^-(H_2O)_n]^*$ ($n \geq 5$) [*24, 26, 46, 47*] and $[I^-(CH_3CN)_n]^*$ ($n \geq 5$),[*29*] the excited electron vertical detachment energy (VDE), which is directly related to the stability of the excited electron relative to detachment from the cluster, decreases sharply by up to 0.5 eV for several hundred femtoseconds following vertical excitation. Subsequently, the excited electron VDE increases over several picoseconds, typically to values that are substantially larger than the initial values. In smaller clusters, $[I^-(H_2O)_n]^*$ (n = 5-10) and $[I^-(CH_3CN)_n]^*$ (n = 5-8), the excited electron VDE eventually decreases by around 0.05eV at longer times. Both $[I^-(H_2O)_n]^*$ and $[I^-(CH_3CN)_n]^*$ decay *via* vibrational autodetachment of the excited electron, but in the case of $[I^-(CH_3CN)_n]^*$, the time scale of this process is too long to be observed experimentally. While the qualitative features of the time profiles of the excited electron VDE of $[I^-(CH_3OH)_n]^*$ bears some resemblance to the corresponding profiles of smaller $[I^-(H_2O)_n]^*$ and $[I^-(CH_3CN)_n]^*$, the final decrease of the excited electron VDE is far more pronounced for $[I^-(CH_3OH)_n]^*$, which also decays by excited electron autodetachment over a much shorter time scale.[*27, 28*] Time profiles of the $[I^-(NH_3)_n]^*$ excited electron VDE lack the fluctuations observed for the other complexes; the excited electron VDE increases before becoming relatively constant, after which the clusters decay, presumably by autodetachment over time scales that are similar to those for $[I^-(CH_3OH)_n]^*$.[*25*] While stabilisation of the

excited electron at early times following excitation of $I^-(Solv)_n$ appears to be a common feature of all $[I^-(Solv)_n]^*$, the longer-time evolution of the stability of the excited electron exhibits substantial variation with the identity of the solvent, a reflection of the profound influence of the nature of the solvent on the longer-time dynamics and stability of $[I^-(Solv)_n]^*$.

Based on the features of the experimentally determined time profiles of the excited electron VDEs and early ("single-point") quantum-chemical calculations of the excited electron VDE for a collection of $[I^-(H_2O)_n]^*$ cluster configurations differing only in the relative position of the iodine atom with respect to a rigid solvent cluster, two models of $[I^-(Solv)_n]^*$ relaxation dynamics emerged, one emphasising the role of the solvent molecules[*24, 46, 47*] while the other emphasising the role of the iodine formed post-excitation.[*32, 33*] While these models were mainly proposed to describe the relaxation dynamics of $[I^-(H_2O)_n]^*$, they have also been applied to understand the relaxation processes of other $[I^-(Solv)_n]^*$.[*27, 29*]

Neumark and co-workers were the first to discuss the effects of solvent reorganisation on the stability of the excited electron,[*24*] based on earlier work in which multiple isomers of water cluster anions with different excess electron VDEs had been identified.[*30, 31, 135*] In the cases of water and acetonitrile clusters, the solvent cluster moiety was believed to undergo reorganisation that led to an increased stability of the excited electron.[*24, 29, 46-48*]. On the other hand, the observed destabilisation of the excited electron in methanol clusters, which had a much shorter lifetime than the water and acetonitrile clusters, was explained by the occurrence of solvent reorganisation to destabilise the excited electron.[*27*] In this so-called 'solvent-driven' model of $[I^-(Solv)_n]^*$ relaxation dynamics, $[I^-(Solv)_n]^*$ were viewed as an electron-solvent cluster with an extra iodine atom acting as a spectator, with limited effects on the excess electron.

Chen and Sheu were the first to describe the potential role of iodine in the $[I^-(Solv)_n]^*$ (Solv = $H_2O$) relaxation process, proposing the so-called 'iodine-driven' model of $[I^-(Solv)_n]^*$ relaxation dynamics.[*32*] Using quantum-chemical calculations, it was found that the iodine atom exerted a destabilising effect on the excited electron distribution of $[I^-(H_2O)_n]^*$ due to the exclusion effects resulting from the valence electrons of the iodine atom.[*21*] Ejection of the iodine atom from the cluster would thus result in an increased stability of the excited electron, accounting for the observed increase in the excited electron VDE of $[I^-(H_2O)_n]^*$ following photoexcitation.[*32, 33*] Although the original calculations assumed a fixed water

cluster geometry (*i.e.* the geometry of the solvent moiety was kept unchanged as iodine was removed from the cluster), they nevertheless provided valuable insights into the effects of iodine on the stability of the excited electron, and highlighted the importance of taking into account the iodine atom in the interpretation of $[I^-(Solv)_n]^*$ relaxation dynamics.

The solvent-driven and iodine-driven models of $[I^-(Solv)_n]^*$ relaxation dynamics provided, together, a useful framework for understanding the relaxation mechanisms of $[I^-(Solv)_n]^*$, but they failed to provide a concrete, comprehensive picture of the actual relaxation processes. In addition, a more detailed analysis of the relative importance of solvent reorganisation and iodine detachment in $[I^-(Solv)_n]^*$ relaxation dynamics was not possible based on the available experimental observations and quantum-chemical calculations, and a detailed understanding of the solvent specificity of $[I^-(Solv)_n]^*$ relaxation dynamics remained beyond the reach of these relatively simplistic models. It was the development of highly sophisticated first-principles molecular dynamics simulation approaches for $[I^-(Solv)_n]^*$, discussed in the following section, that allowed the elucidation of the actual relaxation mechanisms, made it possible to untangle the roles of solvent and iodine in the relaxation processes and provided a comprehensive understanding of the solvent specificity of the electron solvation dynamics.

### 5.3. First-principles molecular dynamics simulation approaches for $[I^-(Solv)_n]^*$

First-principles molecular dynamics simulations of $[I^-(Solv)_n]^*$ have proven highly valuable for providing a detailed molecular-level picture of their relaxation dynamics, and such simulations have been used to investigate $[I^-(Solv)_n]^*$ (Solv = $H_2O$, $CH_3CN$ and $CH_3OH$), leading to a picture of rich and varied relaxation and electron solvation dynamics.[*34-38, 87, 88, 97, 129, 131*] The basic approach employed in these simulations is conceptually relatively simple; classical molecular dynamics simulations of $[I^-(Solv)_n]^*$ are performed, typically initiated from a representative ground-state $I^-(Solv)_n$ geometry (often simply the minimum energy geometry), with the energies and forces that are required for the propagation of the equations of motion obtained from quantum-chemical calculations performed at each step. Electronic properties of the clusters, such as their dipole moments, excited electron VDEs and excited electron distributions can be computed for configurations sampled along the trajectory for analysis and connection with experiment. Nevertheless, first-principles molecular dynamics simulations of $[I^-(Solv)_n]^*$ represent numerous significant challenges due to the complex potential energy surfaces of ground and excited

$I^-(Solv)_n$, the subtle dispersion interactions that are involved in the binding of the extremely diffuse excited electron with the neutral cluster framework, the uncertainties in the initial temperatures of $I^-(Solv)_n$, and possible zero point vibrational energy leakage that could corrupt the dynamics, leaving significant room for improvement of the simulation methodology.

The first reported first-principles molecular dynamics simulation of $[I^-(Solv)_n]^*$ (Solv = $H_2O$, n = 3), by Timerghazin and Peslherbe, was initiated from the ground-state global minimum energy geometry of $I^-(H_2O)_3$, with no initial kinetic energy in the cluster vibrational modes.[*34*] While this work provided the first glimpse of the molecular details of $[I^-(Solv)_n]^*$ relaxation dynamics, it also highlighted the need to take into account numerous trajectories initiated from an ensemble of cluster configurations at finite temperature in order to draw a proper connection with experiment. Despite subsequent efforts to explore the effects of the Franck-Condon geometry[*36, 37, 88, 97*] and temperature[*38*] on $[I^-(Solv)_n]^*$ relaxation dynamics, and our recent simulations of CTTS excited $I^-(CH_3CN)$ taking into account a large collection of initial conditions[*131*], there has thus far not been any attempt to perform large-scale first-principles molecular dynamics simulations of the larger $[I^-(Solv)_n]^*$ for which substantial electron solvation dynamics have been observed in experiment, due to the immense computational cost they would involve.

Due to the classical treatment of the motion in molecular dynamics simulations of $[I^-(Solv)_n]^*$, transfer of kinetic energy from the high-frequency intramolecular vibrational modes of the solvent molecules to the lower frequency intermolecular vibrational modes of the cluster is in principle allowed, a process known as zero-point energy leakage,[*59, 60, 133*] which can lead to artefacts in the simulated dynamics, such as the potential overestimation of cluster fragmentation. Bowman and co-workers have shown that in quasiclassical trajectory simulations of the water trimer in which unconstrained energy transfer between all cluster vibrational modes is allowed, rapid dissociation of the cluster into free water molecules is observed within a few picoseconds since the total kinetic energy present in the system at 0 K (~46 kcal/mol) significantly exceeds the water trimer dissociation energy of *ca*. 16 kcal/mol.[*136*] On the other hand, no cluster dissociation is observed within the same time frame, which reflects a physically more realistic picture, when the simulations are performed using a constrained quasiclassical method in which the energy in each cluster vibrational mode is constrained to remain above the zero-point level,

effectively eliminating zero-point energy leakage during the simulations. While the constrained quasiclassical method described by Bowman and co-workers rigorously treats zero-point energy in cluster vibrational modes during molecular dynamics simulations, the computational cost would be prohibitive for first-principles molecular dynamics simulations of $[I^-(Solv)_n]^*$. In our recent work on $[I^-(H_2O)_n]^*$ and $[I^-(CH_3OH)_n]^*$,[*87, 88*] we have instead used rigid solvent molecules in simulations performed in quaternion coordinates[*56*] using a Gear predictor-corrector algorithm,[*58*] which also eliminates the possibility of zero-point energy leakage from high-frequency solvent vibrational modes.

One of the greatest challenges associated with first-principles molecular dynamics simulations of $[I^-(Solv)_n]^*$ is the development of a suitable electronic structure method for describing the interaction between the excited electron distribution and the neutral cluster framework in the CTTS state. The excited electron distributions of $[I^-(Solv)_n]^*$ are extremely diffuse and the excited electron occupies a region of space much larger than the neutral cluster framework, often with a fairly small binding energy. As shown in previous work on small electron-polar molecule complexes, the proper description of the interaction of a highly diffuse excess electron with a neutral molecule or collection of neutral molecules dictates the use of electronic structure calculations involving an extremely high level of electron correlation, such as Coupled Cluster theory with Single, Double and perturbative Triple excitations [CCSD(T)], and a very large basis set that includes an ample number of diffuse functions to describe the distribution of the excess electron.[*102, 104-107*] However, the prohibitive computational cost associated with calculations employing such model chemistries preclude their use in first-principles molecular dynamics simulations, which typically require energy and gradient calculations to be performed over several thousand molecular dynamics steps. Furthermore, the use of a large numbers of diffuse basis functions may lead to linear dependence issues in the basis set and convergence problems, that can be exacerbated when these functions are placed on multiple atomic centres to describe the rapidly changing excited electron distribution during $[I^-(Solv)_n]^*$ relaxation.[*102*] Due to these difficulties, it has to date not been possible to simulate the relaxation and electron solvation dynamics of $[I^-(Solv)_n]^*$ with model chemistries providing reliable excited electron VDEs that can be directly connected with experiment.

In order to be able to efficiently simulate the relaxation processes of $[I^-(Solv)_n]^*$ while, at the same time, computing reliable excited electron VDEs which can be used to understand the

effects of the relaxation process on the stability of the excited electron in the cluster, almost all first-principles molecular dynamics simulations of $[I^-(Solv)_n]^*$ that have been reported to date employ a dual-level approach.[*36-38, 87, 88, 129, 131*] In this approach, a lower level of theory and relatively compact basis sets are used for the description of the excited-state potential energy surface in the course of the dynamics, while a far more rigorous model chemistry is used for the calculation of the excited electron VDEs, which are more heavily influenced by subtle electron correlation effects. We note that this dual-level approach has long been used by quantum chemists, who typically optimise molecular geometries with a more approximate model chemistry than the one they use for recalculating energetics and other molecular or electronic properties.[*137*] Since the primary purpose of the actual molecular dynamics simulations of $[I^-(Solv)_n]^*$ is to obtain a real-time dynamical picture of the evolution of the cluster configuration in the excited state and produce configurations for analysis of the evolution of the electronic properties of the CTTS states as the clusters relax, the model chemistry selected for the energy and gradient calculations of the CTTS state must reproduce correctly the features of the excited-state potential energy surface of the cluster. To this end, relatively inexpensive quantum-chemical calculations employing Configuration Interaction with Single (CIS) excitations,[*114*] Complete-Active-Space Self-Consistent-Field (CASSCF) theory [*61, 62*] and Density-Functional Theory (DFT) with the B3LYP[*138*] functional, combined with modest double-zeta-quality basis sets, have been shown to provide a reliable description of the CTTS state potential energy surface when compared with more rigorous calculations employing second-order Complete-Active-Space Perturbation Theory (CASPT2),[*63*] Multireference Configuration Interaction (MRCI)[*139-141*] or CCSD(T)[*108, 109*] and larger basis sets with more diffuse functions.[*36-38, 88, 97, 131*]

First-principles molecular dynamics simulations are performed with the less computationally intensive model chemistries, and geometric configurations are then selected from the propagated trajectories. More rigorous model chemistries are then used in calculations of the excited electron VDE and other properties of the CTTS states for these configurations. The rigorously computed excited electron VDEs and CTTS state electronic properties are then used to develop a connection between simulations and experiment and to understand how the relaxation process influences the stability of the excited electron. It is of importance to note that, while the excited electron VDEs of $[I^-(Solv)_n]^*$, which depend on the energy difference between the excited and ionised states of the cluster, are heavily dependent on high-order electron correlation effects, the numerical values of the binding energies of the highly diffuse

excited electron to the neutral cluster are small, accounting for less than 10% of the total binding energy of $[I^-(Solv)_n]^*$.[*88*] As such, the features of the excited-state potential energy surfaces of $[I^-(Solv)_n]^*$ are to a great extent determined by the other interactions within the cluster, such as the solvent-solvent and iodine-solvent interactions, which appear to be well described with lower levels of electronic structure theory and more modest basis sets. Therefore, such model chemistries adequately describe the excited-state potential energy surfaces of $I^-(Solv)_n$ despite being questionable for the computation of excited electron VDEs, providing a sound theoretical justification for the dual-level approach commonly employed in first-principles molecular dynamics simulations of $[I^-(Solv)_n]^*$.

### 5.4. Relaxation pathways of $[I^-(Solv)_n]^*$

In this section, a brief summary of the main features of the relaxation and electron solvation dynamics of different $[I^-(Solv)_n]^*$ (Solv = $H_2O$, $CH_3OH$ and $CH_3CN$) is provided to facilitate the discussion of the solvent specificity of the relaxation and electron solvation dynamics, which follows in Section 5.

#### *5.4.1. $[I^-(H_2O)_n]^*$*

As water is the most frequently encountered of all solvents on earth, it is not surprising that $[I^-(H_2O)_n]^*$ was the first $[I^-(Solv)_n]^*$ to have been investigated with first-principles molecular dynamics simulations,[*34*] and there is now a clear molecular-level picture of the relaxation and electron solvation dynamics of $[I^-(H_2O)_n]^*$. While the precise details of the simulated $[I^-(H_2O)_n]^*$ dynamics can vary with cluster size, the Franck-Condon cluster configuration and the precise model chemistry employed to describe the cluster potential energy surface,[*34-38, 87, 129*] the main features of the $[I^-(H_2O)_n]^*$ relaxation process are similar in all cases. Snapshots of cluster configurations from our recent CASSCF molecular dynamics simulations of $[I^-(H_2O)_5]^*$[*87*] are shown with the excited and excess electron distributions, respectively, of $[I^-(H_2O)_5]^*$ and $(H_2O)_5^-$ (computed at the geometry of the former) in Figure 5.1, while simulated time profiles of the excited and excess electron VDEs of these two clusters (computed at the CASPT2 level of theory) are shown together in Figure 5.2. The time evolution of the excited electron VDEs derived from these simulations closely resemble those obtained from other $[I^-(H_2O)_5]^*$ simulations initiated from the same initial cluster configuration in which other approximate model chemistries, including density-functional theory[*37*] and the CASSCF method with a different basis set,[*38*] are used to compute the

required energies and energy gradients at each simulation step. The general features of the simulated relaxation and electron solvation dynamics of $[I^-(H_2O)_n]^*$ do not appear to be particularly sensitive to the precise model chemistry used in the description of the excited-state potential energy surface as long as the iodine-solvent and solvent-solvent interactions in the excited cluster are reasonably well-described, consistent with the fact that these interactions to a large extent determine the stability and geometric features of $[I^-(Solv)_n]^*$.[*142*] The relaxation process of $[I^-(H_2O)_n]^*$ is in general characterised by the rapid initial rotational motion of the water molecules originally forming hydrogen bonds with iodide in the ground state, leading to a rapid decrease in the excited electron VDE, followed by reorganisation of the solvent cluster to higher dipole moment configurations with higher excited electron VDEs. Throughout the relaxation process, the excited electron locates away from the iodine atom as it adjusts to the changing dipole moment of the cluster (Figure 5.1), and the iodine atom-excited electron interaction becomes negligible within 200 fs of excitation, as indicated by the nearly identical VDEs of the excited and excess electron for $[I^-(H_2O)_5]^*$ and $(H_2O)_5^-$ after 200 fs (Figure 5.2). The relaxation of $[I^-(H_2O)_n]^*$ can thus be viewed as a process of separation of iodine from the excited electron, followed by a solvent-cluster reorganisation process to stabilise the excited electron, a mechanism that appears to incorporate elements of both the iodine-driven and solvent-driven models of $[I^-(H_2O)_n]^*$ relaxation dynamics.

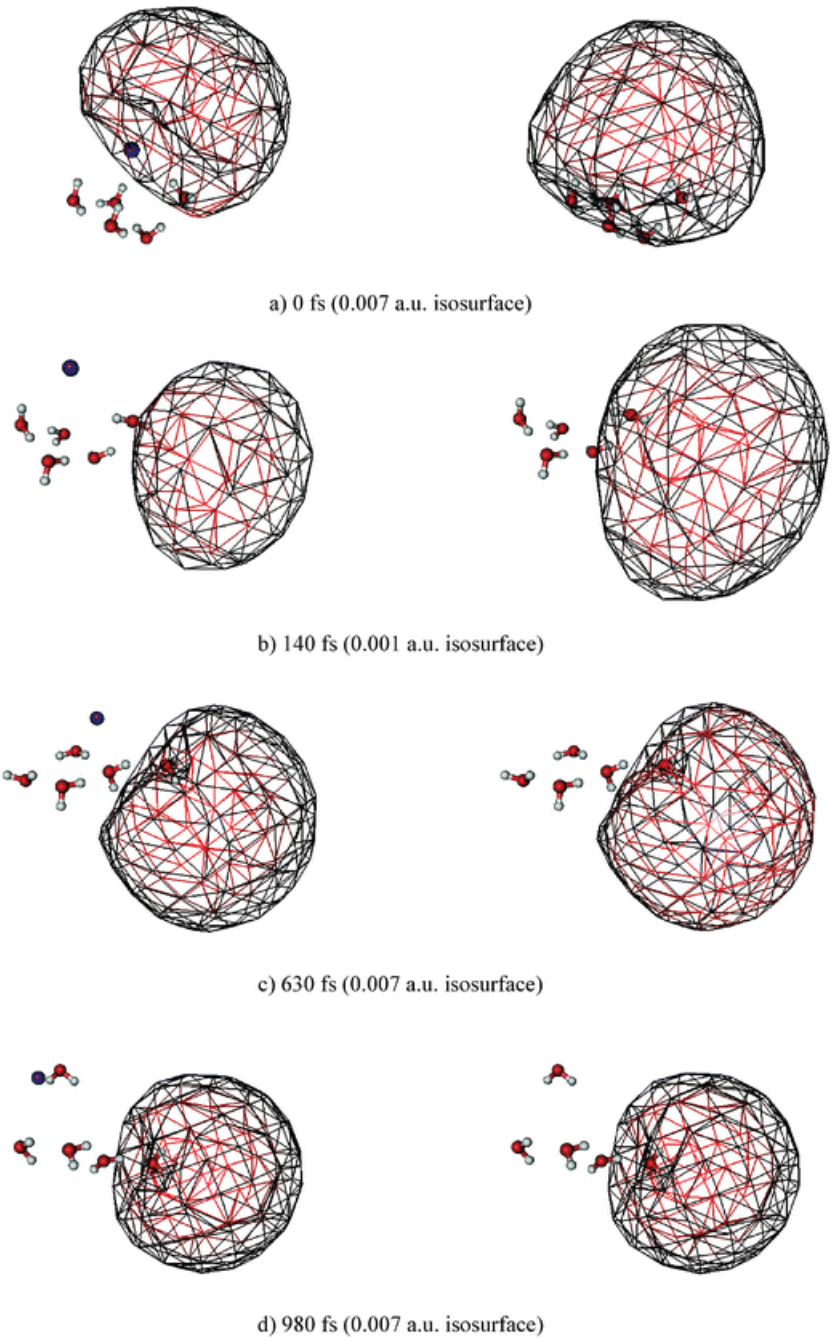


Figure 5.1. Cluster configurations and excited/excess electron distributions of $[I^-(H_2O)_5]^*$ and $(H_2O)_5^-$ at the geometries of $[I^-(H_2O)_5]^*$ obtained from molecular dynamics simulations (reproduced with permission from ref. 29 and identical to Figure 2.1). The iodine atom and the excited electron are essentially separated at 140 fs; after this time the excited and excess electron distributions of $[I^-(H_2O)_5]^*$ and $(H_2O)_5^-$ become increasingly similar as the clusters undergo further reorganisation.

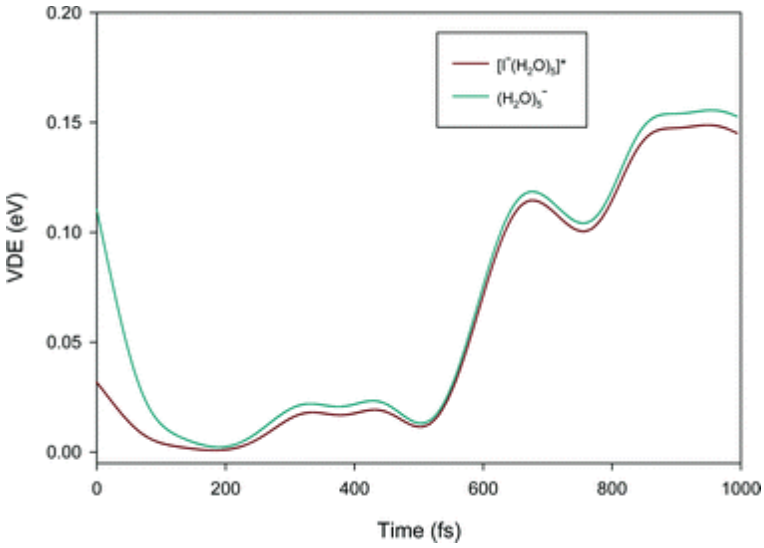


Figure 5.2. Time profiles of the excited/excess electron VDEs of $[I^-(H_2O)_5]^*$ and $(H_2O)_5^-$ computed at the water cluster geometries of $[I^-(H_2O)_5]^*$ obtained from molecular dynamics simulations (reproduced with permission from ref. 29 and identical to Figure 2.7). $[I^-(H_2O)_5]^*$ and $(H_2O)_5^-$ have almost identical excited/excess electron VDEs after 200 fs, and the gradual increase in both VDEs after this time can be attributed almost entirely to solvent cluster reorganisation.

### *5.4.2. $[I^-(CH_3OH)_n]^*$*

Despite the similarities between water and methanol as hydroxylic solvents, preliminary first-principles molecular dynamics simulations of $[I^-(CH_3OH)_n]^*$ (n = 3), which employed a similar CASSCF-based model chemistry to compute the energy and gradients as in the previously described $[I^-(H_2O)_5]^*$ simulations, indicate that there are critical differences in the relaxation dynamics of $[I^-(CH_3OH)_n]^*$ and $[I^-(H_2O)_n]^*$,[*88*] consistent with the differing experimental time profiles of the excited electron VDEs of these two clusters reported.[*26-28*] These simulations were initiated from two $I^-(CH_3OH)_n$ configurations, ***ch3*** and ***dm***, with different hydrogen-bond networks, shown in Figure 5.3a. In the ***ch3*** configuration, ***3*** methanol molecules are ***ch***ained together through hydrogen bonds with each other, and iodide is attached to the terminal methanol through the single dangling hydrogen atom, while in the ***dm*** configuration, a methanol ***d***imer and a methanol ***m***onomer each form separate hydrogen bonds with iodide. Simulation results indicate that the early stages of $[I^-(CH_3OH)_n]^*$ relaxation, which involve rapid initial rotation of the solvent molecules originally forming hydrogen bonds with iodide in the ground state, leading to an initial decrease in the excited

electron VDE and location of the excited electron away from the iodine atom, and a subsequent cluster reorganisation process leading to a temporary increase in the excited electron VDE, in fact appear to be quite similar to the corresponding stages of $[I^-(H_2O)_n]^*$ relaxation. The subsequent relaxation processes, however, differ starkly from those of $[I^-(H_2O)_n]^*$ depending on the initial $[I^-(CH_3OH)_n]^*$ cluster configuration. In ***ch3*** $[I^-(CH_3OH)_3]^*$, iodine and the solvent cluster moiety gradually separate from each other eventually forming a methanol trimer anion and an iodine atom (Figure 5.3b, top), while ***dm*** $[I^-(CH_3OH)_3]^*$ undergoes a more dramatic fragmentation process in which the original cluster framework separates into an iodine atom, a methanol molecule and a methanol dimer anion with lower excess electron VDE than the original $[I^-(CH_3OH)_3]^*$ (Figure 5.3b, bottom). The propensity for ***dm*** $[I^-(CH_3OH)_3]^*$ to undergo fragmentation was attributed to the more limited hydrogen-bonded network of the solvent moiety and the lower dissociation energy relative to ***ch3*** $[I^-(CH_3OH)_3]^*$.[*88*] Due to the fact that methanol, unlike water, is a single hydrogen-bond donor, the ground-state configurations of $I^-(CH_3OH)_n$ are expected to be determined by the competition between $CH_3OH$ ••• $CH_3OH$ and $I^-$ ••• $CH_3OH$ interactions, resulting in cluster configurations with a more disrupted solvent network than for $I^-(H_2O)_n$. This feature of iodide-methanol clusters is expected to increase the propensity for cluster fragmentation in the excited state, explaining the substantial decrease in the excited electron VDE of $[I^-(CH_3OH)_n]^*$ at longer times, as observed experimentally by Neumark and co-workers.[*26-28*]

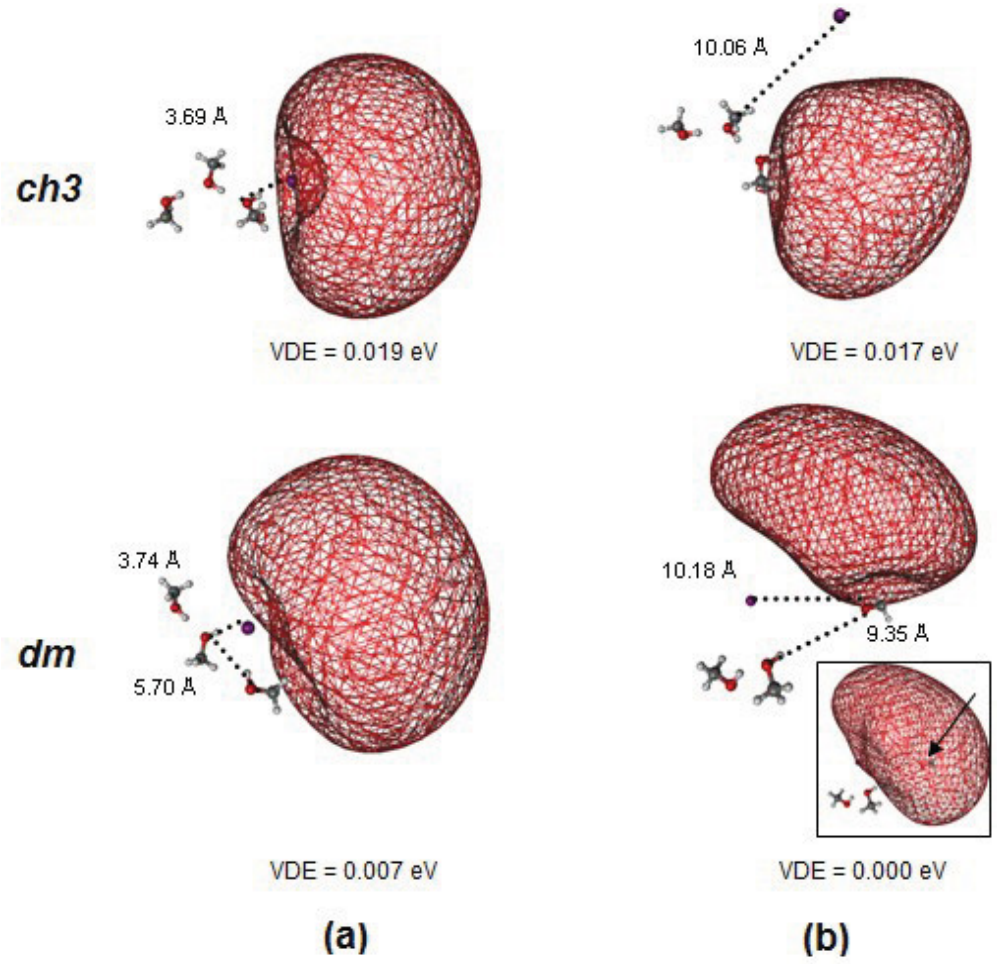


Figure 5.3. Cluster configurations and excited electron distribution of ***ch3*** and ***dm*** $[I^-(CH_3OH)_3]^*$ at (a) 0 fs and (b) 2240 fs obtained from molecular dynamics simulations. The inset in (b) shows the excess electron distribution of $(CH_3OH)_2^-$, formed by removal of I and the departing $CH_3OH$ from ***dm*** $[I^-(CH_3OH)_3]^*$ at 2240 fs. ***Ch3*** $[I^-(CH_3OH)_3]^*$ dissociates into I and $(CH_3OH)_3^-$ while ***dm*** $[I^-(CH_3OH)_3]^*$ fragments to form I, $CH_3OH$ and $(CH_3OH)_2^-$ (adapted from Figure 4.2).

### *5.4.3 $[I^-(CH_3CN]^*$*

The relaxation dynamics of $[I^-(CH_3CN)_n]^*$ (n = 1-3) has been investigated with first-principles molecular dynamics simulations in order to gain insight into the role and motion of an individual solvent molecule in CTTS relaxation dynamics[*131*] and to probe the effects of initial solvation structure on the formation of anionic solvent clusters from CTTS excited iodide-polar molecule clusters.[*97*] Results of first-principles molecular dynamics

simulations of $[I^-(CH_3CN)]^*$ performed on a potential energy surface computed at the CIS level of theory with a small double-zeta-quality basis set and initiated from 128 ground-state $I^-(CH_3CN)$ initial conditions at 150 K indicate that $[I^-(CH_3CN)]^*$ undergoes fairly rapid dissociation into I and $CH_3CN^-$ (Figure 5.4), leading to a decrease in the excited electron VDE (Figure 5.5). The iodine-acetonitrile distance increases rapidly, and for most of the trajectories, this distance exceeds 10 Å after 2 ps, while for a few trajectories, this distance can reach up to 20 Å. Furthermore, unlike for $[I^-(H_2O)_n]^*$ and $[I^-(CH_3OH)_n]^*$, the relaxation process is dominated by the relative translational motion between iodine and acetonitrile, although rotational motion of acetonitrile may also be important. The $[I^-(CH_3CN)]^*$ relaxation pathway predicted by our simulations appears to be supported by the results of recent time-resolved photoelectron imaging experiments performed on $[I^-(CH_3CN)]^*$, which indicate that the complex does indeed undergo fairly rapid dissociation into an iodine atom and an acetonitrile anion, which subsequently undergoes electron autodetachment on a much slower time scale.[*143*] Translational motions of $CH_3CN$ also appear to be the dominant aspect of $[I^-(CH_3CN)_n]^*$ (n = 2, 3) relaxation dynamics. Takayanagi showed, using first-principles molecular dynamics simulations employing a density functional theory based description of the cluster potential energy surface, that symmetric $[I^-(CH_3CN)_n]^*$ relaxes to produce $CH_3CN^-$ and neutral acetonitrile molecules, while asymmetric $[I^-(CH_3CN)_n]^*$ undergoes relaxation to form acetonitrile cluster anions $(CH_3CN)_n^-$.[*97*] These simulation results provide evidence that the molecular motions involved in the relaxation process of $[I^-(CH_3CN)_n]^*$ may differ substantially from those involved in $[I^-(H_2O)_n]^*$ and $[I^-(CH_3OH)_n]^*$ relaxation. These differences appear to originate from the molecular structure of $CH_3CN$, which has a much higher moment of inertia and thus greater resistance to rotational excitation than either $H_2O$ or $CH_3OH$, and the prevalence of symmetric solvation structures in which iodide is essentially surrounded by the acetonitrile molecules, which are unique to $I^-(CH_3CN)_n$, at least for the small clusters that are of interest here.[*89, 144*] A more detailed understanding of the actual processes leading to electron stabilisation and solvation in $[I^-(CH_3CN)_n]^*$ as observed by Neumark and co-workers[*29*] will, however, require additional molecular dynamics simulations of $[I^-(CH_3CN)_n]^*$ (n > 1) initiated from a collection of representative local minimum energy configurations, and rigorous computations of the excited electron VDEs as the clusters relax in the CTTS state.

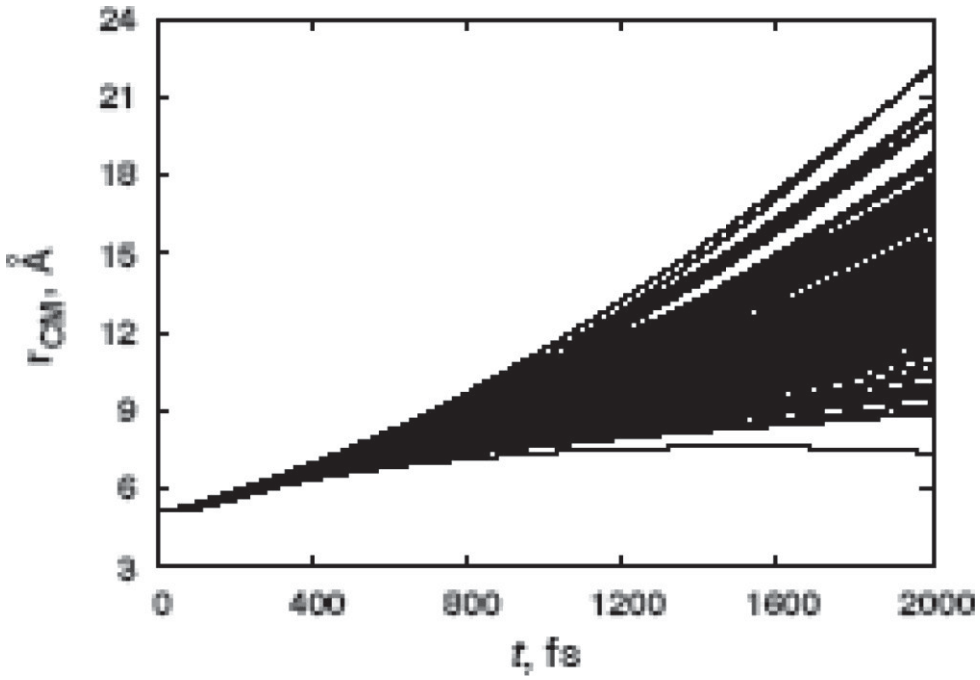


Figure 5.4. Time evolution of the iodine-carbon distance along 128 trajectories of $[I^-(CH_3CN)]^*$ (reproduced with permission from ref. 30 and identical to Figure 3.7). The iodine and acetonitrile moieties are more than 10 Å apart for most trajectories after 2 ps.

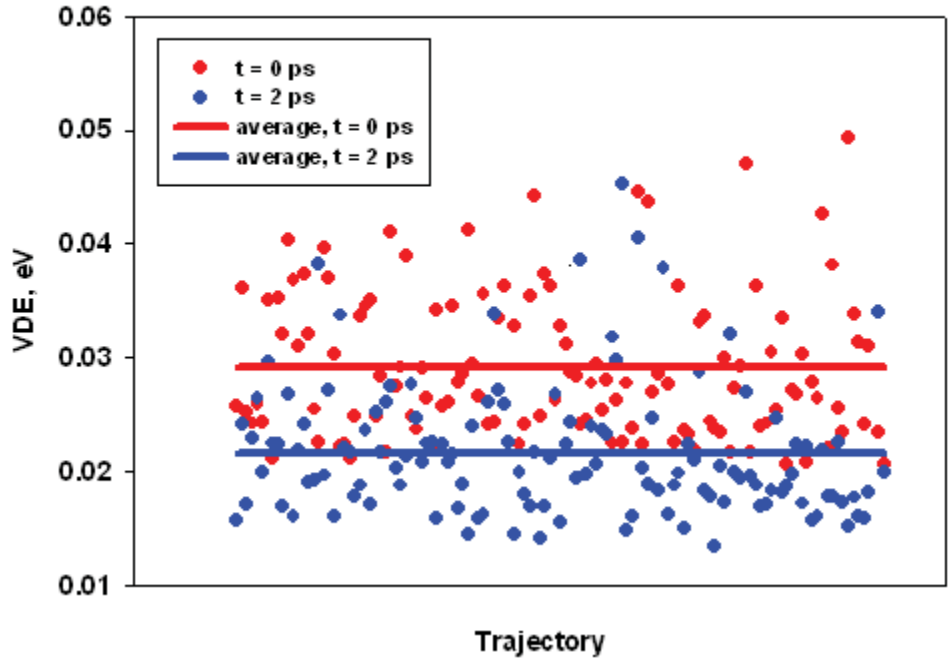


Figure 5.5. Excited electron VDEs of $[I^-(CH_3CN)]^*$ 0 ps and 2 ps after excitation taken from 128 trajectories (reproduced with permission from ref. 30 and identical to Figure 3.9). The

$[I^-(CH_3CN)]^*$ excited electron VDEs are on average lower than they were initially after 2 ps following excitation.

### 5.5. Molecular interactions in $[I^-(Solv)_n]^*$ and solvent specificity of electron solvation dynamics

The rich and varied relaxation dynamics of $[I^-(Solv)_n]^*$ provide a valuable opportunity to develop a fundamental understanding of the role of individual molecules and molecular interactions in trapping and stabilising a diffuse excess electron in clusters to form gas-phase molecular analogues of the solvated electron. By analysing the contrasting relaxation and electron solvation dynamics of $[I^-(Solv)_n]^*$ for which the molecular details of the relaxation dynamics are well characterised, it is possible to develop an understanding of the factors governing electron solvation in small iodide-polar solvent molecule clusters excited to the CTTS state. In this section we describe some general features of $[I^-(Solv)_n]^*$ that are common to all the solvent clusters that have been investigated computationally and show how intricate differences in the properties of the solvent molecules forming the cluster can lead to the intriguing solvent specificity of the electron solvation dynamics. Iodine effects on the electron solvation processes of different $[I^-(Solv)_n]^*$ are also discussed in order to provide a more complete view of $[I^-(Solv)_n]^*$ relaxation dynamics.

A comparison of the simulated relaxation dynamics of $[I^-(Solv)_n]^*$ (Solv = $H_2O$, $CH_3OH$ and $CH_3CN$) indicates that the relaxation process can be roughly viewed as comprising two somewhat distinct phases, which involve a rapid initial relaxation process that results in the separation of the excited electron and the iodine atom formed in the vertical CTTS excitation process, followed by a more gradual reorganisation process with variable effects on the stability of the excited electron, depending on the identity of the solvent. The early-time relaxation process, which takes place within 200 fs in the case of $[I^-(H_2O)_n]^*$[*34-38, 87, 129*] and $[I^-(CH_3OH)_n]^*$[*88*] and around 500 fs in the case of $[I^-(CH_3CN)_n]^*$[*97*], appears to be due to the repulsive nature of the potential energy surfaces of $[I^-(Solv)_n]^*$ in the Franck-Condon region,[*76, 88, 97, 131*] which results in rapid solvent motion leading to a rapid decrease in the cluster potential energy and a concomitant increase in the cluster kinetic energy. The kinetic energy acquired in the early phase of $[I^-(Solv)_n]^*$ relaxation drives the subsequent cluster reorganisation process, the nature of which varies with the solvent and the intermolecular interactions within the cluster. While the first stage of the cluster relaxation process generally leads to a decrease in the excited electron VDE due mainly to the decrease

in the dipole moment of the solvent cluster network resulting from the rotational motion of the solvent molecules, the effects of the subsequent cluster reorganisation process on the excited electron VDEs can be highly variable, depending heavily on the nature of the solvent cluster configuration and the intermolecular interactions within the cluster; electron stabilisation occurs in the case of $[I^-(H_2O)_n]^*$ and $[I^-(CH_3CN)_n]^*$, but electron destabilisation is apparent for $[I^-(CH_3OH)_n]^*$.

In order to understand the intriguing solvent specificity of the electron solvation dynamics of $[I^-(Solv)_n]^*$, it is essential to consider the intermolecular interactions within the cluster, and their effects on the stability of the cluster framework in the excited state. While ground-state $I^-(Solv)_n$ are stabilised by solvent-solvent hydrogen-bonding interactions, ion-dipole interactions, and in the case of $I^-(H_2O)_n$ and $I^-(CH_3OH)_n$, ionic hydrogen-bonding interactions, the latter two interactions are replaced with the much weaker iodine-solvent and diffuse electron-solvent cluster interactions in the excited state. As such, the structural integrity of the excited clusters can be significantly compromised if the solvent cluster moiety does not possess an extensive network of solvent-solvent interactions that stabilise the cluster network, and the excited clusters may dissociate into smaller fragments due to the kinetic energy acquired in the excitation and initial relaxation process. The key role played by the strong solvent-solvent interactions in supporting a diffuse excess electron in small CTTS excited iodide-polar solvent molecule clusters is evident from the stark contrast between $[I^-(H_2O)_n]^*$ and $[I^-(CH_3OH)_n]^*$ relaxation dynamics. In the case of $[I^-(H_2O)_n]^*$, the kinetic energy acquired in the initial relaxation process drives cluster reorganisation to stabilise the excited electron, with no evidence of water evaporation or cluster fragmentation taking place within the time scale of the simulations,[*36-38, 87, 129*] while cluster fragmentation is evident within 2 ps of excitation in the case of $[I^-(CH_3OH)_n]^*$, resulting in the excited electron destabilisation[*88*]; the extensively hydrogen-bonded water cluster moiety resists dissociation in $[I^-(H_2O)_n]^*$,[*72*] but methanol clusters fragment during $[I^-(CH_3OH)_n]^*$ relaxation, leading to smaller cluster fragments, which tend to have lower excess electron binding energies.[*134*] While simulations of $[I^-(CH_3CN)_n]^*$ that have been performed to date have not painted a clear picture of the cluster reorganisation process leading to electron stabilisation, one may expect the $(CH_3CN)_n$ moiety to be reasonably stable with respect to fragmentation, as larger $I^-(CH_3CN)_n$ ($n > 5$) clusters are also characterised by extensive solvent-solvent interactions due to the high dipole moment of the acetonitrile molecule and the propensity for acetonitrile to engage in dipole-dipole interactions.[*144*] Indeed, a stable

solvent cluster moiety that resists fragmentation is required for the experimentally observed electron stabilisation to occur in $[I^-(CH_3CN)_n]^*$. The solvent specificity of the electron solvation dynamics in $[I^-(H_2O)_n]^*$, $[I^-(CH_3OH)_n]^*$ and $[I^-(CH_3CN)_n]^*$ can thus be rationalised in terms of differences in the stability of the solvent cluster framework with respect to fragmentation, which is influenced by the nature of the solvent molecules in the cluster. $H_2O$ and $CH_3CN$ can interact with both $I^-$ and other solvent molecules *via* hydrogen-bonding and dipole-dipole interactions in the ground state, resulting in a solvent cluster moiety that resists fragmentation in the excited state. On the other hand, $CH_3OH$ can hydrogen bond with $I^-$ or another $CH_3OH$ in the ground state but not both, resulting in a solvent cluster moiety that easily fragments in the excited state. As a result, prominent electron solvation dynamics are observed for $[I^-(H_2O)_n]^*$ and $[I^-(CH_3CN)_n]^*$ but not $[I^-(CH_3OH)_n]^*$.

While there is no question about the important role of solvent reorganisation in the relaxation and electron solvation dynamics of $[I^-(Solv)_n]^*$, there has also been some interest in the influence of iodine in the electron stabilisation process of $[I^-(Solv)_n]^*$.[*21, 22, 32, 33, 43, 87, 129, 131*] Peslherbe and co-workers were the first to rigorously analyse the role of iodine in the electron solvation dynamics of $[I^-(H_2O)_5]^*$ and its effects on the stability of the excited electron as the cluster relaxes in the CTTS state.[*87*] By comparing the relaxation and rearrangement dynamics of $[I^-(H_2O)_5]^*$ and $(H_2O)_5^-$ from first-principles molecular dynamics simulations initiated with the same water cluster geometry, it was shown that iodine was important for initiating the repulsive dynamics in the Franck-Condon region and causing an increase of the kinetic energy available to drive the cluster reorganisation process that stabilises the excited electron. In addition, by computing the excited electron VDEs of $[I^-(H_2O)_5]^*$ with and without the neutral iodine atom, it was shown unequivocally that, while iodine exerts an initial destabilising effect on the excited electron due to exclusion effects between the iodine atom and the excited electron, iodine has essentially no effect on the excited electron past 200 fs, as evidenced by the similarity between the excited and excess electron distributions and VDEs of $[I^-(H_2O)_5]^*$ and $(H_2O)_5^-$ respectively after 200 fs (Figures 5.1 and 5.2).

Interestingly, it was more recently shown that iodine may also have a slight stabilising effect on the excited electron in some cases; profiles of the excited electron VDE of $[I^-(CH_3CN)]^*$ along the I•••$CH_3CN$ separation coordinate computed with CCSD(T) combined with a large

triple-zeta basis set augmented with a large set of diffuse functions indicate that the iodine atom can confer around 0.010 eV of additional stability to the excited electron, and this was attributed to subtle dispersion effects that were not captured at the CASPT2 level of theory used to compute $[I^-(H_2O)_5]^*$ VDEs earlier .[*131*] On the other hand, Sheu and Chiou recently proposed an interesting alternate explanation of the stabilising effect of the iodine atom on the excited electron in $[I^-(H_2O)_n]^*$; by comparing the excited/excess electron VDEs and neutral cluster framework dipole moments of $[I^-(H_2O)_4]^*$ and $(H_2O)_4^-$ configurations sampled from density-functional theory molecular dynamics simulations of the former, they showed that iodine can exert a stabilising effect of around 0.1 eV on the excited electron beginning 350 fs after excitation by enhancing the cluster dipole moment through dipole-induced dipole interactions.[*129*] Furthermore, it was pointed out that it is the gradual departure of iodine from the cluster over a period of tens to hundreds of picoseconds that can account for the 0.050 eV decrease in the excited electron VDE of $[I^-(H_2O)_n]^*$ observed by Neumark and co-workers.[*47*]

These subtle stabilising effects of iodine on the excited electron in $[I^-(Solv)_n]^*$ appear to be relevant only after the initial relaxation process has resulted in separation of the iodine from the excited electron, at least in the case of clusters with hydroxylic solvents, such as $[I^-(H_2O)_n]^*$; it appears that in these cases, the initial exclusion effects which result in the increased distance between the excited electron and the solvent cluster moiety decreases the attractive interaction between the excited electron and the partially positively charged hydrogen atoms of the water molecules, resulting in a smaller excited electron VDE for $[I^-(H_2O)_n]^*$ than for $(H_2O)_n^-$ until iodine has moved away from the region occupied by the excited electron. This effect may be much less significant in the case of $[I^-(CH_3CN)]^*$, in which the hydrogen atoms presumably carry a much smaller positive charge; enhancement of the cluster dipole moment by the presence of iodine, resulting in stabilisation of the excited electron relative to $(CH_3CN)^-$ is expected to be the more important effect in this case. It is also important to realise that, with the exception of the initial destabilisation of the excited electron arising from exclusion effects between iodine and the excited electron of $[I^-(Solv)_n]^*$, the iodine effects on the excited electron VDE appear to be quite small relative to the effects arising from solvent reorganisation. Thus, it appears that the relaxation process of $[I^-(Solv)_n]^*$ can mostly be viewed as a process of electron transfer from $I^-$ to the solvent cluster moiety, followed by a solvent-dependent rearrangement process of $(Solv)_n^-$ in which iodine primarily acts as a spectator.

## 5.6. Conclusions and Outlook

In this review article, we have provided an overview of the use of first-principles molecular dynamics simulations to develop a clear picture of the rich and varied $[I^-(Solv)_n]^*$ (Solv = $H_2O$, $CH_3OH$, $CH_3CN$) relaxation dynamics, which exhibits remarkable solvent specificity. By contrasting the simulated relaxation dynamics of $[I^-(H_2O)_n]^*$, $[I^-(CH_3OH)_n]^*$ and $[I^-(CH_3CN)_n]^*$, important insights into the molecular interactions that govern the electron solvation dynamics have been obtained; in order for small $I^-(Solv)_n$ to be able to support and maintain a diffuse excited electron in the CTTS state, the solvent molecules must be able to form a stable solvent cluster network that resists fragmentation in the excited state. While the iodine atom can also exert both stabilising and destabilising effects on the excited electron in $[I^-(Solv)_n]^*$, it appears that the relaxation and electron solvation processes in these clusters are essentially defined by the nature of the solvent reorganisation processes involved.

Despite the substantial progress that has been made in understanding the relaxation and electron solvation processes of iodide-polar solvent molecule clusters excited to the CTTS state since our original work on $[I^-(H_2O)_3]^*$,[*34*] there remain a number of unanswered questions and opportunities for future work in this area. In particular, it is of great importance to examine both experimentally and computationally a larger range of $[I^-(Solv)_n]^*$ than have been investigated thus far, encompassing a wide variety of solvents with different molecular characteristics, in order to develop a more refined picture of the complex relationship between the solvent molecular structure, the ground-state $I^-(Solv)_n$ cluster configurations and the relaxation and electron solvation dynamics in the CTTS state. In addition, it would be of significant interest to develop approaches for first-principles molecular dynamics simulations of excited iodide-polar solvent molecule complexes in which the polar molecules bound to iodide may also undergo chemical reactions in the excited state. Experimental studies of the dynamics of excited iodide-nucleobase complexes have recently been reported,[*145, 146*] and an extension of the first-principles molecular dynamics simulation approach previously employed in the investigation of $[I^-(Solv)_n]^*$ to such complexes may prove highly valuable for understanding the chemical reactivity induced by low energy electron attachment, an area with substantial implications for both chemistry and biology. None of this would be possible without the development of efficient first-principles excited-state molecular dynamics simulation approaches.

# 6. Conclusions and Future Directions

In this work, a combination of high-level quantum chemical calculations and state-of-the-art first-principles molecular dynamics simulations has been employed to obtain a detailed molecular-level picture of the relaxation process of $[I^-(Solv)_n]^*$, and to develop a thorough understanding of the molecular basis of the solvent specificity in the electron solvation process occurring during $[I^-(Solv)_n]^*$ relaxation, as observed in ongoing femtosecond photoelectron spectroscopy experiments conducted by the Neumark group.[*24-29, 46-48*] By examining the similarities and differences in the relaxation processes of $[I^-(Solv)_n]^*$ (Solv = $H_2O$, $CH_3OH$ and $CH_3CN$), valuable insights into the general features of $[I^-(Solv)_n]^*$ relaxation dynamics and the role of individual molecules in the electron solvation process have been obtained.

For all $[I^-(Solv)_n]^*$ investigated in this work, simulation results indicate that the relaxation and electron solvation processes involve two rather distinct sequential stages. Immediately following photoexcitation of $I^-(Solv)_n$, which results in transfer of an electron from an iodide-localised orbital to a diffuse orbital supported by the cluster framework, the first stage of the relaxation process begins. During this stage, rapid motions of the solvent molecules originally hydrogen-bonded to the iodide anion in the ground state result in a sharp increase in the kinetic energy present within the cluster and the rapid separation of the excited electron distribution from the iodine atom formed upon CTTS excitation. The kinetic energy acquired in the first stage of the $[I^-(Solv)_n]^*$ relaxation process then drives the gradual cluster reorganisation process that follows in the second stage, which can, depending on the nature of the solvent molecules, lead to the ultimate stabilisation and solvation of the excited electron. While both stages of $[I^-(Solv)_n]^*$ relaxation are dominated by solvent motion, repulsive iodine-solvent molecule interactions play an important role in the relaxation dynamics, and furthermore, the iodine atom can exert subtle stabilising and destabilising effects on the excited electron, depending on the nature of the electron-cluster interactions present.

Despite the similarities in the general features of the relaxation dynamics of the $[I^-(Solv)_n]^*$ investigated in this work, the nature of the electron solvation pathways in these clusters is heavily influenced by the identity of the solvent molecules within the cluster due to differences in the molecular structure of the solvent molecules that give rise to differences in the stability of the solvent cluster network of $[I^-(Solv)_n]^*$, which plays a critical role in supporting the diffuse excited electron. While solvent cluster reorganisation to stabilise the

excited electron is evident in all three $[I^-(Solv)_n]^*$ (Solv = $H_2O$, $CH_3OH$ and $CH_3CN$), it appears that solvent fragmentation competes with electron solvation processes in $[I^-(CH_3OH)_n]^*$, accounting for the ultimate destabilisation of the excited electron in $[I^-(CH_3OH)_n]^*$ and the more rapid decay by autodetachment of the excited electron in the case of $[I^-(CH_3OH)_n]^*$ than in the case of $[I^-(H_2O)_n]^*$ or $[I^-(CH_3CN)_n]^*$. The contrasting electron solvation dynamics of different $[I^-(Solv)_n]^*$ reflects the important role of subtle molecular interactions in stabilising and solvating an excess electron, in gas-phase clusters and presumably also in bulk solutions.

Due to the limited number of solvent molecules in small $[I^-(Solv)_n]^*$, results of the present theoretical investigation of these relatively simple systems have provided the most refined picture to date of the intricate molecular interactions that may drive the CTTS relaxation dynamics of anions in bulk solution. Despite some crucial differences in the solvent environment surrounding the anion in small solvent clusters and in solution, which may result in significant differences in the electronic distribution of the CTTS excited state and the associated relaxation dynamics in the two cases,[*23*] very similar molecular-level interactions underlie the relaxation dynamics in both cases. As such, there is an intimate connection between the relaxation and electron solvation processes in $[I^-(Solv)_n]^*$ and in CTTS excited iodide in solution, and certain important insights into the role of the interactions between the excited electron, the solvent molecules, and the iodine atom in the process of solvated electron formation from CTTS excited anions in solution may be inferred from the present work. In solution, as in clusters, the CTTS relaxation process begins with the rapid separation of the excited electron from the neutral iodine atom,[*14*] and based on the results of the research reported herein, it may be expected that exclusion effects between the diffuse excited electron and the iodine atom and the nearby solvent molecules contribute to the rapid solvent motions involved in the process. Since the excited electron is mostly confined within the solvent shell of the original ground-state iodide, it appears that these exclusion effects result in the rapid expansion of the solvent cavity and the eventual localisation of the excited electron into nearby voids arising from the random motions of the solvent molecules in the liquid phase,[*148*] a process analogous to the rapid solvent reorientation-driven excited electron-iodine separation process in $[I^-(Solv)_n]^*$. In $[I^-(Solv)_n]^*$, results of the present work also suggest that subtle dispersion effects between the excited electron and the iodine atom can influence the stability of the excited electron, and although these attractive effects are generally small relative to the much stronger exclusion effects, their contribution to the

stability of the CTTS excited electron in small clusters certainly raises important questions regarding the need to take into account such effects in a quantitative description of CTTS excited-state relaxation dynamics in solution. There, however, appears to be no question that in both clusters and solution, the longer-time relaxation processes are essentially driven by the propensity to maximise attractive polar solvent-excited electron electrostatic interactions. It is of course critical to emphasise that, despite parallels that can be drawn between $[I^-(Solv)_n]^*$ and the related CTTS excited states of iodide in solution, there are fundamental differences in the interaction between the excited electron and its solvent environment in the two cases, if only because of the finite extent of gas-phase clusters, which lack the long-range electrostatic effects that have been shown to be important in stabilising CTTS excited states of iodide in solution.[*23*] In spite of these limitations, the present work has clarified the role of some of the fundamental molecular interactions that contribute to the intriguing behaviour of the solvated electron, hereby highlighting the fact that insight into electron solvation processes intrinsically associated with bulk solutions may be gained from related processes taking place in small gas-phase clusters and involving only a few solvent molecules.

As the next step towards strengthening the connection between electron solvation dynamics in clusters and in solution, it will be of great interest to investigate in more detail the relaxation and electron solvation dynamics of $[I^-(CH_3CN)_n]^*$ ($n > 1$), which differ from $[I^-(H_2O)_n]^*$ and $[I^-(CH_3OH)_n]^*$ in that the iodide anion is internalised in the ground state.[*89, 90, 147*] As such, the excited electron is also expected to be more internalised in $[I^-(CH_3CN)_n]^*$ than in $[I^-(H_2O)_n]^*$ or $[I^-(CH_3OH)_n]^*$, and $[I^-(CH_3CN)_n]^*$ may thus present an excellent opportunity to investigate the unique features of the dynamics of an excess electron surrounded by solvent molecules. While experimental work suggests that $[I^-(CH_3CN)_n]^*$, like $[I^-(H_2O)_n]^*$, undergoes relaxation that results in stabilisation and possibly solvation of the excited electron,[*29*] results of the first-principles molecular dynamics simulations of $[I^-(CH_3CN)]^*$ reported in this thesis suggest that the molecular motions involved in the relaxation process of $I^-(CH_3CN)_n$ may be quite different from those observed in other $[I^-(Solv)_n]^*$, due to the unique molecular structure of $CH_3CN$, which gives rise to a much higher moment of inertia and hindrance to rotational excitation as compared with $H_2O$ and $CH_3OH$. Despite important differences between an excess electron surrounded by a finite number of solvent molecules and a solvated electron trapped in a polar liquid, obtaining a clear picture of the electron solvation dynamics of a diffuse excess electron localised in the interior of a solvent cluster will be a critical step towards the development of a complete picture of the

relationship between the electron solvation dynamics in the two environments.

While the findings reported in this thesis have resulted in substantial new insights into the electron-molecule and molecule-molecule interactions that form the backbone of the solvated electron, much remains to be explored with regard to the mechanisms by which solvated electrons can induce chemical reactions, especially those of biological relevance. Indeed, precursors of the hydrated electron, which are formed in aqueous systems upon exposure to ionising radiation, have been implicated in the mechanism of DNA damage, and as a result, there is currently much interest in reactions of DNA components induced by attachment of an excess electron.[*17*] To this end, Neumark and co-workers have begun to probe using femtosecond photoelectron spectroscopy the dynamics of transient nucleobase anions formed by photoexcitation of binary iodide-nucleobase complexes, $I^-$(Nuclb), which results in the transfer of an electron from the iodide anion to the nucleobase molecule, in a process similar to the formation of CTTS states upon photoexcitation of iodide-polar solvent molecule clusters.[*145, 146*] In contrast to the CTTS excited iodide-polar solvent molecule clusters investigated in this thesis, however, the photoexcitation of $I^-$(Nuclb) appears to result in the transfer of the excited electron to a valence orbital of the nucleobase, forming a presumably loosely-bound iodine-nucleobase anion complex, I•••(Nuclb)$^-$, that can decay by multiple possible pathways, including ejection of the iodine atom or the excess electron, or loss of hydrogen atoms from the nucleobase molecule. In order to assist in the interpretation of these experimental findings, it will as a first step be important to develop a reliable theoretical approach that can properly describe the electronic properties and potential energy surfaces of ground, excited and ionised $I^-$(Nuclb); as a starting point, it may prove fruitful to modify the approaches previously employed for treating the dipole-bound $[I^-(Solv)_n]^*$ to treat the valence-bound I•••(Nuclb)$^-$; the availability of a sound description of the electronic structure and potential energy surface of the various states of $I^-$(Nuclb) should then make possible reliable classical trajectory simulations of the decay process of I•••(Nuclb)$^-$. A detailed picture of the decay dynamics of I•••(Nuclb)$^-$ resulting from theoretical work should ultimately contribute to a better understanding of the mechanisms of reactions involving solvated electrons and related species, which are important aspects of radiation chemistry and biochemistry.

## References:


(1) Edwards, P.P., The electronic properties of metal solutions in liquid ammonia and related solvents. In *Advances in Inorganic Chemistry*; Academic Press: 1982; Vol. 25, pp 135-185.
(2) Weyl, W., Ueber metallammonium-verbindungen. *Annalen der Physik* **1864,** *121*,606-612.
(3) Kraus, C.A., Solutions of metals in non-metallic solvents; I. General properties of solutions of metals in liquid ammonia. *Journal of the American Chemical Society* **1907,** *29*,1557-1571.
(4) Hart, E.J.; Boag, J.W., Absorption spectrum of the hydrated electron in water and in aqueous solutions. *Journal of the American Chemical Society* **1962,** *84*,4090-4095.
(5) Dorfman, L.M., The solvated electron in organic liquids. In *Solvated Electron*; American Chemical Society: 1965; Vol. 50, pp 36-44.
(6) Birch, A.J., Reduction by dissolving metals. Part I. *Journal of the Chemical Society (Resumed)* **1944,** 430-436.
(7) Birch, A.J., Reduction by dissolving metals. Part II. *Journal of the Chemical Society (Resumed)* **1945,** 809-813.
(8) Birch, A.J., Reduction by dissolving metals. Part III. *Journal of the Chemical Society (Resumed)* **1946,** 593-597.
(9) Bouveault, L.; Blanc, G., Préparation des alcools primaires au moyen des acides correspondants. *Comtes Rendus Hebdomadaires des Séances de l'Académie des Sciences* **1903,** *136*,1676-1678.
(10) Bouveault, L.; Blanc, G., Transformation des acides monobasiques saturés dans les alcools primaires correspondants. *Bulletin de la Société Chimique de France* **1904,** *31*,666-672.
(11) Ferris, J.P.; Antonucci, F.R., Hydrated electron in organic synthesis. Reduction of nitriles to aldehydes. *Journal of the American Chemical Society* **1972,** *94*,8091-8095.
(12) Casey, J.R.; Kahros, A.; Schwartz, B.J., To be or not to be in a cavity: The hydrated electron dilemma. *The Journal of Physical Chemistry B* **2013,** *117*,14173-14182.
(13) Turi, L.; Rossky, P.J., Theoretical studies of spectroscopy and dynamics of hydrated electrons. *Chemical Reviews* **2012,** *112*,5641-5674.
(14) Chen, X.; Bradforth, S.E., The ultrafast dynamics of photodetachment. *Annual Review of Physical Chemistry* **2008,** *59*,203-231.
(15) Rabinowitch, E., Electron transfer spectra and their photochemical effects. *Reviews of Modern Physics* **1942,** *14*,112-131.
(16) Blandamer, M.J.; Fox, M.F., Theory and applications of charge-transfer-to-solvent spectra. *Chemical Reviews* **1970,** *70*,59-93.
(17) Alizadeh, E.; Sanche, L., Precursors of solvated electrons in radiobiological physics and chemistry. *Chemical Reviews* **2012,** *112*,5578-5602.
(18) Dessent, C.E.H.; Bailey, C.G.; Johnson, M.A., Observation of the dipole-bound excited state of the $I^-$ • acetone ion-molecule complex. *The Journal of Chemical Physics* **1995,** *102*,6335-6338.
(19) Dessent, C.E.H.; Bailey, C.G.; Johnson, M.A., Dipole-bound excited states of the $I^-$ • $CH_3CN$ and $I^-$ • $(CH_3CN)_2$ ion--molecule complexes: evidence for asymmetric solvation. *The Journal of Chemical Physics* **1995,** *103*,2006-2015.
(20) Serxner, D.; Dessent, C.E.H.; Johnson, M.A., Precursor of the $I_{aq}^-$ charge-transfer-to-solvent (CTTS) band in $I^-$ • $(H_2O)_n$ clusters. *The Journal of Chemical Physics* **1996,** *105*,7231-7234.

(21) Chen, H.-Y.; Sheu, W.-S., Precursors of the charge-transfer-to-solvent states in $I^-(H_2O)_n$ clusters. *Journal of the American Chemical Society* **2000,** *122*,7534-7542.
(22) Timerghazin, Q.K.; Peslherbe, G.H., Theoretical investigation of charge transfer to solvent in photoexcited iodide-acetonitrile clusters. *Chemical Physics Letters* **2002,** *354*,31-37.
(23) Bradforth, S.E.; Jungwirth, P., Excited states of iodide anions in water: A comparison of the electronic structure in clusters and in bulk solution. *The Journal of Physical Chemistry A* **2002,** *106*,1286-1298.
(24) Lehr, L.; Zanni, M.T.; Frischkorn, C.; Weinkauf, R.; Neumark, D.M., Electron solvation in finite systems: femtosecond dynamics of iodide • $(water)_n$ anion clusters. *Science* **1999,** *284*,635-638.
(25) Frischkorn, C.; Zanni, M.T.; Davis, A.V.; Neumark, D.M., Electron solvation dynamics in $I^-(NH_3)$ clusters. *Faraday Discussions* **2000,** *115*,49-62.
(26) Davis, A.V.; Zanni, M.T.; Frischkorn, C.; Neumark, D.M., Time-resolved dynamics of charge transfer to solvent states in solvated iodide clusters. *Journal of Electron Spectroscopy and Related Phenomena* **2000,** *108*,203-211.
(27) Young, R.M.; Yandell, M.A.; Neumark, D.M., Dynamics of electron solvation in $I^-(CH_3OH)_n$ clusters ($4 \leq n \leq 11$). *The Journal of Chemical Physics* **2011,** *134*,124311.
(28) Yandell, M.A.; Young, R.M.; King, S.B.; Neumark, D.M., Effects of excitation energy on the autodetachment lifetimes of small iodide-doped ROH clusters (R = H-, $CH_3$-, $CH_3CH_2$-). *The Journal of Physical Chemistry A* **2012,** *116*,2750-2757.
(29) Ehrler, O.T.; Griffin, G.B.; Young, R.M.; Neumark, D.M., Photoinduced electron transfer and solvation in iodide-doped acetonitrile clusters *The Journal of Physical Chemistry B* **2009,** *113*,4031-4037.
(30) Bailey, C.G.; Johnson, M.A., Determination of the relative photodetachment cross sections of the two isomers of $(H_2O)_6^-$ using saturated photodetachment. *Chemical Physics Letters* **1997,** *265*,185-189.
(31) Lee, S.; Kim, J.; Lee, S.J.; Kim, K.S., Novel structures for the excess electron state of the water hexamer and the interaction forces governing the structures. *Physical Review Letters* **1997,** *79*,2038-2041.
(32) Chen, H.-Y.; Sheu, W.-S., Iodine effect on the relaxation pathway of photoexcited $I^-(H_2O)_n$ clusters. *Chemical Physics Letters* **2001,** *335*,475-480.
(33) Chen, H.-Y.; Sheu, W.-S., Reply to the comment on `Iodine effect on the relaxation pathway of photoexcited $I^-(H_2O)_n$ clusters' [Chem. Phys. Lett. 335 (2001) 475]. *Chemical Physics Letters* **2002,** *353*,459-462.
(34) Timerghazin, Q.K.; Peslherbe, G.H., Further insight into the relaxation dynamics of photoexcited $I^-(H_2O)_n$ clusters. *Journal of the American Chemical Society* **2003,** *125*,9904-9905.
(35) Kolaski, M.; Lee, H.M.; Pak, C.; Dupuis, M.; Kim, K.S., Ab initio molecular dynamics simulations of an excited state of $X^-(H_2O)_3$ (X = Cl, I) complex. *The Journal of Physical Chemistry A* **2005,** *109*,9419-9423.
(36) Takayanagi, T.; Takahashi, K., Direct dynamics simulations of photoexcited charge-transfer-to-solvent states of the $I^-(H_2O)_6$ cluster. *Chemical Physics Letters* **2006,** *431*,28-33.
(37) Takahashi, K.; Takayanagi, T., Direct Dynamics Simulations of Photoexcited Charge-Transfer-to-Solvent States of the $I^-(H_2O)_n$ (n = 4, 5 and 6) Clusters. *Chemical Physics* **2007,** *342*,95-106.
(38) Kolaski, M.; Lee, H.M.; Pak, C.; Kim, K.S., Charge-transfer-to-solvent-driven dissolution dynamics of $I^-(H_2O)_{2-5}$ upon excitation: excited-state ab initio molecular dynamics simulations. *Journal of the American Chemical Society* **2008,** *130*,103-112.

(39) Jortner, J.; Ottolenghi, M.; Stein, G., On the photochemistry of aqueous solutions of chloride, bromide, and iodide Ions. *The Journal of Physical Chemistry* **1964,** *68*,247-255.
(40) Hart, E.J.; Anbar, M., *The Hydrated Electron*; Wiley-Interscience: New York, 1970.
(41) Boudaiffa, B.; Cloutier, P.; Hunting, D.; Huels, M.A.; Sanche, L., Resonant formation of DNA strand breaks by low-energy (3 to 20 eV) electrons. *Science* **2000,** *287*,1658-1660.
(42) Simons, J., How do low-energy (0.1-2 eV) electrons cause DNA-strand breaks? *Accounts of Chemical Research* **2006,** *39*,772-779.
(43) Sheu, W.-S.; Liu, Y.-T., Charge-transfer-to-solvent (CTTS) precursor states of $X^-(H_2O)_n$ clusters (X=Cl, Br, I). *Chemical Physics Letters* **2003,** *374*,620-625.
(44) Balzani, V., *Electron Transfer in Chemistry*; Wiley-VCH: Weinheim, 2001.
(45) Bolton, J.R.; Mataga, N.; McLendon, G., *Electron Transfer in Inorganic, Organic and Biological Systems*; American Chemical Society and Canadian Chemical Society: Washington and Ottawa, 1991.
(46) Verlet, J.R.R.; Kammrath, A.; Griffin, G.B.; Neumark, D.M., Electron solvation in water clusters following charge transfer from iodide. *The Journal of Chemical Physics* **2005,** *123*,231102-231104.
(47) Kammrath, A.; Verlet, J.R.R.; Bragg, A.E.; Griffin, G.B.; Neumark, D.M., Dynamics of charge-transfer-to-solvent precursor states in $I^-(water)_n$ (n = 3-10) clusters studied with photoelectron imaging. *The Journal of Physical Chemistry A* **2005,** *109*,11475-11483.
(48) Davis, A.V.; Zanni, M.T.; Weinkauf, R.; Neumark, D.M., Comment on `Iodine effect on the relaxation pathway of photoexcited $I^-(H_2O)_n$ clusters' [Chem. Phys. Lett. 335 (2001) 475]. *Chemical Physics Letters* **2002,** *353*,455-458.
(49) Coe, J.V.; Lee, G.H.; Eaton, J.G.; Arnold, S.T.; Sarkas, H.W.; Bowen, K.H.; Ludewigt, C.; Haberland, H.; Worsnop, D.R., Photoelectron spectroscopy of hydrated electron cluster anions, $(H_2O)_{n=2-69}$. *The Journal of Chemical Physics* **1990,** *92*,3980-3982.
(50) Kim, J.; Becker, I.; Cheshnovsky, O.; Johnson, M.A., Photoelectron spectroscopy of the `missing' hydrated electron clusters $(H2O)_n$, n=3, 5, 8 and 9: Isomers and continuity with the dominant clusters n=6, 7 and ≥ 11. *Chemical Physics Letters* **1998,** *297*,90-96.
(51) Shin, J.-W.; Hammer, N.I.; Headrick, J.M.; Johnson, M.A., Preparation and photoelectron spectrum of the 'missing' $(H_2O)_4^-$ cluster. *Chemical Physics Letters* **2004,** *399*,349-353.
(52) Verlet, J.R.R.; Bragg, A.E.; Kammrath, A.; Cheshnovsky, O.; Neumark, D.M., Observation of Large Water-Cluster Anions with Surface-Bound Excess Electrons. *Science* **2005,** *307*,93-96.
(53) Szpunar, D.E.; Kautzman, K.E.; Faulhaber, A.E.; Neumark, D.M., Photofragment coincidence imaging of small $I^-(H_2O)_n$ clusters excited to the charge-transfer-to-solvent state. *The Journal of Chemical Physics* **2006,** *124*,054318-054318.
(54) Lee, H.M.; Kim, K.S., Solvent rearrangement for an excited electron of the iodide-water pentamer. *Molecular Physics* **2004,** *102*,2485-2489.
(55) Lee, H.M.; Suh, S.B.; Kim, K.S., Solvent rearrangement for an excited electron of $I^-(H_2O)_6$: Analog to structural rearrangement of $e^-(H_2O)_6$. *The Journal of Chemical Physics* **2003,** *119*,7685-7692.
(56) Evans, D.J.; Murad, S., Singularity free algorithm for molecular dynamics simulation of rigid polyatomics. *Molecular Physics* **1977,** *34*,327-331.
(57) The experimental gas-phase geometry of the water molecules was used in the present study. However, using the water geometry predicted by the model chemistries employed to compute the energy and forces - which differs only slightly from the experimental one - did not affect the outcome of the simulations, which was found to be essentially insensitive to the precise choice of water geometry.

(58) Gear, C.W., *Numerical Initial Value Problems in Ordinary Differential Equations*; Prentice-Hall: Englewood Cliffs, 1971.
(59) Peslherbe, G.H.; Hase, W.L., Analysis and extension of a model for constraining zero-point energy flow in classical trajectory simulations. *The Journal of Chemical Physics* **1994,** *100*,1179-1189.
(60) Czakó, G.; Kaledin, A.L.; Bowman, J.M., A practical method to avoid zero-point leak in molecular dynamics calculations: application to the water dimer. *The Journal of Chemical Physics* **2010,** *132*,164103.
(61) Werner, H.-J.; Knowles, P.J., A second order multiconfiguration SCF procedure with optimum convergence. *The Journal of Chemical Physics* **1985,** *82*,5053-5063.
(62) Knowles, P.J.; Werner, H.-J., An efficient second-order MC SCF method for long configuration expansions. *Chemical Physics Letters* **1985,** *115*,259-267.
(63) Werner, H.-J., Third-order multireference perturbation theory The CASPT3 method. *Molecular Physics* **1996,** *89*,645-661.
(64) Hampel, C.; Peterson, K.A.; Werner, H.-J., A comparison of the efficiency and accuracy of the quadratic configuration interaction (QCISD), coupled cluster (CCSD), and Brueckner coupled cluster (BCCD) methods. *Chemical Physics Letters* **1992,** *190*,1-12.
(65) Amos, R.D.; Andrews, J.S.; Handy, N.C.; Knowles, P.J., Open-shell Møller-Plesset perturbation theory. *Chemical Physics Letters* **1991,** *185*,256-264.
(66) Hehre, W.J.; Ditchfield, R.; Pople, J.A., Self-consistent molecular orbital methods. XII. Further extensions of gaussian-type basis sets for use in molecular orbital studies of organic molecules. *The Journal of Chemical Physics* **1972,** *56*,2257-2261.
(67) Clark, T.; Chandrasekhar, J.; Spitznagel, G.W.; Schleyer, P.V.R., Efficient diffuse function-augmented basis sets for anion calculations. III. The 3-21+G basis set for first-row elements, Li–F. *Journal of Computational Chemistry* **1983,** *4*,294-301.
(68) Hariharan, P.C.; Pople, J.A., The influence of polarization functions on molecular orbital hydrogenation energies. *Theoretica Chimica Acta* **1973,** *28*,213-222.
(69) Bergner, A.; Dolg, M.; Küchle, W.; Stoll, H.; Preuβ, H., Ab initio energy-adjusted pseudopotentials for elements of groups 13-17. *Molecular Physics* **1993,** *80*,1431-1441.
(70) This arrangement of the diffuse functions leads to a reasonable distribution of the excess electron, and placement of the diffuse functions at other locations does not significantly affect the outcome of the calculations. For a discussion of the effect of the choice of diffuse functions on the electronic distribution of the excess electron, see Timerghazin, QK, Rizvi, I, and Peslherbe, GH. Can a dipole-bound electron form a pseudo-atom? An atoms-in-molecules study of the hydrated electron. *The Journal of Physical Chemistry A*. 2011, 115:13201-13209.
(71) Werner, H.-J.; Knowles, P.J.; Knizia, G.; Manby, F.R.; Schütz, M.; Celani, P.; Korona, T.; Lindh, R.; Mitrushenkov, A.; Rauhut, G.; Shamasundar, K.R.; Adler, T.B.; Amos, R.D.; Bernhardsson, R.D.; Berning, A.; Cooper, D.L.; Deegan, M.J.O.; Dobbyn, A.J.; Eckert, F.; Goll, E.; Hampel, C.; Hesselmann, A.; Hetzer, G.; Hrenar, T.; Jansen, G.; Köppl, C.; Liu, Y.; Lloyd, A.W.; Mata, R.A.; May, A.J.; McNicholas, S.J.; Meyer, W.; Mura, M.E.; Nicklass, A.; O'Neill, D.P.; Palmieri, P.; Pflüger, K.; Pitzer, R.; Reiher, M.; Shiozaki, T.; Stoll, H.; Stone, A.J.; Tarroni, R.; Thorsteinsson, T.; Wang, M.; Wolf, A.; *Molpro*, version 2010.1; http://www.molpro.net.
(72) Lee, H.M.; Kim, K.S., Structures and spectra of iodide-water clusters $I^-(H_2O)_n$=1-6: an ab initio study. *The Journal of Chemical Physics* **2001,** *114*,4461-4471.
(73) This represents only one of many possible choices of initial conditions. However, using other cluster configurations sampled from ground-state molecular dynamics simulations of $I^-(H_2O)_5$ and initial velocities resulted in overall similar relaxation dynamics, primarily governed by the strong I-H repulsive interactions in the Franck-Condon geometry.

In all cases, the dynamics is characterised by the initial rapid synchronous rotational motion of the water molecules and the accompanying sharp decrease in the cluster potential energy within 0.2 ps. This is not surprising, since the initial thermal energy assigned to the cluster is negligible, compared to the kinetic energy acquired in the simulations, due to the strong I-H repulsive interactions.
(74) Klots, C.E., Temperatures of evaporating clusters. *Nature* **1987,** *327*,222-223.
(75) Herbert, J.M.; Head-Gordon, M., First-principles, quantum-mechanical simulations of electron solvation by a water cluster. *Proceedings of the National Academy of Sciences* **2006,** *103*,14282-14287.
(76) Vila, F.D.; Jordan, K.D., Theoretical study of the dipole-bound excited states of $I^-(H_2O)_4$. *The Journal of Physical Chemistry A* **2002,** *106*,1391-1397.
(77) The iodine-hydrogen repulsion energy was estimated by comparing the energy difference of $[I^-(H_2O)_5]^*$ with and without iodine, for cluster configurations at 0 fs (strong repulsions) and 50 fs (little or no repulsion).
(78) Jortner, J.; Levine, R.; Ottolenghi, M.; Stein, G., Photochemistry of the iodide ion in aqueous solution. *Journal of Physical Chemistry* **1961,** *65*,1232-1238.
(79) Kloepfer, J.A.; Vilchiz, V.H.; Lenchenkov, V.A.; Germaine, A.C.; Bradforth, S.E., The ejection distribution of solvated electrons generated by the one-photon photodetachment of aqueous I- and two-photon ionization of the solvent. *The Journal of Chemical Physics* **2000,** *113*,6288-6307.
(80) Kloepfer, J.A.; Vilchiz, V.H.; Lenchenkov, V.A.; Bradforth, S.E., Femtosecond dynamics of photodetachment of the iodide anion in solution: resonant excitation into the charge-transfer-to-solvent state. *Chemical Physics Letters* **1998,** *298*,120-128.
(81) Crowell, R.A.; Lian, R.; Shkrob, I.A.; Bartels, D.M.; Chen, X.; Bradforth, S.E., Ultrafast dynamics for electron photodetachment from aqueous hydroxide. *Journal of Chemical Physics* **2004,** *120*,11712-11725.
(82) Martini, G.B.; Barthel, E.R.; Schwartz, B.J., Optical control of electrons during electron transfer. *Science* **2001,** *293*,462-465.
(83) Martini, I.B.; Barthel, E.R.; Schwartz, B.J., Manipulating the production and recombination of electrons during electron transfer: Femtosecond control of the charge-transfer-to-solvent (CTTS) dynamics of the sodium anion. *Journal of the American Chemical Society* **2002,** *124*,7622-7634.
(84) Jordan, K.D.; Wang, F., Theory of dipole-bound anions. *Annual Review of Physical Chemistry* **2003,** *54*,367-396.
(85) Robertson, W.H.; Johnson, M.A., Molecular aspects of halide ion hydration: The cluster approach. *Annual Review of Physical Chemistry* **2003,** *54*,173-213.
(86) Combariza, J.E.; Kestner, N.R.; Jortner, J., Energy-structure relationships for microscopic solvation of anions in water clusters. *The Journal of Chemical Physics* **1994,** *100*,2865-2870.
(87) Mak, C.C.; Timerghazin, Q.K.; Peslherbe, G.H., Photoinduced electron transfer and solvation dynamics in aqueous clusters: comparison of the photoexcited iodide-water pentamer and the water pentamer anion. *Physical Chemistry Chemical Physics* **2012,** *14*,6257-6265.
(88) Mak, C.C.; Peslherbe, G.H., Relaxation pathways of photoexcited iodide-methanol clusters: a computational investigation. *The Journal of Physical Chemistry A* **2014,** *118*,4494-4501.
(89) Nguyen, T.-N.V.; Peslherbe, G.H., Microsolvation of alkali and halide ions in acetonitrile clusters. *The Journal of Physical Chemistry A* **2003,** *107*,1540-1550.

(90) Nguyen, T.-N.V.; Hughes, S.R.; Peslherbe, G.H., Microsolvation of the sodium and iodide ions and their ion pair in acetonitrile clusters: A theoretical study *The Journal of Physical Chemistry B* **2008,** *112*,621-635.
(91) Koch, D.M.; Peslherbe, G.H., On the transition from surface to interior solvation in iodide-water clusters. *Chemical Physics Letters* **2002,** *359*,381-389.
(92) Robertson, W.H.; Karapetian, K.; Ayotte, P.; Jordan, K.D.; Johnson, M.A., Infrared predissociation spectroscopy of $I^- \cdot (CH_3OH)_n$, n=1,2: Cooperativity in asymmetric solvation. *The Journal of Chemical Physics* **2002,** *116*,4853-4857.
(93) Cabarcos, O.M.; Weinheimer, C.J.; Martinez, T.J.; Lisy, J.M., The solvation of chloride by methanol---surface versus interior cluster ion states. *The Journal of Chemical Physics* **1999,** *110*,9516-9526.
(94) Corbett, C.A.; Martinez, T.J.; Lisy, J.M., Solvation of the fluoride anion by methanol *The Journal of Physical Chemistry A* **2002,** *106*,10015-10021.
(95) Beck, J.P.; Lisy, J.M., Cooperatively enhanced ionic hydrogen bonds in $Cl^-(CH_3OH)_{1-3}Ar$ clusters. *The Journal of Physical Chemistry A* **2010,** *114*,10011-10015.
(96) Ayala, R.; Martinez, J.M.; Pappalardo, R.R.; Sanchez Marcos, E., Theoretical study of the microsolvation of the bromide anion in water, methanol, and acetonitrile: Ion-solvent vs solvent-solvent interactions. *The Journal of Physical Chemistry A* **2000,** *104*,2799-2807.
(97) Takayanagi, T., Dynamical calculations of charge-transfer-to-solvent excited states of small $I^-(CH_3CN)_n$ clusters. *The Journal of Physical Chemistry A* **2006,** *110*,7011-7018.
(98) Mbaiwa, F., Wei, Jie, Van Duzor, Matthew, Mabbs, Richard, Threshold effects in $I^-CH_3CN$ and $I^-H_2O$ cluster anion detachment: The angular distribution as an indicator of electronic autodetachment. *The Journal of Chemical Physics* **2010,** *132*,134304-134309.
(99) Hehre, W.J.; Radom, L.; Schleyer, P.v.R.; Pople, J.A., *Ab Initio Molecular Orbital Theory*; John Wiley and Sons: New York, 1985.
(100) Dunning, T.H., Gaussian basis sets for use in correlated molecular calculations. I. The atoms boron through neon and hydrogen. *The Journal of Chemical Physics* **1989,** *90*,1007-1023.
(101) Stoll, H.; Metz, B.; Dolg, B., Relativistic energy-consistent pseudopotentials - recent developments. *Journal of Computational Chemistry* **2002,** *23*,767-778.
(102) Skurski, P.; Gutowski, M.; Simons, J., How to choose a one-electron basis set to reliably describe a dipole-bound anion. *International Journal of Quantum Chemistry* **2000,** *80*,1024-1038.
(103) Alfonso, D.R.; Jordan, K.D., Rearrangement pathways of the water trimer and tetramer anions. *The Journal of Chemical Physics* **2002,** *116*,3612-3616.
(104) Gutowski, M.; Skurski, P.; Boldyrev, A.I.; Simons, J.; Jordan, K.D., Contribution of electron correlation to the stability of dipole-bound anionic states. *Physical Review A* **1996,** *54*,1906-1909.
(105) Gutowski, M.; Skurski, P., Theoretical study of the dipole-bound anion $(HF)_2^-$. *The Journal of Chemical Physics* **1997,** *107*,2968-2973.
(106) Gutowski, M.; Skurski, P., Dispersion stabilization of solvated electrons and dipole-bound anions. *The Journal of Physical Chemistry B* **1997,** *101*,9143-9146.
(107) Gutowski, M.; Jordan, K.D.; Skurski, P., Electronic structure of dipole-bound anions. *The Journal of Physical Chemistry A* **1998,** *102*,2624-2633.
(108) Knowles, P.J.; Hampel, C.; Werner, H.-J., Coupled cluster theory for high spin, open shell reference wave functions. *The Journal of Chemical Physics* **1993,** *99*,5219-5227.
(109) Knowles, P.J.; Hampel, C.; Werner, H.-J., Erratum: coupled cluster theory for high spin, open shell reference wave functions [ J. Chem. Phys. 99, 5219 (1993)]. *The Journal of Chemical Physics* **2000,** *112*,3106-3107.

(110) Martin, J.M.L.; Sundermann, A., Correlation consistent valence basis sets for use with the Stuttgart-Dresden-Bonn relativistic effective core potentials: The atoms Ga-Kr and In-Xe. *The Journal of Chemical Physics* **2001,** *114*,3408-3420.
(111) Bolton, K.; Hase, W.L.; Peslherbe, G.H., *Direct dynamics simulations of reactive systems*. World Scientific Publishing Co.: 1998.
(112) Labello, N.P.; Ferreira, A.M.; Kurtz, H.A., An augmented effective core potential basis set for the calculation of molecular polarizabilities. *Journal of Computational Chemistry* **2005,** *26*,1464-1471.
(113) Labello, N.P.; Ferreira, A.M.; Kurtz, H.A., Correlated, relativistic, and basis set limit molecular polarizability calculations to evaluate an augmented effective core potential basis set. *International Journal of Quantum Chemistry* **2006,** *106*,3140-3148.
(114) Foresman, J.B.; Head-Gordon, M.; Pople, J.A.; Frisch, M.J., Toward a systematic molecular orbital theory for excited states. *The Journal of Physical Chemistry* **1992,** *96*,135-149.
(115) Mitin, A.V.; Hirsch, G.; Buenker, R.J., Accurate small split-valence 3-21SP and 4-22SP basis sets for the first-row atoms. *Chemical Physics Letters* **1996,** *259*,151-158.
(116) Stevens, W.J.; Krauss, M.; Basch, H.; Jasien, P.G., Relativistic compact effective potentials and efficient, shared-exponent basis-sets for the 3rd-row, 4th-row, and 5th-row atoms. *Canadian Journal of Chemistry-Revue Canadienne De Chimie* **1992,** *70*,612-630.
(117) Check, C.E.; Faust, T.O.; Bailey, J.M.; Wright, B.J.; Gilbert, T.M.; Sunderlin, L.S., Addition of polarization and diffuse functions to the LANL2DZ basis set for p-block elements. *The Journal of Physical Chemistry A* **2001,** *105*,8111-8116.
(118) Peslherbe, G.H.; Wang, H.B.; Hase, W.L., Monte Carlo sampling for classical trajectory simulations. *Monte Carlo Methods in Chemical Physics* **1999,** *105*,171-201.
(119) Hase, W.L.; Duchovic, R.J.; Hu, X.; Komornicki, A.; Lim, K.; Lu, D.; Peslherbe, G.H.; Swamy, K.N.; Van de Linde, S.R.; Wang, H.B.; Wolf, R.J., Venus, a general chemical dynamics computer program. *Quantum Chemistry Program Exchange Bulletin* **1996,** *16*,671.
(120) Stewart, J.J.P.; Davis, L.P.; Burggraf, L.W., Semi-empirical calculations of molecular trajectories: Method and applications to some simple molecular systems. *Journal of Computational Chemistry* **1987,** *8*,1117-1123.
(121) Schmidt, M.W.; Baldridge, K.K.; Boatz, J.A.; Elbert, S.T.; Gordon, M.S.; Jensen, J.H.; Koseki, S.; Matsunaga, N.; Nguyen, K.A., General atomic and molecular electronic structure system. *Journal of Computational Chemistry* **1993,** *14*,1347-1363.
(122) Sanov, A.; Faeder, J.; Parson, R.; Lineberger, W.C., Spin-orbit coupling in I.CO2 and I.OCS van der Waals complexes: Beyond the pseudo-diatomic approximation. *Chemical Physics Letters* **1999,** *313*,812-819.
(123) Timerghazin, Q.K.; Koch, D.M.; Peslherbe, G.H., Accurate ab initio potential for the Na+.I complex. *The Journal of Chemical Physics* **2006,** *124*,014313-014310.
(124) Sansonetti, J.E.; Martin, W.C., *Handbook of Basic Atomic Spectroscopic Data (http://physics.nist.gov/PhysRefData/Handbook/index.html)*; Editor Ed.^Eds.;National Institute of Standards and Technology: Gaithersburg, MD 20899, 2005.
(125) Meot-Ner (Mautner), M.M.; Lias, S.G., Binding Energies Between Ions and Molecules, and The Thermochemistry of Cluster Ions. In *NIST Chemistry WebBook, NIST Standard Reference Database Number 69*; Linstrom, P.J., Mallard, W.G., Eds. National Institute of Standards and Technology: Gaithersburg MD (http://webbook.nist.gov), 2003.
(126) Desfrancois, C.; Abdoulcarime, H.; Khelifa, N.; Schermann, J.P., From 1/R to 1/R(2) potentials - electron-exchange between Rydberg atoms and polar-molecules. *Physical Review Letters* **1994,** *73*,2436-2439.
(127) Timerghazin, Q.K. Structure, Photochemistry and Charge-Transfer-to-Solvent Relaxation Dynamics of Anionic Clusters. Concordia University, Montréal, 2006.

(128) Peterson, K.A.; Figgen, D.; Goll, E.; Stoll, H.; Dolg, M., Systematically convergent basis sets with relativistic pseudopotentials. II. Small-core pseudopotentials and correlation consistent basis sets for the post-d group 16-18 elements. *The Journal of Chemical Physics* **2003,** *119*,11113-11123.
(129) Sheu, W.-S.; Chiou, M.-F., Effects of iodine on the relaxation dynamics of a photoexcited $I^-(H_2O)_4$ cluster. *The Journal of Physical Chemistry A* **2013,** *117*,13946-13953.
(130) Watts, J.D.; Gauss, J.; Bartlett, R.J., Coupled-cluster methods with noniterative triple excitations for restricted open-shell Hartree-Fock and other general single determinant reference functions. Energies and analytical gradients. *The Journal of Chemical Physics* **1993,** *98*,8718-8733.
(131) Mak, C.C.; Timerghazin, Q.K.; Peslherbe, G.H., Photoexcitation and charge-transfer-to-solvent relaxation dynamics of the $I^-(CH_3CN)$ complex. *The Journal of Physical Chemistry A* **2013,** *117*,7595-7605.
(132) Kendall, R.A.; Dunning, T.H.; Harrison, R.J., Electron affinities of the first-row atoms revisited. Systematic basis sets and wave functions. *The Journal of Chemical Physics* **1992,** *96*,6796-6806.
(133) Peslherbe, G.H.; Hase, W.L., Comparison of zero-point energy constrained and quantum anharmonic Rice-Ramsperger-Kassel-Marcus and phase space theory rate constants for $Al_3$ dissociation. *The Journal of Chemical Physics* **1996,** *104*,9445-9460.
(134) Turi, L., A quantum chemical study of negatively charged methanol clusters. *Journal of Chemical Physics* **1999,** *110*,10364-10369.
(135) Ayotte, P.; Weddle, G.H.; Bailey, C.G.; Johnson, M.A.; Vila, F.; Jordan, K.D., Infrared spectroscopy of negatively charged water clusters: evidence for a linear network. *The Journal of Chemical Physics* **1999,** *110*,6268-6277.
(136) Czakó, G.; Kaledin, A.L.; Bowman, J.M., Zero-point energy constrained quasiclassical, classical, and exact quantum simulations of isomerizations and radial distribution functions of the water trimer using an ab initio potential energy surface. *Chemical Physics Letters* **2010,** *500*,217-222.
(137) Cramer, C.J., *Essentials of Computational Chemistry*; Editor Ed.^Eds.; Second ed.; John Wiley & Sons Ltd: Chichester, 2004.
(138) Becke, A.D., Density functional thermochemistry. III. The role of exact exchange. *The Journal of Chemical Physics* **1993,** *98*,5648-5652.
(139) Werner, H.-J.; Knowles, P.J., An efficient internally contracted multiconfiguration reference configuration interaction method. *The Journal of Chemical Physics* **1988,** *89*,5803-5814.
(140) Knowles, P.J.; Werner, H.-J., An efficient method for the evaluation of coupling coefficients in configuration interaction calculations. *Chemical Physics Letters* **1988,** *145*,514-522.
(141) Knowles, P.; Werner, H.-J., Internally contracted multiconfiguration-reference configuration interaction calculations for excited states. *Theoretica chimica acta* **1992,** *84*,95-103.
(142) Mak, C.C.; Peslherbe, G.H., Relaxation pathways of photoexcited iodide-methanol clusters: a computational investigation. *The Journal of Physical Chemistry A* **2014,** *submitted*.
(143) Yandell, M.A.; King, S.B.; Neumark, D.M., Decay Dynamics of Nascent Acetonitrile and Nitromethane Dipole-Bound Anions Produced by Intracluster Charge-Transfer. *The Journal of Chemical Physics* **2014,** *140*,184317.
(144) Markovich, G.; Perera, L.; Berkowitz, M.L.; Cheshnovsky, O., The solvation of $Cl^-$, $Br^-$, and $I^-$ in acetonitrile clusters: photoelectron spectroscopy and molecular dynamics simulations. *The Journal of Chemical Physics* **1996,** *105*,2675-2685.

(145) Yandell, M.A.; King, S.B.; Neumark, D.M., Time-resolved radiation chemistry: photoelectron imaging of transient negative ions of nucleobases. *Journal of the American Chemical Society* **2013,** *135*,2128-2131.
(146) King, S.B.; Yandell, M.A.; Neumark, D.M., Time-resolved photoelectron imaging of the iodide-thymine and iodide-uracil binary cluster systems. *Faraday Discussions* **2013,** *163*,59-72.
(147) Timerghazin, Q.K.; Nguyen, T.-N.; Peslherbe, G.H., Asymmetric solvation revisited: The importance of hydrogen bonding in iodide-acetonitrile clusters. *The Journal of Chemical Physics* **2002,** *116*,6867-6870.
(148) Sheu, W-S.; Rossky, P.J., Electronic and solvent relaxation dynamics of a photoexcited aqueous halide ion. *The Journal of Physical Chemistry* **1996,** *100,* 1295-1302.